IN VITRO-IN VIVO, CROSS-LIFE STAGE AND INTER-SPECIES EXTRAPOLATION OF THE BIOTRANSFORMATION AND UPTAKE OF BENZO[*A*]PYRENE IN TWO FISH SPECIES USING TOXICOKINETIC MODELS

A Thesis Submitted to the College of
Graduate and Postdoctoral Studies
In Partial Fulfillment of the Requirements
For the Degree of Master of Science
In the Toxicology Graduate Program
University of Saskatchewan
Saskatoon, Saskatchewan, Canada

By

CHELSEA GRIMARD

PERMISSION TO USE

In presenting this thesis in partial fulfillment of the requirements for a postgraduate degree from the University of Saskatchewan, I agree that the Libraries of the University may make freely available for inspection. I further agree that permission for copying of this thesis in any manner, in whole or in part, for scholarly purpose may be granted by the professors who supervised my thesis work or, in their absence, by the Head of the Department of the Dean of the College in which my thesis work was done. It is understood that any copying or publication of use of this thesis or parts thereof for financial gain shall not be allowed without my written permission. It is also understood that due recognition shall be given to me and the University of Saskatchewan in any scholarly use which may be made of any material in my thesis.

Requests for permission to copy or to make other use of material in this thesis in whole or parts should be addressed to:

Chair of the Toxicology Graduate Program

Toxicology Centre

University of Saskatchewan

44 Campus Drive

Saskatoon, Saskatchewan

S7N 5B3

Canada

Dean

College of Graduate and Postdoctoral Studies

University of Saskatchewan

116 Thorvaldson Building, 110 Science Place

Saskatoon, Saskatchewan

S7N 5C9

Canada

ABSTRACT

Toxicokinetic (TK) models are *in silico* tools that are used to assess the uptake, biotransformation, and elimination of environmental contaminants. Such models can be used in ecological risk assessment (ERA) and in research to evaluate chemical bioaccumulation. This information is especially useful for fish, which are an important taxonomic group used in ERA. Presently, the TK models developed for fish are accurate for neutral organic chemicals; however, the models do not commonly consider chemicals that are actively biotransformed. Furthermore, most TK models for aquatic organisms focus strictly on the adult life stage, while few are explicitly developed for early-life stages (ELS). Thus, the overall objective of this thesis was to develop life-stage specific TK models for the rapidly biotransformed model chemical, benzo[*a*]pyrene (B[*a*]P), in two physiologically distinct species of fishes, i.e., the fathead minnow (*Pimephales promelas*) and the white sturgeon (*Acipenser transmontanus*).

The first study (Chapter 2) focused on integrating biotransformation of B[*a*]P into life stage-specific TK models for a standard laboratory fish model, the fathead minnow. Whole-body embryos, and adult liver and gall bladder (bile) were collected from fish aqueously exposed to B[*a*]P. The respective tissues were analyzed for the activity of phase I and phase II enzymes to assess biotransformation capacity, and B[*a*]P metabolites were measured to act as a model validation data set. The biotransformation rate of B[*a*]P was determined using measurements of *in vitro* intrinsic clearance and implemented into a multi-compartment adult model using *in vitro-in vivo* extrapolation. For the embryo-larval stage, whole-body biotransformation was allometrically scaled from the calculations of adult biotransformation and directly implemented into a one-compartment embryo-larval TK model. No difference in phase I or II activity was observed with exposure to increasing concentrations to aqueous B[*a*]P; however, a significant increase in B[*a*]P metabolites was observed in both life stages. Both models showed good predictive power with model predictions within one order of magnitude of measured values.

The second study (Chapter 3) focused on developing life-stage specific TK models for white sturgeon. Similar to chapter 2, whole-body embryos were sampled from white sturgeon larvae aqueously exposed to B[*a*]P for assessment of phase I and II activity, and for measurements of whole-body B[*a*]P metabolites. In contrast to chapter 2, however, whole-body biotransformation of B[*a*]P could not be scaled from the calculated value of sub-adult B[*a*]P biotransformation, and therefore, was internally calibrated. The calibrated value of whole-body

biotransformation was implemented into a one-compartment embryo-larval TK model and used to make predictions of the internal concentrations of B[*a*]P metabolites. Due to logistical and ethical reasons (white sturgeon are an endangered species in Canada), an aqueous B[*a*]P exposure with the adult life stage could not be conducted. Instead, an experimental data set of four chemicals was compiled from previously conducted sub-adult sturgeon bioaccumulation studies found in the scientific literature to be used as a model validation data set. A multi-compartment TK model was parameterized using direct measurements of wet mass, tissue volume, tissue lipid fraction, tissue water content and cardiac output, and literature values of oxygen consumption, from sub-adult white sturgeon, and used to make predictions of the internal concentrations of organic contaminants in the sub-adult life stage. The model results showed that both models could accurately predict the bioaccumulation of organic contaminants within one order of magnitude.

In chapter 4, the life-stage and species specific models were used to characterize the differences in the uptake and biotransformation of B[*a*]P between life-stages and species. In the fathead minnow, the results of the life-stage analysis showed that the embryo-larval life-stage accumulated a greater abundance of parent B[*a*]P and B[*a*]P metabolites; however, the accumulation was slower than what was observed in the adults. The results of the life-stage analysis in white sturgeon showed a similar uptake of parent B[*a*]P between life stages, but a larger abundance of B[*a*]P metabolites was predicted in the sub-adult life stage. In both species, the results suggest that the embryo-larval stage might have a lesser capacity to generate the enzymes required for biotransformation B[*a*]P. The comparative species analysis showed that in both the embryo-larval and sub-adult/adult life stages, white sturgeon showed substantially slower biotransformation of B[*a*]P. Accordingly, in both life stages, a lesser abundance of metabolites was predicted/measured in the white sturgeon. It was concluded that the embryo-larval life stage of white sturgeon would be comparatively more susceptible to the effects of aryl hydrocarbon receptor binding, as a result of the slower rates of biotransformation, while the sub-adult/adult life stage of the fathead minnow would be comparatively more susceptible to the genotoxic effects associated with B[*a*]P exposure, as a result of the faster rates of biotransformation.

Overall, the models developed in this thesis contribute to the increasing scope of applications in which TK models can be used in ERA and research by providing a basis in which cross-life stage and interspecies extrapolation can be conducted for the bioaccumulation of actively biotransformed chemicals.

ACKNOWLEDGEMENTS

First and foremost, I would like to acknowledge my supervisors Dr. Markus Brinkmann and Dr. Markus Hecker for their continuous support and guidance throughout the past three years of my master's degree.

I will be forever grateful to the countless hours that Markus Brinkmann dedicated to helping me with the numerous obstacles I came across in my research project. There a few people with the amount passion and drive that Markus puts into his work, while also dedicating his time to helping students, despite if they are part of his lab or not. I am honoured to be Markus' first graduate student of his professorship and I am proud of the work we accomplished together.

I would like to thank Markus Hecker for the encouragement, support, and advice he provided during my graduate studies. Markus was always supportive and open to discuss any ideas I wanted to pursue and any problems I had. Markus encompasses what an astounding supervisor is, and his passion in the field of environmental toxicology is undeniable. I am thankful to him for allowing me to realize the potential I had while perusing my research.

I would like to thank my committee members, Dr. Lynn Weber and Dr. Paul Jones, for their insightful reviews and comments on my research work. Thank you to Dr. Jason Raine, the staff at the Aquatic Toxicology Research Centre, the countless technicians that assisted me in my exposures, and to all the administrative staff at the Toxicology Centre. I would not have been able to complete my degree without their invaluable help.

I would like to acknowledge my funding sources; Genome Canada, NSERC Discovery, and the Toxicology Centre, for providing financial support for my research, Mitacs for allowing me the opportunity to conduct research abroad, and for the organizations that provided the numerous travel awards I received to attend local, national and international conferences.

I would like to acknowledge the life-long friendships that were created throughout my graduate studies. Thank you to the members of the Hecker lab; Anita, Carly, Dayna, Derek, James, Katherine, Laura, Taylor, Susari, Ulyana, and honouring member Nicole, as well as the rest of the students at the Tox Centre (there are too many to name!) for your friendship and support throughout the past three years.

I am especially thankful to the international students that came to study at the U of S during my studies. Annika for her continuous support, expertise, and assistance with coding, Markus for

TABLE OF CONTENTS

LIST OF TABLES

LIST OF FIGURES

LIST OF ABBREVIATIONS

6-MeO-BDE-47	6-methoxylated-brominated diphenyl ether-47
ACN	acetonitrile
ADME	absorption, distribution, metabolism, excretion
AhR	aryl hydrocarbon receptor
AOP	adverse outcome pathway
AR	androgen receptor
ARNT	aryl hydrocarbon nuclear translocator
ATP	adenosine triphosphate
ATRF	aquatic toxicology research facility
B[a]P	benzo[a]pyrene
BAX	BCL2 Associated
BP2	benzophenone-2
BPDE	benzo[a]pyrene diol epoxide
Bpm	beats per minute
BPS	bisphenol S
BSA	bovine serum albumin
CDNB	1-Chloro-2,4-dinitrobenzene
C_{int}	whole-body internal chemical concentration
$CL_{int,\ in\ vivo}$	*In vivo* intrinsic clearance
C_m	muscle chemical concentration
C_{OX}	dissolved oxygen
CYP	cytochrome P450
CYP1a1	Cytochrome P450 family 1, subfamily A, polypeptide 1
DMSO	dimethyl sulfoxide
DNA	deoxyribonucleic acid
DLC	dioxin-like compounds
DTT	DL-dithiothreitol
Dpf	days post fertilization
EC_{50}	median effective concentration

EDTA	
E_G	gill uptake efficiency
ELS	early-life stages
ERa	estrogen receptor alpha
ERA	ecological risk assessment
EROD	ethoxyresorufin-O-deethylase
EURL ECVAM	European Union Reference Laboratory for Alternatives to Animal Testing
FET	fish embryo test
f_H	ventricular contractile rates
FHM	fathead minnow
G6P	glucose-6-phosphate
GC-MS	gas chromatography-mass spectrometry
Gluc-B[a]P	3-hydroxy-benzo[a]pyrene-glucuronide
GSH	glutathione
GST	glutathione S-transferase
G_V	gill ventilation rate
HESI	heated electrospray ionization
HPLC	high-performance liquid chromatography
IOC	ionizable organic chemicals
IVIVE	*in vitro-in vivo* extrapolation
K_{BW}	whole-body fish wet mass
KCL	potassium chloride
k_{MET}	whole-body biotransformation
K_{OW}	octanol/water partition coefficient
LOD	lowest observable detection
$logK_{OW}$	*log* octanol/water partition coefficient
MFO	mixed-function oxidase
NADPH	nicotinamide adenine dinucleotide phosphate
NAM	new approach methodologies
NLOM	non-lipid organic matter

OAT	organic anion transporter
OC	organochlorine
OECD	Organisation for Economic Co-operation and Development
OH-B[*a*]P	3-hydroxy-benzo[*a*]pyrene
PAH	polycyclic aromatic hydrocarbon
PAPS	3'-phosphoadenosine-5'-phosphosulfate
PBTK	physiologically based toxicokinetic model
PCB	polychlorinated biphenyl
pKa	acid dissociation constant
PNP	para-nitrophenol
PPT	poorly perfused tissues
PRM	parallel reaction monitoring
Q_{bile}	bile flow rate
QSAR	quantitative structure-activity relationship
RMSE	root mean squared error
RNA	ribonucleic acid
ROS	reactive oxygen species
RPT	richly perfused tissues
S9	post-mitochondrial supernatant fraction
SC	solvent control
SD	standard deviation
S.E.M.	standard error of the mean
SM_2	sulfamethazine
SPE	solid-phase extraction
SPV	sulfophosphovanillin
TD	toxicodynamic
TK	toxicokinetics
UDPGA	uridine 5'-diphosphoglucuronic acid
UDPGT	uridine 5'-diphospho-glucuronyltransferase
U of S	University of Saskatchewan

UPLC-HRMS	ultra-high-performance liquid chromatography high-resolution mass spectrometry
U.S.	United States
V_{bile}	bile volume
V_{OX}	oxygen consumption
V_S	ventricular stroke volume
VTG	vitellogenin
WC	water control
WS	white sturgeon

PREFACE

The focus of this thesis was to develop life stage and species specific toxicokinetic models that characterize and integrate the uptake and biotransformation of benzo[*a*]pyrene (B[*a*]P) in the embryo-larval and adult life stages of two fish species, fathead minnow *(Pimephales promelas)* and white sturgeon (*Acipenser transmontanus)*. This thesis was written in manuscript style.

Chapter 1 is a review of the available literature data. This review includes topics regarding general toxicokinetics and toxicokinetic models, toxicokinetic models in regard to aquatic species, an overview of fathead minnow and white sturgeon, and lastly, a review of benzo[*a*]pyrene including environmental fate, mechanisms of action, and biological effects.

Chapters 2 and 3 describe and discuss the data collected from fathead minnows and white sturgeon, respectively. These chapters have been prepared in manuscript style, and thus, there may be repetition amongst their respective materials and methods sections. Chapter 2 was published in the peer-reviewed scientific journal *Aquatic Toxicology* (Grimard et al., 2020), and Chapter 3 was submitted to be published in *Environmental Science and Technology*.

Chapter 4 is a general discussion. This chapter compares the findings between chapters 2 and 3. Specifically, comparisons between life stages and species, the relevance of the present work, and recommendations for future research are discussed.

CHAPTER 1: GENERAL INTRODUCTION

Environmental contaminants originating from various sources, such as urban communities and industrial outputs, are continuously being released into aquatic environments. If not assessed and managed appropriately, these contaminants pose a risk to both human health and wildlife (Government of Canada, 2016). To adequately assess the risk associated with environmental contaminants in aquatic systems, the relation between chemical exposure and hazards (i.e., toxic effects) is evaluated through ecological risk assessment (ERA). ERA consists of three phases; problem formulation, analysis, and risk characterization (U.S. EPA, 1998). Previously, the analysis phase of ERA characterized chemical effects strictly based on the characterization of external exposure metrics. This approach, however, can only determine the effects triggered by external concentrations and does not consider how much of the toxicant reaches the systemic circulation of an organism and, ultimately, its site of toxic action (Escher & Hermans, 2005). Therefore, toxicokinetics (TK) are being integrated into ERA for aquatic systems as a better approach to relate exposure and hazards. The key advantage of integrating toxicokinetics is that it describes physiological processes that determine the fate of a chemical within the body, and therefore, can link external exposure concentration to internal exposure concentration. The internal concentrations can then be related to the quantity of an active compound that reaches target organs and elicits a toxic response (Grech et al., 2017). Using toxicokinetics, cross life stage and inter-species differences in toxicity can be better understood because life-stage and species differences in physiology can be used to explain the difference in the amount of chemical that reaches the target site. Understanding these differences is critical for characterizing species and life stage differences in sensitivity to contaminants. This is particularly important for the ERA of diverse taxonomic groups such as fish, one of the most diverse groups of vertebrates.

The applicability of the current TK models for ERA, however, is limited for chemicals that are actively biotransformed and for the early-life stages (ELS) of fish. Biotransformation of chemicals, such as polycyclic aromatic hydrocarbons (PAHs), is an essential consideration for TK models used in ERA as biotransformation acts to both detoxify and bioactivate chemicals and will influence the total chemical body burden and the resulting toxic effect. Biotransformation in the ELS of fish has been shown to differ from adults, and the ELS are frequently shown to be more sensitive to contaminants compared to the adult life stage. Therefore, the aim of the following

thesis is to bridge the described data gaps for TK models by integrating the biotransformation of the model PAH, benzo[*a*]pyrene (B[*a*]P), into life stage-specific TK models for two physiologically distinct fish species; the fathead minnow (*Pimephales promelas*) and the white sturgeon (*Acipenser transmontanus*).

1.1 Toxicokinetics

TK quantitatively describes the time course of disposition of a chemical in a whole organism. Disposition is characterized by the processes of absorption, distribution, metabolism, and excretion (ADME) of a chemical. TK applies ADME parameters and processes to describe the connection between the external exposure concentration and the concentration that reaches the target organ, defined as the biologically effective dose (Ashauer & Escher, 2010; Paustenbach, 2000). Additionally, for chemicals that are extensively biotransformed, TK can describe the relationship between the exposure concentration and the number, proportion, and concentration of metabolites produced through activation and detoxification pathways (Grech et al., 2017).

1.1.1 Absorption

Absorption describes the process by which a chemical from the external environment crosses a biological membrane to enter the systemic circulation of an organism (Klaasen, 2010). In fish, the primary site of absorption for waterborne chemicals is the blood-water interface at the gills. The gill is made up of brachial arches, filaments, and secondary lamellae that form a "sieve"-like structure (Hughes, 1984; Laurent, 1984; Evans, 1987). The gill lamellae have a large surface area (McKim & Erickson, 1991) and are covered by a thin epithelial layer with diffusion distances ranging from ≤ 1 to 22.5 µm (Hughes, 1984). These two physiological features, in addition to countercurrent blood and water flows (Randall, Lin & Wright, 1991) and high rates of blood and water perfusion at the gill, support the exchange of waterborne chemicals (McKim & Erickson, 1991).

The processes that facilitate absorption include passive diffusion, facilitated diffusion, active transport, filtration through membrane channels, and specialized transport such as endocytosis (Tierney et al., 2013). Most chemicals are absorbed through simple passive diffusion in which chemicals move from areas of high to low concentration with no additional energy requirements (Klassen, 2010). The main processes that facilitate absorption across the gills can be

described in two parts. First, a water-borne chemical passes through the gill lamellar "sieve" (McKim & Erickson, 1991), and secondly, the chemical passively diffuses across the lamellae into the blood (Hunn & Allen, 1974; McKim, Schmieder & Veith, 1985). There are many physicochemical properties, however, which can influence the rate and extent of absorption across a biological membrane *via* passive diffusion. They include the molecular volume and weight, ionization, and lipophilicity of a chemical (Hunn & Allen, 1974; Spacie & Hamelink, 1982). Lipophilicity and ionization are important chemical parameters that directly correspond to the potential lipid membrane permeability and rate of absorption *via* passive diffusion. Lipophilicity is described by a chemical's octanol/water partition coefficient (log K_{OW}) and has a positive correlation with the rate and extent of absorption across membranes (Gluth et al., 1985; Klassen, 2010). Studies using fish have shown a direct relationship between log K_{OW} and rate of absorption for chemicals with a log K_{OW} between one and six, in which the rate of absorption increased with increasing log K_{OW} (Saarikoski et al., 1986). This phenomenon is thought to be because chemicals with increased lipophilicity have a greater ability to permeate membranes (McKim, Schmieder & Veith, 1985). These chemicals are also more likely to bind to plasma proteins, which has been shown to be directly related to increasing log K_{OW} (Schmieder & Henry, 1988). However, for chemicals with a log K_{OW} greater than six, the rate of absorption is shown to decrease with increasing log K_{OW}. This decrease is attributed to increased molecular weight and volume, which may disrupt diffusion across the membrane (McKim, Schmieder & Veith, 1985).

The extent of molecular ionization is described by a chemical's acid dissociation constant (pKa), an expression of acidity that indicates the pH at which 50% of molecules are ionized. For acids, a low pKa indicates a strong acid, while a high pKa indicates a weak acid, and vice versa for bases (Klassen, 2010). A molecule in its ionized state cannot readily permeate across membranes (McKim & Erickson, 1991). Therefore, the pH at the site of absorption, in combination with pKa of the chemical, will have a vast influence on the extent of absorption (Klassen, 2010). The effects of pH on the uptake of waterborne ionizable organic chemicals (IOCs) by fish have been reported multiple times. These studies showed that uptake of IOCs began to decrease when the pH of the aqueous medium reached the pKa of the studied chemical and accordingly, toxicity decreased (Hunn & Allen, 1974; Saarikoski et al., 1986; Howe et al., 1994; Kishino & Kobayashi, 1995). It has also been suggested that the effect of pH may not be solely related to the waterborne

chemical phase, but also the internal space between the water and mucous layer covering the gills (Saarikoski et al., 1986).

Physiological processes can also influence the rate of absorption at the gill, namely the water flow to and from the gill attributed to the respiration rate (McKim & Erickson, 1991). It has been shown that increases in respiration, due to factors such as an increase in temperature, can increase chemical absorption rates at the gill (Murphy & Murphy, 1971).

1.1.2 Distribution

Distribution refers to the transfer of a chemical from the systemic circulation to organs or tissues (Kishnan & Peyret, 2009; Klaassen, 2010). The factors that determine the rate and extent of distribution of chemicals are complex. They involve many parameters, including physicochemical properties, such as the chemical's affinity and capacity for protein and tissue binding, as well as its lipophilicity. Physiological parameters, such as the blood flow to the tissues, tissue volumes, tissue composition, and diffusion rates between capillary beds and tissues are equally important (Krishnan Peyret, 2009; Klassen, 2010).

Blood flow and capillary diffusion rate are considered the most influential physiological parameters during the initial phases of distribution (Klassen, 2010). These parameters govern whether uptake is perfusion-limited or diffusion-limited (Krishnan and Peyret, 2009). When membranes are not a barrier to chemical uptake, distribution is limited by perfusion. Therefore, the chemical will more readily distribute into highly perfused tissues compared to poorly perfused tissues and tissue: blood equilibrium of the unbound chemical is quickly established (Rowland & Towzer, 2011). Perfusion limitations, in combination with chemical-tissue affinity, will govern the overall distribution of a chemical into a tissue. This concept is essential in physiologically based toxicokinetic (PBTK) modeling to accurately predict chemical accumulation in specific tissues (Nichols et al., 1990). When a membrane presents a barrier to uptake, distribution is diffusion-limited. This is often the case for large or polar chemicals as lipophilicity and ionization are the main drivers of their ability to cross a membrane. Such diffusion limitations at the gill have been shown to also occur in fish (Opperhulzen et al., 1985; Erickson & McKim, 1990). In these cases, perfusion rates have no discernable effect on distribution into tissues, and equilibriums are slow to establish (Rowland & Tozer, 2011).

The physicochemical properties of a chemical will influence its overall distribution and resulting toxic effects. First, a chemical's affinity and capacity to bind plasma proteins is an important driver of toxicity because only the unbound chemical fraction can cross membranes and elicit a toxic effect (Gülden et al., 2002; Seibert & Gülden, 2002; Heringa et al., 2004). Therefore, chemicals that are highly protein-bound in plasma may show a lesser extent of toxicity compared to chemicals that have low plasma protein binding affinity. This concept has been studied with mouse cells *in vitro*, where the median effective concentration (EC_{50}) for organochlorine pesticide exposure increased with increasing albumin concentrations indicating a higher proportion of plasma protein binding and a lesser proportion of unbound chemical to elicit a toxic effect (Gülden et al., 2002). The relationship between EC_{50} and the unbound fraction has also been shown to be applicable to aquatic species (Gülden & Seibert, 2007).

Secondly, both protein binding and chemical lipophilicity will influence the affinity of a chemical to distribute to a tissue. For example, highly lipophilic chemicals are more likely to distribute into fatty tissues than to remain in the systemic circulation. This concept was studied by Gluth et al. (1985), who showed that chemical accumulation in the liver of carp (*Cyprinus carpio*) was directly related to the lipophilicity of the chemical in which accumulation increased with increasing $logK_{OW}$. Sequentially, from this concept, tissue lipid content and $\log K_{OW}$, became the main parameters in determining chemical partitioning coefficients (Bertelsen et al., 1998). Chemicals may also concentrate in a specific tissue due to affinity to certain proteins in this tissue. An example of this is reported by Ng & Hungerbühler (2013), where the authors recognized the specific protein binding of perfluorinated alkyl acids to serum albumin, fatty-acid binding proteins in the liver, and organic anion transporters (OATs) in the kidney when they were creating an accumulation model for rainbow trout (*Oncorhynchus mykiss*) and common carp. This research shows that the inclusion of specific binding affinity in the model was essential to achieve accurate distribution and bioconcentration predictions. Once distributed into a tissue, an equilibrium of the free compound between the systemic circulation and the tissue occurs. As the chemical is metabolized or excreted from the body, it will be released from the tissue to maintain this equilibrium (Klassen, 2010).

1.1.3 Metabolism

Metabolism in the context of ADME most often describes the biotransformation of a lipophilic chemical to an excretable hydrophilic molecule. In fish, biotransformation largely occurs in the liver (Chambers & Yarbrough, 1976; Cok et al., 1998), but can also occur at lower rates in the kidney (Fukami et al., 1969; Lindström-Seppä, Koivusaar, & Hänninen, 1981), blood (Cok et al., 1998), gastrointestinal tract (Fukami et al., 1969; Lindström-Seppä, Koivusaar, & Hänninen 1981; Cok et al., 1998), gill (Lindström-Seppä, Koivusaar, & Hänninen, 1981; Leugen et al., 2000), heart (Lindström-Seppä, Koivusaar, & Hänninen 1981), and brain (Fukami et al., 1969; Cok et al., 1998). It has also been suggested that some metabolism may occur in muscle tissue (Cok et al., 1998). The mechanisms that govern biotransformation are similar between all vertebrate species and can include any one or more of the following systems: conjugation, hydroxylation, epoxidation, dealkylation, sulfuration, oxidation, reductions, and ester and ether cleavage (Chambers & Yarbrough, 1976). These transformation processes are governed by enzyme systems, which are categorized by their function into phase I or phase II biotransformation. Phase I biotransformation moderately increases the hydrophilicity of a chemical by affixing a functional group, such as a hydroxy (-OH), through oxidation, reduction, hydration, or hydrolysis (Livingstone, 1998). In aquatic species, the enzymes most often associated with phase I biotransformation are cytochrome P450 and mixed-function monooxygenases (Stegeman & Lech, 1991; Andersson & Förlin, 1992). Phase II biotransformation affixes a large polar endogenous compound, such as glutathione or sulphate, to the phase I metabolite through conjugation, which results in a highly hydrophilic excretable compound (Livingstone, 1998). The primary enzymes found in aquatic species associated with phase II biotransformation are glutathione *S*-transferase (GST), uridine 5'-diphospho-glucuronyltransferase (UDPGT), sulfotransferases (George, 1994). While biotransformation of a chemical predominately results in detoxification, some metabolites generated can be more toxic than the parent compound. This process is referred to as bioactivation (Buhler & Williams, 1988). B[*a*]P (benzo[*a*]pyrene), a prominent environmental contaminant and infamous carcinogen, provides an excellent example, as it has been shown to be bioactivated into the toxic metabolite BPDE (benzo[*a*]pyrene diol epoxide), amongst other metabolites, which are associated with various toxic effects. Here, it is the proportion of detoxification compared to activation that is an important driver of toxicity.

1.1.4 Elimination

Elimination involves the removal of a chemical or its metabolite from the body (Klaasen, 2010). In aquatic organisms, elimination occurs through the gills, bile, and kidney (Nichols et al., 1990). The kidney is the primary organ of elimination and uses three mechanisms: glomerular filtration, tubular secretion, and tubular reabsorption, in which only glomerular filtration and tubular secretion are involved in the elimination of IOCs (Pritchard & Bend, 1984; Rowland & Tozer, 2011). The extent of elimination by glomerular filtration depends on the glomerular filtration rate, which is determined by the blood flow to the kidney, the molecular weight of a molecule, and the extent of plasma protein binding, as bound molecules are too large to pass through the glomeruli pores (Pritchard & Bend, 1984; Klaasen, 2010). An example is 2,2-bis[*p*-chlorophenyl] acetic acid, a metabolite of the insecticide dichlorodiphenyltrichloroethane, which has been shown to be highly plasma protein-bound in fish and unable to be filtered at the glomerulus (Prichtard et al., 1977). Once a chemical is filtered at the glomerulus, it will be excreted into the urine. Chemicals that are not filtered at the glomerulus may undergo tubular secretion in which transporters located along the tubular epithelium actively transport molecules across the tubular membrane to be excreted through the urine (Klaasen, 2010). This mechanism is especially prevalent in fish compared to mammals as the blood from the portal system saturates the kidney tubules, potentially due to the existence of the renal portal vein that diverts blood from the posterior half of the body to the kidney (Henderson & Daniel, 1978; Pritchard & Bend, 1984). Therefore, there is a greater dependence on transporters for the excretion of chemicals and their metabolites in aquatic vertebrates. An example of this in fish are OATs that have been shown to contribute to the excretion of B[*a*]P metabolites into the urine (Pritchard & Bend, 1991). Reabsorption of chemicals back into the systemic circulation may occur if the chemical is lipophilic as only polar compounds will be eliminated through the kidneys (Pritchard & Bend, 1984; Klaasen, 2010).

Excretion through the gill occurs through passive diffusion and is therefore limited to the unionized form of a chemical (McKim & Erickson, 1991). The elimination rate at the gill, similarly to distribution, can be limited by either perfusion or diffusion, depending on whether the membrane at the gills acts as a barrier to chemical elimination (Maren et al., 1968; Erickson & McKim, 1990; Nichols et al., 1990). As in absorption and distribution, the rate of elimination at the gill has been shown to be dependent on $logK_{OW}$, in which elimination rates decline with

increasing logK$_{OW}$ because of an associated increase in plasma binding (Schmeider & Henry, 1988).

Biliary excretion contributes to the fecal elimination of a chemical where metabolites generated in the liver are secreted into the bile and then excreted with the feces (Klassen, 2010). Factors that determine if a compound will be excreted in the bile are related to increased molecular weights and polarity. For this reason, metabolites such as glucuronides, which have a greater molecular weight and are more polar than the parent compound, are often found in the bile (Levine, 1978). If the chemical is not sufficiently conjugated and polar, it may be reabsorbed into the systemic circulation due to increased lipophilicity (Klaasen, 2010). This process is referred to enterohepatic circulation, and while it is thought to be unlikely to occur in fish for some metabolites, such as large polar glucuronides (Kasokat, Nagel & Urich, 1987), it has been proven to occur in several fish species for compounds such as bile alcohols (Fricker et al., 1997) and steroids (Pelissero & Sumpter, 1992).

1.2 Toxicokinetic models

TK models are computational tools used to describe the ADME properties and processes of an organism in relation to chemical exposure (Coeke et al., 2013). This *in silico* modeling approach is gaining interest from the scientific community as a method of integrating TK into ERA. The key advantage of integrating TK is that it describes physiological processes that determine the fate of a chemical within the body, and therefore, can link external exposure concentration to internal exposure concentration. The internal concentrations can then be related to the quantity of active compound that reaches target organs and elicits a toxic response (Grech et al., 2017). Using TK, cross life stage and inter-species differences in toxicity can be better understood because life-stage and species differences in physiology can be used to explain the difference in the amount of chemical that reaches the target site.

Two types of TK models exist, classic models (empirical) and mechanistic (physiologically based) models. Empirical models are structured as simple one or more complex multi-compartment models adequate for determining the basic concentration-to-time relationship. One-compartment models represent the whole body of an organism as a single compartment and assume the chemical concentration to be homogenous throughout the organism. In contrast, multi-compartment models represent individual organs/tissues or groups of organs/tissues as separate

compartments and assume that chemical concentrations will differ among them depending on their characteristics (Grech et al. 2017).

Empirical models apply experimentally determined uptake and elimination rate coefficients that can describe the kinetics of chemicals in many organs and tissues. However, because parameters are determined experimentally, empirical models are only appropriate for interpolation between the chemical concentrations at which the uptake and elimination constants were established and therefore are not suitable for any type of extrapolation (Krishnan & Peyret, 2009).

PBTK models are mechanistic models. Such models compartmentalize an organism into organs or tissue/organ groups of physiological importance. They use the physiological functions cardiac output, effective respiratory volume, tissue volumes, tissue lipid and moisture content, and tissue perfusion rates to calculate partitioning coefficients (i.e., between water:blood and blood:tissue) determined by physiological and physicochemical properties, to describe the kinetic behavior of a chemical (Nichols et al., 1990). As a result of the mechanistic nature, PBTK models can be used to describe and extrapolate the toxicokinetics of numerous chemicals in relation to interspecies differences in exposure patterns, physiology, enzyme expression, and life cycle, as the model is specifically parameterized based on the physiology of the species of interest (EFSA, 2016). Regardless of the intended use, all PBTK models have the main objectives to integrate diverse sets of kinetic data for a particular chemical and to predict and extrapolate tissue dose for situations in which it cannot be measured (U.S. EPA, 2006).

1.2.1 One-compartment model

One-compartment models describe an organism as one homogenous system, which makes the assumption that the accumulation of a chemical will be the same throughout the whole organism (Grech et al., 2017). The first order uptake and elimination rate coefficients are the two main parameters that drive the kinetics in a one-compartment model. Uptake rate coefficients are expressed in relation to the exposure concentration, while elimination rate coefficients are expressed in relation to the whole-body internal concentration (Landrum et al. ,1992; Grech et al., 2017). However, when appropriate other model formulations can be used: zero-order kinetics, where the rate of change of internal concentration is constant in relation to changes in exposure concentration, second-order kinetics, where the rate is proportional to the concentration of two

products, and quasi-zero order kinetics, where a rate reaches a maximum value, can be integrated into a one-compartment model (Newman, 1995, Grech et al., 2017).

Additional biological parameters, external stressors, and kinetic rates can also be integrated into a one-compartment model to assist in refining the outputs of a given model. Biological parameters can include lipid contents and biotransformation rates (Arnot & Gobas, 2004). External environmental factors, such as temperature and pH, can influence the bioavailability of chemicals (Grech et al., 2017). For example, as described above (Section 1.1.1), the pH of the exposure medium will influence the ionization of a chemical, influencing the extent of absorption (Erickson et al., 2006). Last, growth dilution can be integrated into a model through mathematical descriptions of growth or first-order growth rate constants to improve model applicability and specificity (Landrum et al., 1992; Koojman 2008).

This research project uses the one-compartment bioaccumulation model described by Arnot & Gobas (2004). Originally designed as a food web bioaccumulation model, we adapted the model to be applicable to the developmental stages, i.e., egg, yolk, and free-feeding embryolarval stages of fish. This adaptation is based on the one-compartment TK model developed for common sole (*Solea solea*) larvae by Foekema et al. (2012). The Arnot & Gobas (2004) model is comprised of rate coefficients for the major routes of uptake and elimination, as well as whole-body metabolism and growth dilution (Figure 1.1). Calculations of partitioning coefficients between the water and the whole-body fish (K_{BW}), oxygen consumption (V_{OX}), gill ventilation rate (G_V), gill uptake efficiency (E_G), and dissolved oxygen (C_{OX}) are used to calculate the associated rate coefficients. These parameters, i.e., $K_{BW}, V_{OX}, G_V, E_G, C_{OX}$, are determined using the measurement of wet mass, whole-body lipid fraction, and the nonlipid organic matter (NLOM) in addition to a proportionality constant (β), which refers to the sorption capacity of NLOM in relation to octanol, the octanol/water partitioning coefficient (K_{OW}) of the chemical of interest, and the temperature and percent oxygen saturation of the exposure. Using this model, the whole-body chemical concentration, as well as the whole-body metabolite concentration, can be predicted throughout the time-course of exposure and/or the embryo-larval development of fishes.
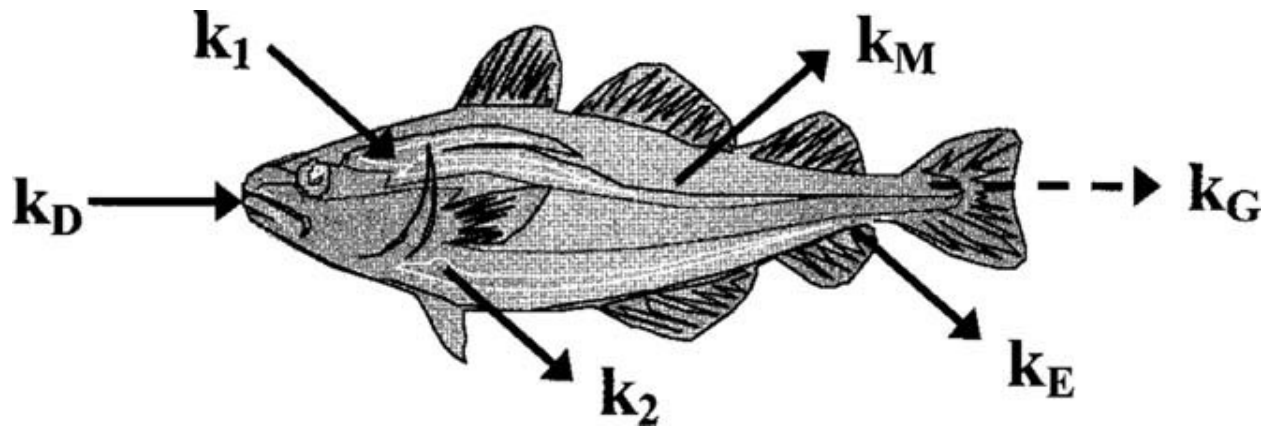
Figure 1.1. A conceptual representation of a one-compartment bioaccumulation model fish where k_1 is the uptake constant through the gills, k_2 is the elimination constant through the gills, k_D is the dietary uptake constant, k_M is the metabolism constant, k_E is the elimination constant through egestion, and k_G is the growth dilution constant (Figure from Arnot & Gobas, 2004).

1.2.2 Physiologically based toxicokinetic model

A PBTK model is a computational tool that estimates target tissue concentrations by considering the ADME processes in relation to important physiological, physicochemical, and biochemical properties (U.S. EPA, 2006; Jongeneelen & Berge, 2011). PBTK models are structured with multiple compartments that separate an organism into representative organs and tissues that are connected by the blood circulatory system. There is no limit to the number and complexity of compartments chosen to represent the biological functions of the model organism (U.S. EPA, 2006). However, the compartments must always include the portal of entry, metabolizing tissues, adipose tissues, and the tissues that comprise the "rest of the body" in order to achieve mass balance (U.S. EPA 2006; Krishnan & Peyret, 2009). Most often, the tissues and organs chosen as compartments are those that drive the ADME processes, are of high physiological and/or biochemical relevance for the chemical of interest and are a target tissue for toxicity (U.S. EPA, 2006; Grech et al., 2017). Representative compartments chosen for fish models typically include the kidney, liver, adipose tissue, richly perfused tissues (RPT), and poorly perfused tissues (PPT), where RPT includes intestine, brain, and spleen and PPT include skin and muscle (Nichols et al., 1990; Grech et al., 2017). The intestine may also be included as a separate compartment when modeling dietary exposures (Wan et al., 2013; Yang et al., 2013). This research project uses the PBTK model developed for fathead minnows described by Stadnicka et al. (2012). The model consists of four compartments; the liver, fat, RPT, and PPT.

The representative compartments are described by four types of parameters; physiological, anatomical, biochemical, and physicochemical. Physiological and anatomical parameters include cardiac output, effective respiratory volume, tissue volumes, tissue lipid and moisture content, and tissue perfusion rates. Biochemical parameters include estimations of gill metabolism and hepatic clearance. Physiochemical parameters describe the chemical of interest through the respective log K_{OW}. It is from this set of parameters that partitioning coefficients, i.e., water:blood; blood:tissue, can be calculated. These influence the proportion of uptake, distribution, and elimination from a compartment (Jongeleen & Berge, 2011).

The parameters are calibrated with either *in vitro* studies, *in vivo* studies, quantitative structure-activity relationships (QSARs) and/or allometric scaling (Grech et al., 2017). Parameters established *in vitro*, such as biotransformation rates through measurements of *in vitro* intrinsic clearance, can be integrated into PBTK models through *in vitro-in vivo* extrapolation (IVIVE)

(Nichols et al., 2006; Nichols et al., 2007; Nichols et al., 2013). Partitioning coefficients in fish can also be studied *in vitro* through gas equilibrium (Bertelsen et al., 1998; Hoffman et al., 1992) or equilibrium dialysis (Law et al., 1991). Experimental *in vivo* studies are useful for calibrating physiological parameters such as wet mass and tissue volumes through direct measurements, perfusion data through radiolabeled or fluorescent microspheres (Barron et al., 1987; Schultz et al., 1999; White et al., 1988; Brinkmann et al., 2014; Brinkmann et al., 2016), and respiratory volume and cardiac output through respirometer-metabolism chambers (McKim et al., 1999; Fitzsimmons et al., 2001). QSARs are an additional *in silico* tool which uses statistical models to relate chemical structure and descriptors to chemical activity within an organism (Bertelsen et al., 1998; Nichols et al., 2006; Escher et al., 2011; Grech et al., 2017). Allometric scaling is most often used in instances where parameters are to be extrapolated across species and life stages in which the parameter cannot be directly established through *in vitro*, *in vivo,* or QSAR studies (Hendriks et al., 2001; Vives i Batle et al., 2007).

The above parameters are used in mass balance differential equations to describe the rate of change in the chemical amount in each compartment over time (Chiu et al., 2007; Krishnan & Peyret, 2009). To achieve mass balance, the rate of change of a chemical in a compartment must equal the difference in the rates of entry and elimination. A computational program is required to solve the differential equations and create a numerical simulation (Chiu et al., 2007; Krishnan & Peyret, 2009). Numerous integration algorithms and programming languages exist to code and solve PBTK model equations. The code written into the program structures the equations, physiological and chemical parameters as a dynamic model. Comparisons with experimental data are then used to validate and/or refine the model (Krishnan & Peyret, 2009).
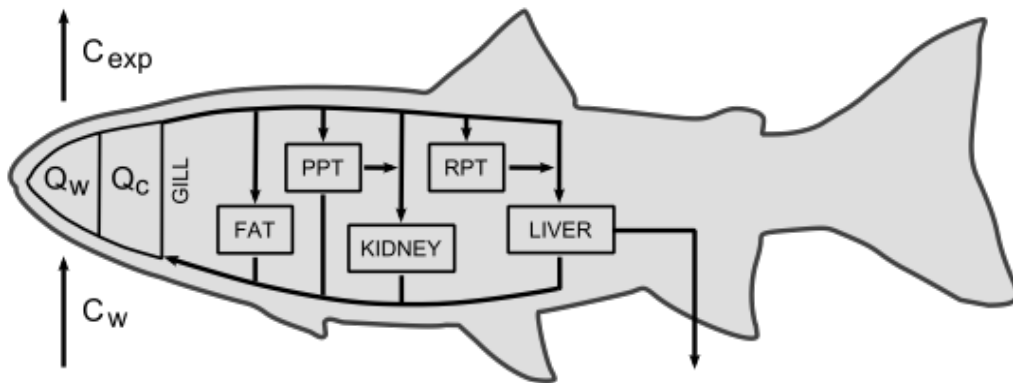
Figure 1 2. A conceptional representation of the PBTK model framework in a fish. C_w and C_{exp} represent the water concentration inspired and expired respectively, Q_W represents the effective respiratory volume, and Q_C represents the cardiac output. Each compartment is represented as a box where PPT represents the poorly perfused tissues, and RPT represents the richly perfused tissue, with the exception of the gill compartment, which is the organ of uptake. The lines show the systemic circulation and flow of the chemical from uptake to elimination (Figure modified from Brinkmann et al., 2014).

1.2.3 Model evaluation

Model evaluation tests the validity of a model structure and consists of verification and validation. Verification involves assessing whether the model performs as expected, while validation assessing and comparing the model predictions with measured data, that must be independent of data used to parameterize the model. Models should have the ability to accurately predict the kinetics of chemicals against a variety of conditions and data sets. For example, a model for a chemical that demonstrates saturable kinetics (i.e., metabolism) should be able to make accurate predictions for both low and high input concentrations where the kinetic behavior would be different (U.S. EPA, 2006). Several methods exist to evaluate the adequacy of the models. The most common method currently used is the visual inspection of the model prediction plots against experimental values. Adequacy using this method is determined by how close the correlation is between the simulated curve and discrete experimental data points where the closer the correlation, the more adequate the model is deemed. The less common approach to the evaluation of models is through statistical tests. The goal is to test whether the model can predict the kinetic behavior of a chemical to make accurate conclusions or if there are large differences between the biological system and the model to deem conclusions inaccurate (U.S. EPA. 2006). A multivariate analysis of variance was determined to be the most appropriate statistical test to evaluate this correlation (Haddad et al., 1995).

In addition to testing the adequacy of the overall model structure, additional analyses that evaluate the model's sensitivity, variability, and uncertainty are used to evaluate the adequacy of model input parameters. Local sensitivity analyses are used to determine how a change in a single input parameter (i.e., cardiac output, lipid content, etc.) affects the output of the model (i.e., dose-response). This magnitude of change in the dose metrics given a change in the input parameter is measured by a sensitivity ratio (U.S. EPA, 2006; Chiu et al., 2007). For example, a ratio of two correlates a one percent increase in parameter value to a two percent increase in output (Simmons et al., 2002; Chiu et al., 2007). Presently, global sensitivity analyses, in which multiple parameters are varied in parallel, are also gaining interest in evaluating PBTK models because they assess synergies and influences among parameters (Gueorgeuiva et al., 2006; Sobol et al., 2007; Grech et al., 2019).

Variability analyses evaluate the variability in an individual parameter and the subsequent variability in outputs (U.S. EPA, 2006). This type of analysis is useful in analyzing the inter-

individual differences in physiology (Chiu et al. 2007). Monte Carlo simulations are most often used to evaluate variability (Haber et al., 2002; Timchalk et al., 2002; Lipscomb et al., 2003). Using the Monte Carlo method, repeated computations are conducted in which the model randomly selects input values from a statistical distribution for each parameter. The result is a statistical distribution of model outputs that can be used to evaluate the impact of variability in the input parameters (U.S. EPA, 2006; Chiu et al., 2007).

Uncertainty analysis is used to determine how the lack of precise information for an input parameter and/or model structure affects the model output. Lack of precision may be due to lack of biological information, errors in the experimental determination of parameters, or errors in model structure (U.S. EPA, 2006; Chiu et al., 2007). Uncertainty analyses are conducted using classic Monte Carlo approaches or Bayesian Markov chain Monte Carlo analysis (integrating new TK data with the previously used TK data to conduct Monte Carlo simulations) (Jonsson & Johanson, 2001; Chiu et al., 2007). In scenarios where statistical distributions are not available, a fuzzy simulation approach can be used in which uncertainty is correlated to the relative frequency of the parameter value (Nestorov, 2001). If uncertainty regarding a parameter exists, these types of analyses will identify the impact it may have on model output. Therefore, uncertainty analyses are most beneficial when the model is producing inadequate simulations but is also favorable in providing credibility for well-calibrated models (U.S. EPA, 2006).

1.3 Toxicokinetic modelling in fishes

TK models have been developed for several aquatic organisms to predict the accumulation of a variety of chemicals under a variety of conditions. Initially, TK models were created to extrapolate kinetic data among mammalian species. These models were then adapted to create the first models for aquatic species, the stingray (*Myliobatoidei*) and the dogfish shark (*Squalas acanthias*) (Zaharako et al., 1972; Bungay et al., 1976). However, these aquatic species models were limited in applications as they were created based on the intravenous injection of a chemical and not environmentally relevant routes of exposure (i.e., brachial, oral, or dermal). Therefore, future TK models such as those developed by Nichols et al. (1990) for aqueous exposures of organic chemicals using the rainbow trout as the model species were developed. This approach to TK modelling was advantageous as it took into consideration the uptake and elimination of a chemical *via* the gills (Nichols et al., 1991). Since then, TK models have been created for various aquatic

species for a variety of conditions. Among the species are the brook trout (*Salvelinus fontinalis*) (Nichols et al., 1998), rainbow trout (Nichols et al., 1990; Law et al., 1991; Nichols et al., 1991; Nichols et al., 1994; Nichols et al., 1996; Abbas et al., 1997; Freidig et al., 2000; Garnier-Laplace et al., 2000; Nichols et al., 2004; Stadnicka et al., 2012; Brinkmann et al., 2014; Brinkmann et al., 2016; Salmina et al., 2016), lake trout (*Salvelinus namaycush)* (Lien et al., 2001; Brinkmann et al., 2016), fathead minnow (Lien et al., 1994; Li et al,. 2011; Stadnicka et al., 2012; Breen et al., 2013; Parhizgari & Li, 2014; Brinkmann et al., 2016), medaka (*Oryzias latipes)* (Parhizgari & Li, 2014), zebrafish (*Danio rerio*) (Pery et al., 2014; Brinkmann et al., 2016), roach (*Rutilus rutilus*) (Brinkmann et al., 2016), sole (Foekema et al., 2012), Chinese sturgeon (*Acipenser sinensis*) (Wan et al., 2013), crucian carp (*Carassiuis carassius*) (Yang et al., 2013), channel catfish (*Ictalurus punctatus*) (Nichols et al., 1993, Nichols et al., 1996), and European eel (*Anguilla anguilla*) (Brinkmann et al., 2015).

1.3.1 Fathead minnow

The fathead minnow, a member of the Cyprinidae family, is a native North American fish species found in rivers and freshwater lakes (Zimmer et al., 2001; Ankley & Villeneuve, 2006; Herwig et al., 2007). Due to their small size, distinctive reproductive behavior and patterns, and broad tolerance to different water quality conditions, fathead minnows are a popular test organism for environmental toxicity studies (Ankley & Villeneuve, 2006). As such, the species has been used in thousands of toxicity tests ranging from acute to sub-chronic to chronic exposures for characterization of the toxicity of a multitude of chemicals (Ankley & Villenevue, 2006). Most often, fathead minnows are used to assess effects of contaminants on reproductive fitness and sexual development (OECD, 2012), but the species has been used for a vast number of other assessments, including acute lethality tests and longer-term exposures assessing growth and mortality, along with a variety of mechanistic and diagnostic endpoints (Ankley & Villeneuve, 2006).

Several TK models for fathead minnow are presently described (Table 1.1; Lien et al., 1994; Li et al., 2011; Stadnicka et al., 2012; Breen et al., 2013; Parhizgari & Li, 2014; Brinkmann et al., 2016). Most fathead minnow models are developed as PBTK models, with the exception of Stadnicka et al. (2012), who compared two types of one-compartment models to a PBTK model. The PBTK model was superior as it predicted 88% of the internal concentrations within one order

of magnitude compared to the two one-compartment models, which only predicted 68% and 76% of the internal concentrations within one order of magnitude (Stadnicka et al., 2012). It is important to note that in most of the present fathead minnow PBTK models, the kidney compartment is absent due to a lack of information available for this tissue, specifically perfusion data (Stadnicka et al., 2012, Brinkmann et al., 2016). An exception is made by Parhizgari & Li (2014), where the kidney compartment is included. However, the kidney compartment, in this case, was calibrated using data from rainbow trout (Bertelsen et al., 1998) and lake trout (Lien et al., 2001) and not fathead minnows directly. The fathead minnow models were predominately calibrated and validated using large sets of literature values (Li et al., 2011; Stadnicka et al., 2012, Breen et al., 2013, Parhizgazi & Li, 2014; Brinkmann et al., 2016), with the exception of Lien et al. (1994) who validated the model experimentally.

None of the above models were parameterized for chemicals that were actively biotransformed. Compared to other species, such as rainbow trout, members of the Cyprinidae family show a lesser extent of biotransformation and expression of metabolic enzymes (Liu et al., 2012; van den Hurk et al., 2017). This observation might be correlated to reduced response to contaminants in which biotransformation produces the toxic compound, such as polycyclic aromatic hydrocarbons (PAHs). Accordingly, tumor lesions associated with carcinogenesis from these types of contaminants are not commonly reported in fathead minnows, even when exposed to a potent carcinogen (Hawkins et al., 1988; Hawkins et al., 1991). TK models developed for rapidly biotransformed chemicals, such as B[a]P, would aid in better understanding the effect that bioaccumulation and biotransformation of such contaminants may have on fathead minnows.

Table 1.1. PBTK models developed for fathead minnow (adapted from Grech et al., 2017).

Model Type	Compartments	Chemical (s)	Reference
PBTK	Gill + Carcass + Fat + Viscera + Skin	Pentachloroethane Hexachloroethane 1,1,2,2 – Tetrachloroethane	Lien et al., 1994
PBTK	Gill + Blood + Brain + Gonad + Liver + Other	17α-ethynylestradiol 17β-trenbolone	Li et al., 2011
One-compartment	Gill + Whole-body	24 organic chemicals	Stadnicka et al., 2012
PBTK	Gill + Blood + Fat + Liver + PPT + RPT	24 organic chemicals	Stadnicka et al., 2012
PTBK	Gill + Blood + Brain + Liver + Ovary + Rest of body	Fradazole 17β-estradiol	Breen et al., 2013
PBTK	Gill + Liver + Kidney + Fat + RPT + PPT + Gill + Blood	2,3,7,8- tetracholorodibenzop- dioxin	Parhizgari & Li., 2014
PBTK	Gill + Blood + Fat + Liver + PPT + RPT	24 organic chemicals	Brinkmann et al., 2016 (adapted from Stadnicka et al., 2012)

1.3.2 White sturgeon

The white sturgeon (*Acipenser transmontanus*) is the largest freshwater fish species native to the western rivers of the United States (U.S.) and British Columbia, Canada (U.S. Fish and Wildlife Service, 1999; Fisheries and Oceans Canada, 2014). The species is a slow-growing, long-lived fish; individuals over 100 years of age have been reported (Fisheries and Oceans, 2014). It presents a unique physiology as individuals are comprised predominately of cartilage and bony plates (Fisheries and Oceans, 2014), and demonstrate a higher lipid content compared to most other fish species (Birstein, 1993). White sturgeon are bottom-dwellers and, as such, exhibit primarily benthic feeding habits. Spawning can occur multiple times throughout the lifetime of mature sturgeon (11-26 years of age) and requires a specific habitat to be successful (Fisheries and Oceans, 2014).

Unfortunately, white sturgeon are among 27 ancient fish species for which significant population declines have been reported (Birtsein 1993, Pikitch et al., 2005, McAdam, 2011). Under the Committee on the Status of Endangered Wildlife in Canada and the Species at Risk Act, white sturgeon are listed as an endangered species in the lower and upper Fraser River, upper Columbia River, and upper Kootenay River areas in Canada (COSEWIC, 2012). The observed population declines are attributed to natural recruitment failure (McAdam, 2005; McAdam, 2011) and overfishing (Semakula & Larkin, 1968). Embryo-larval survival of white sturgeon reared naturally during their first year is estimated to be only 0.000396% (Gross et al., 2002). White sturgeon have significant cultural and ecological relevance, and are thus important in terms of species protection. While efforts to conserve the species are actively ongoing, recovery of this species in Canada is currently hampered due to a lack of understanding of the definite causes for the observed recruitment failure (McAdam, 2005). Habitat degradation due to anthropogenic inputs resulting in changes to water flow and substrate quality is considered one of the primary threats to the white sturgeon population in Canada. Additionally, industrial impacts on water quality and the release of pollutants into ecosystems also pose a chronic threat to white sturgeon populations (COSEWIC, 2012; Fisheries and Oceans, 2014).

Since white sturgeon are long-lived, live with sediments, are benthic feeders, and have greater lipid content compared to many other fish species, they are at particular risk from the accumulation and subsequent toxicity of lipophilic and bioaccumulative pollutants (Birstein, 1993; Doering et al., 2014). Accordingly, elevated levels of contaminants have been reported in wild-

caught white sturgeon from northwestern U.S. and Canadian freshwater systems. In the upper Fraser River (British Columbia, CAN), concentrations of metals, polychlorinated biphenyls (PCBs), diphenyl ethers, polychlorinated dibenzo-*p*-dioxins, and chlorophenols exceeding the human consumption guidelines were recorded in red muscle, liver, and roe of the residing white sturgeon (Macdonald et al., 1997). Measurable levels of PCBs and the metabolites of organochlorine (OC) pesticides were also reported in white sturgeon from the Columbia River (British Columbia, CAN) (Fiest et al., 2005; Guncerson et al., 2008). The contaminant concentrations in the Columbia River sturgeon were negatively correlated with plasma triglycerides and androgens, gonad size, and condition factor, which was suggested to have an adverse effect on the growth and reproduction of the resident white sturgeon populations (Fiest et al., 2005). In U.S. freshwater systems (San Francisco Bay area), elevated levels of PCBs, OCs, and numerous heavy metals were detected in several white sturgeon populations (Greenfield et al., 2005; Gunderson et al., 2017). PAH contamination in vulnerable white sturgeon populations is likely also a concern given that their habitats overlap with areas of refineries, chemical manufacturers, industries that rely on fossil fuels, oil tankers, freighters, and ships within the northwestern U.S. freshwater systems (Oros et al., 2007) and PAHs have become a chemical of concern in the Fraser River area (Yunker et al., 2002).

In addition to evidence of contaminant bioaccumulation, white sturgeon have been shown to be more sensitive to some pollutants compared to other species (Bennet & Farrell, 1998; Vardy et al., 2011; Vardy et al., 2013; Doering et al., 2015). Juvenile white sturgeon are shown to be especially susceptible to contaminants such as metals (copper, cadmium, and zinc) and effluents from the forestry industry (Bennet & Farrel, 1998; Vardy et al., 2011; Vardy et al., 2013). Doering et al. (2014) also observed that due to the respective structure of the AhR in white sturgeon, the species might be more susceptible to the effects of dioxin-like compounds. It is suggested that contaminant exposure may result in early life stage mortality, genotoxicity, lowered energy reserves, reduced reproduction, and overall adversely impact white sturgeon health, influencing recovery of the population (Fiest et al., 2005; Gunderson, 2008, Doering et al., 2018).

There are currently no fully developed toxicokinetic models for white sturgeon. Since sturgeon are long-lived, reproduce intermittently, and are slow-growing in addition to being an endangered species, *in vivo* research pertaining to white sturgeon is limited and most often impractical (Birstein, 1993). Toxicokinetic models would serve as a useful tool to help further

understanding the characteristics of chemical behavior in relation to sturgeon physiology and their associated potential toxicological risks. Development of such a model would aid in providing further insights into the potential risks contaminants of concern are posing to this species and could inform targeted future studies to determine their potential contribution to the current population declines.

1.4 Benzo[*a*]pyrene

Benzo[*a*]pyrene, a five-ring polycyclic aromatic hydrocarbon (PAH), is a well-studied environmental pollutant (U.S. EPA, 2017). The compound was first identified in 1931 after years of examining the correlation between coal tar and increased incidence of skin cancer in humans and animals. B[*a*]P has been extensively studied because of its mutagenic and carcinogenic properties (Phillips, 1983). Most notably, the relationship between metabolism of B[*a*]P and the associated carcinogenicity from the covalent binding of B[*a*]P metabolites to DNA, which provided B[*a*]P's label as the 'ultimate' carcinogen (Phillips, 1983). The activation enzymes responsible for the biotransformation of B[*a*]P into toxic metabolites exist in many tissues of fishes. Additionally, many of these enzyme systems are induced by exposure to B[*a*]P (Goksøyr & Förlin, 1992). As a result of B[*a*]P's well-defined biotransformation pathways, B[*a*]P now acts as a model chemical for research evaluating and characterizing metabolic ability in a variety of tissues (Phillips, 1983).

1.4.1 Sources of B[*a*]P and environmental fate

PAHs are known to be ubiquitously distributed and persistent in the environment, having been found globally in atmospheric, terrestrial, and aquatic environments (CCME, 1999). PAHs are produced from both natural and anthropogenic sources, as a result of incomplete combustion (U.S. EPA, 2017) and as a component of petroleum and associated products (Abdel-Shafy & Mansour, 2016). Natural PAH sources include forest and prairie fires, and volcanoes (Blumer, 1976; CCME, 1999). PAH emissions from anthropogenic sources include the incomplete combustion of or leaching from, e.g., fossil fuels (U.S. EPA, 2017), vehicle emissions, power and heat generation, waste incineration, industrial emissions, and contamination from petroleum operations (CCME, 1999; Abdel-Shafy & Mansour, 2016). Runoff from coal treated asphalt vehicle lots also acts as a major contributor to PAH contamination to watersheds (U.S. EPA, 2017).

Atmospheric B[*a*]P primarily exists adsorbed to particulate matter (ATSDR, 1995). In the particulate phase, atmospheric B[*a*]P is a notably persistent PAH and can travel distances of up to 1,000 km (van Pul et al., 1998) and can be deposited and retained in sediments and water bodies (GLC, 2007). Once deposited in an aqueous system, absorption of B[*a*]P onto solid phases in aquatic environments is favored by the compounds hydrophobic nature, relatively low water solubility (3.8 µg/L ± 0.31 µg/L) (Mackay & Shiu, 1977), high lipophilicity (log K_{OW} 6.35) and relatively high molecular weight (252.31 g/mol) (CCME, 1999; IARC, 2010). It is reported that 88% of B[*a*]P in aquatic environments is adsorbed to particulate matter (Broman et al., 1991). Therefore, reported levels of water-borne B[*a*]P measured in the environment are particularly low, compared to other exposure phases such as particulate matter and sediment. Concentrations ranging from <0.0001 µg B[*a*]P/L to 0.05 µg B[*a*]P/L have been found in various water bodies globally (Andelman & Suess, 1970; Basu & Saxena, 1978; Turney et al., 1990; Nirmaier et al., 1996, Fernandes et al., 1997, Nogami et al., 2000; Zhang et al., 2012; Zheng et al., 2016; Santos et al., 2018). The high lipophilicity of B[*a*]P, however, results in its potential for accumulation in aquatic organisms (Eadie et al., 1982; Abdel-Shafy & Mansour, 2016, U.S. EPA, 2017). Many of these aquatic organisms can rapidly metabolize and eliminate B[*a*]P. Still, some organisms, such as plankton, most invertebrates, and a few fish species, have reduced ability to metabolize B[*a*]P, and therefore, are subject to a higher degree of bioconcentration (U.S. EPA, 2017).

1.4.2 Biotransformation pathways of benzo[*a*]pyrene by biological systems

Most vertebrate organisms readily metabolize (i.e., biotransform) B[*a*]P (U.S. EPA, 2017). There are various biotransformation pathways of B[*a*]P, all of which include two stages of biotransformation, phase I and phase II. Phase I is catalyzed by mixed-function oxygenases (MFOs), which are responsible for the conversion of the parent B[*a*]P molecule into oxidated metabolites (Gelboin, 1980). In humans and many animals, including fish, MFOs are cytochrome P450 (CYP) enzymes, the most notable CYP in terms of B[*a*]P biotransformation being CYP1A (Gelboin, 1980; Stegeman & Lech, 1991). Phase II reactions are catalyzed by conjugating enzymes that are responsible for converting the oxidative metabolites produced by phase I biotransformation into hydrophilic excretable compounds (Gelboin, 1980). Each biotransformation pathway of B[*a*]P results in a unique metabolite. Most often, these metabolites are detoxified products, such as in the glucuronide pathway in which the metabolite, 3-hydroxy-

B[*a*]P (OH-B[*a*]P) is produced by the phase I enzymes CYP1A and CYP1B (Kim et al., 1998). OH-B[*a*]P is further converted into 3-hydroxy-B[*a*]P-glucuronide (Gluc-B[*a*]P) by the phase II enzyme, uridine diphosphate glucuronosyltransferase (UDPGT) and excreted (Gelboin, 1980). While this pathway may not be the most relevant from a toxicological perspective, metabolites generated are stable, and therefore, a useful biomarker of exposure. Other pathways, however, result in the production of biologically active products, such as in the epoxide pathway. The epoxide pathway results in several metabolites, the one of greatest concern being 7,8-diol-9,10-epoxide, known as B[*a*]P-diol epoxide (BPDE). This compound is known to be a highly reactive DNA-binding metabolite of B[*a*]P, forming DNA adducts (Gelboin, 1980). The metabolite covalently binds to the guanine residue of DNA or ribonucleic acid (RNA). Occasionally, the metabolite has also been shown to bind to an adenine or cytosine residue (Gelboin, 1980). These adducts pose an increased risk of corresponding mutagenic effects. However, once DNA-bound, the B[*a*]P-DNA adducts have been reported to be excised by the nucleotide excision repair process, eliminating the DNA defect, and therefore decreasing the risk of mutagenic effects (Feldman et al., 1978). Alternatively, if an adduct does not occur, the epoxides undergo phase II biotransformation *via* GST (glutathione-*S*-transferase), resulting in water-soluble glutathione conjugates that can be excreted (Gelboin, 1980).
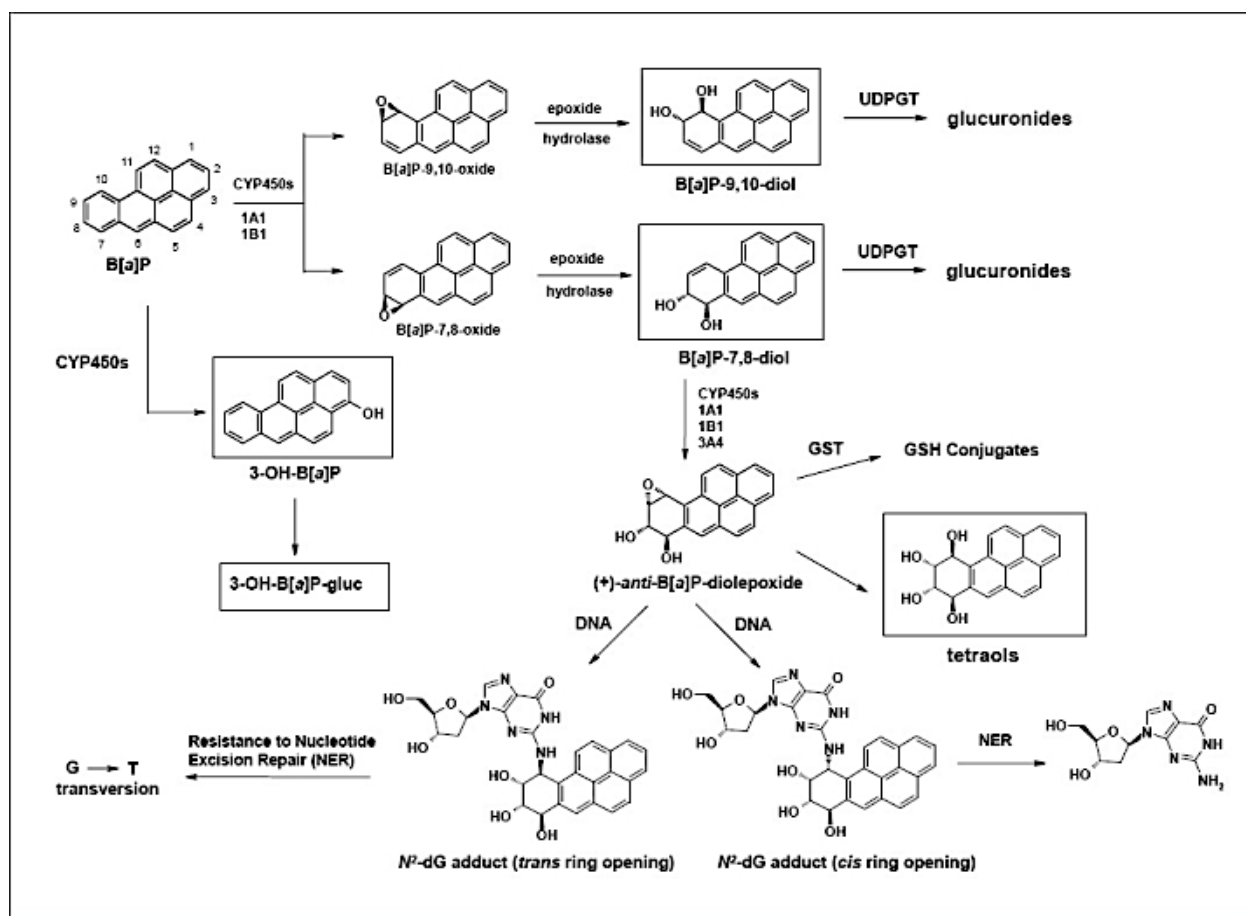
Figure 1.3. A schematic representation of the biotransformation pathways of B[*a*]P that shows the enzymes involved in phase I and phase II biotransformation and the resulting products (Figure from Trushin et al., 2012).

1.4.4 Biological effects of benzo[*a*]pyrene

B[*a*]P elicits several effects on biological systems. Among them are effects at the molecular level, such as activation of the aryl hydrocarbon receptor (AhR), formation of genotoxic metabolites and oxidative stress signalling, which result in effects at higher levels of biological organization, such as embryotoxicity (Hose et al., 1982), immunosuppression (Carlson, Li & Zelikoff, 2002; Carlson, Li & Zelikoff, 2004), pericardial and yolk-sac edema (Cook et al., 2003, Chikae et al., 2004), cardiotoxicity (Corrales et al., 2014; Gerger & Weber, 2015), carcinogenesis (Hawkins et al., 1988), decreased reproduction (Hoffman & Oris, 2006; Corrales et al., 2014; Booc et al., 2014; Gao et al., 2018) and reduced survival and growth (Gravato et al., 2009; Corrales et al., 2014; Gao et al., 2018). The biological effects in fish associated with exposure to B[*a*]P have been extensively studied, primarily through intraperitoneal (IP) injection or dietary studies, and to a lesser extent by water-borne exposure. However, the effects are analogous among exposure routes.

B[*a*]P is a known ligand of the AhR (Miller & Ramos, 2001). The AhR is a ligand-activated transcription factor involved in the regulation of many cellular responses (Nguyen et al., 2013). When a ligand binds to the AhR, the complex is translocated into the nucleus, which interacts with the aryl hydrocarbon nuclear translocator (ARNT), forming an AhR-ARNT complex (Miller & Ramos, 2001). This complex then binds to DNA, modifying the expression of target genes located within the gene battery associated with the metabolism of xenobiotics (Nebert et al., 2000). Accordingly, the most common effect observed at the molecular level, as a result of aqueous B[*a*]P exposure, is a significant increase in the abundance of transcripts of the *cyp1A* gene in the liver, gill, and intestine (Levine et al., 1997; Levine & Oris, 1999; Roy et al., 2002; Costa et al., 2012; Corrales et al., 2014, Lee et al., 2014, Gerger & Weber, 2015; Lee, Yoon & Lee, 2015). Other signal transduction pathways associated with AhR ligand binding also exist, which involve calcium homeostasis (DiGiovanni et al., 1989; Reynaud & Deschaux, 2006), epidermal growth factor (EGF) (Guyda et al., 1990; Haarman-Stemmann, Bothe & Abel, 2009), hypoxia-inducible factor (HIF) (Yu et al., 2008), mitogen-activated protein kinases (MAPKs) (Tan et al., 2002; Puga & Marlowe, 2009), and protein kinase C (PKC)-mediated phosphorylation (Ou et al., 1994; Reynaud & Deschaux, 2006), in addition to being involved in the regulation of cell proliferation and differentiation (Puga, Xia & Elferink, 2002; Marlowe & Puga, 2005), and regulating inflammatory responses of macrophages and T-cells (Nguyen et al., 2013).

The induction of the genes located in the gene battery induces the expression of the CYP1A and CYP1B proteins responsible for metabolizing parent B[a]P into its toxic metabolite BPDE. As such, induction of the CYP1A protein (Levine & Oris, 1999; Smolowitz, Schultz & Stegeman, 1992; Van Veld et al., 1997; Jönsson et al., 2006; Costa et al., 2013; Lee et al., 2014) and ethoxyresorufin-O-deethylase (EROD) activity, a biomarker of CYP1A activity, in the liver and gill (Levine, Oris &Wissing, 1994; Sandvik et al., 1997; Peters et al., 1997; Levine & Oris, 1997; Levine & Oris, 1999; Sandvik et al., 1998, Mdgela et al., 2006; Jönnson et al., 2006; Oritz-Delgado et al., 2007; Yun et al., 2008; Costa et al., 2011; Rey-Salgueiro et al., 2011) are common effects reported in fish aqueously exposed to B[a]P. Consequently, BPDE can bind to DNA forming DNA adducts and result in genotoxic and carcinogenic effects such as neoplasm of the tissues, carcinoma, and adenoma (Hawkins et al., 1988; Hawkins et al., 1990, Stegemen & Lech, 1991; Peters et al., 1997; Baumann, 1988, Jönsson et al., 2004, Wessel et al., 2010; Corrales et al., 2014; Lerebours et al., 2014). Induction of CYP1A through the induction of AhR related responses has also been linked to immunosuppression (Carlson & Zelikoff, 2002; Carlson & Zelikoff, 2004; Reynaud & Dachaux, 2006).

Lastly, B[a]P is known to cause oxidative stress. Metabolism of B[a]P into quinones, such as B[a]P-7,8-dione (BPQ), results in the production of reactive oxygen species (ROS) (Penning et al., 1996). ROS is generated when parent B[a]P undergoes the biotransformation pathway, generating a quinone metabolite. During each metabolic step of the pathway, ROS are released. Redox cycling may also occur throughout the pathway resulting in ROS that can be generated multiple times (Penning et al., 1996). The ROS can damage macromolecules (i.e., DNA, lipids, and proteins). Damage of DNA as a result of ROS is thought to correspond with B[a]P induced carcinogenesis (Peters et al., 1996; Kim & Lee, 1997; Kim & Lee, 2000).
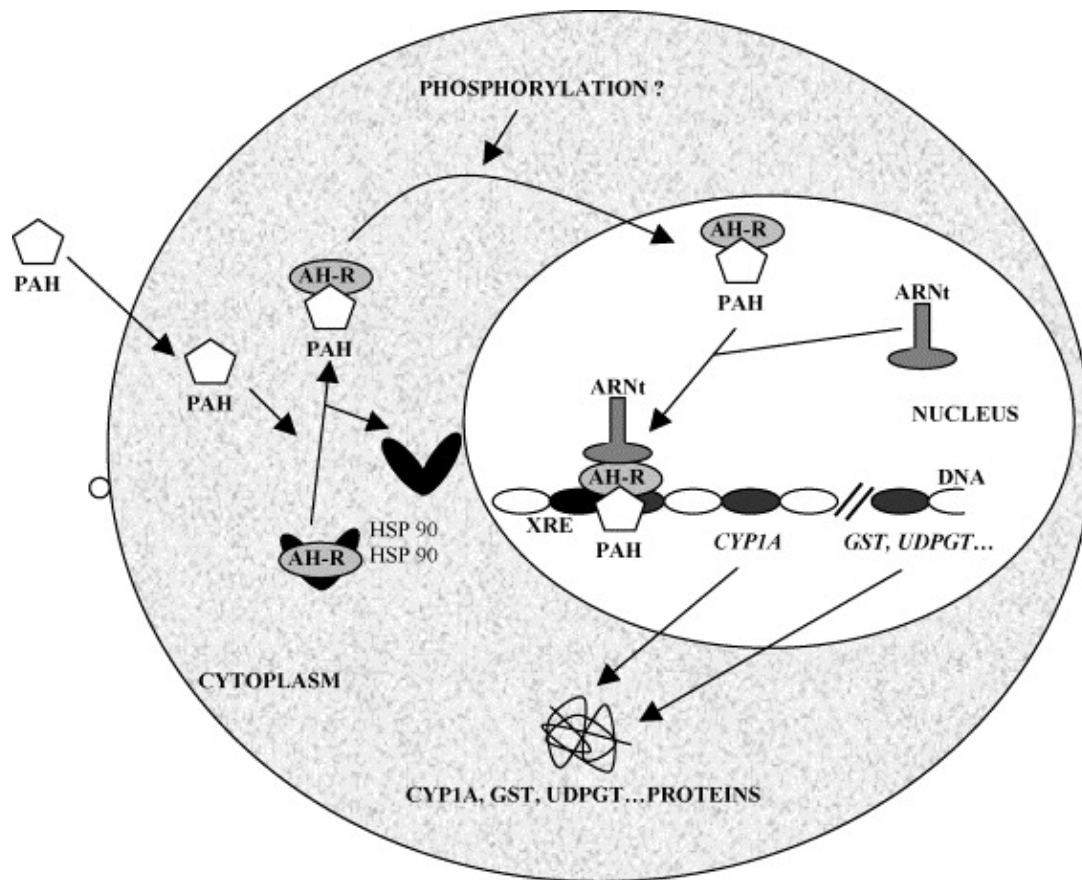
Figure 1.4. A representation of a PAH binding to the AhR inducing transcription of genes located in the gene battery and sequentially inducing the up-regulation of metabolizing proteins (Figure from Reynaud and Deschaux, 2006).
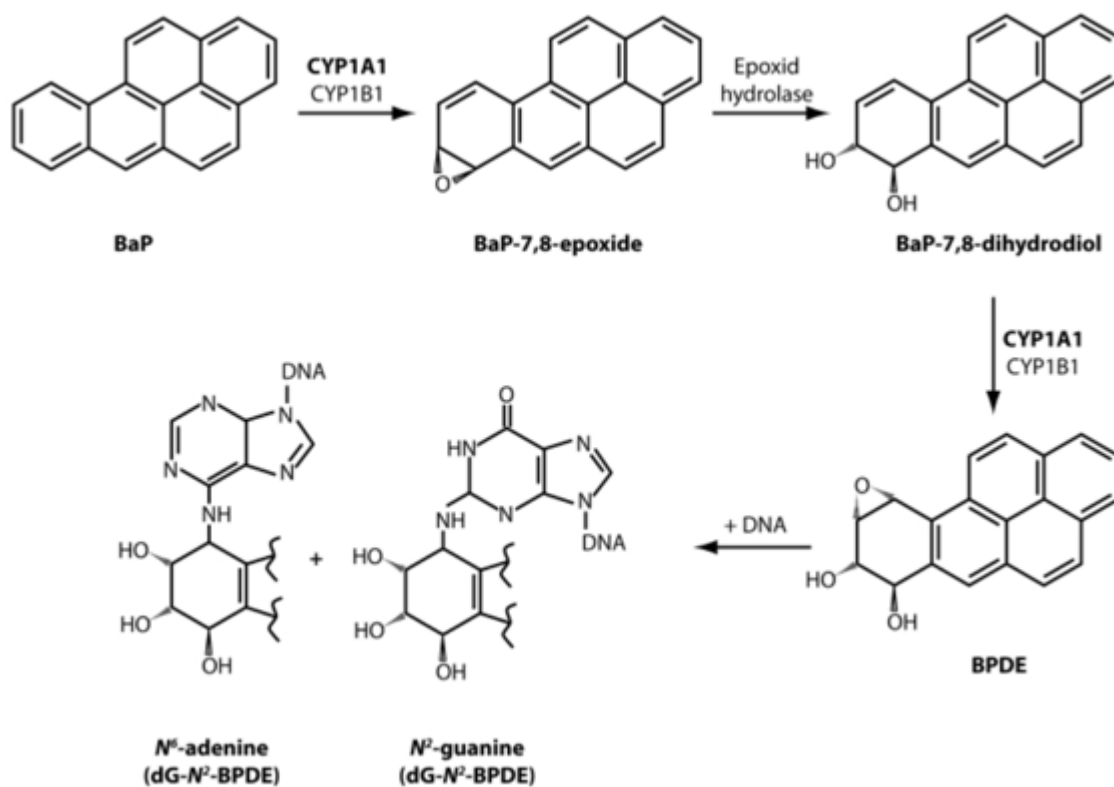
Figure 1.5. An isolated representation of the metabolic pathway of B[*a*]P that results in the genotoxic metabolite BPDE (Figure from Moserová, et al., 2009).

1.4.5 Toxicokinetic models using benzo[*a*]pyrene

The toxicological effects of B[*a*]P in fishes have been extensively studied to date, but exposure modelling of the chemical *via* TK models has been limited, especially in the context of waterborne exposure scenarios. While TK models for exposure to B[*a*]P currently exist for rats and mice (Crowell et al., 2011; Heredia Oritz et al., 2011), there are no models developed for fish. A limitation to parameterizing an aquatic TK model with B[*a*]P is that no information exists regarding *in vivo* biotransformation rates of B[*a*]P in fishes. Therefore, to date, *in vitro-in vivo* extrapolation techniques have been used as measurements of intrinsic clearance, followed by the well-stirred model to calculate hepatic clearance (Nichols et al., 2006). However, these studies were limited to a few species (i.e., rainbow trout) for which results from the relevant *in vitro* systems were available. More research is required to accurately model the kinetics of B[*a*]P for a greater number of aquatic species (Health Canada, 2015).

1.5 Rationale

TK models are an emerging scientific tool to be used in research and ERA. The applicability of most current TK models, however, is limited to neutral organic chemicals. They also do not often consider chemicals that are actively biotransformed. The toxicity of environmental contaminants such as PAHs is often driven by their biotransformation into toxic metabolites. Therefore, assessing the extent and accumulation of metabolites produced by a species would provide a better understanding of the potential adverse effects that may occur as a result of exposure. Additionally, most TK models focus on the adult life stage, with few developed for the early-life stages (ELS) of fishes. ELS are often considered more sensitive and show different metabolic capacity compared to the adult life stage, and thus, life-stage specific TK models are essential to assess and determine these differences in bioaccumulation accurately. This research project developed life stage-specific TK models for the rapidly biotransformed model chemical B[*a*]P two physiologically different species of fish, the fathead minnow and the white sturgeon. The fathead minnow is a small, commonly used research species with ecological relevance, while the white sturgeon is a large, cold-water species, with ecological and cultural relevance and limited available information. The TK models described in the following thesis expand the applicability of TK models that can be used for screening and prioritization of emerging contaminants in aquatic ecosystems for further research and *in vivo* testing.

1.5.1 Research objectives and hypotheses

The overall objective of this thesis research was to develop life-stage specific TK models in two fish species, i.e., fathead minnow and white sturgeon, that integrated the biotransformation of readily metabolized compounds. This thesis focused on characterizing the life-stage specific biotransformation on the rapidly biotransformed model chemical B[*a*]P. The information was subsequently used to conduct *in vitro-in vivo* and cross-life stage extrapolations of the biotransformation of B[*a*]P to parameterize and validate the performance of the corresponding TK models.

The chapter-specific objectives and hypotheses were as follows:

Chapter 2:

To parameterize and optimize life-stage specific TK models for B[*a*]P in the fathead minnow using life-stage specific measurements of B[*a*]P biotransformation

Sub-objectives:

1. To characterize the capacity of the embryo-larval and adult life stages of fathead minnows to biotransform B[*a*]P using *in vitro* assays

   H_{01}: No statistically significant difference in biotransformation capacity will be observed in the embryo-larval life stage of fathead minnows as a function of exposure to increasing concentrations of B[a]P

   H_{02}: No statistically significant difference in biotransformation capacity will be observed in the adult life stage of fathead minnows as a function of exposure to increasing concentrations of B[a]P

2. To parameterize *in silico* life-stage specific TK models that describe the kinetics of B[*a*]P in the embryo-larval and adult life stages of fathead minnow

3. To use *in silico* life-stage specific TK models to predict the internal abundance of B[*a*]P metabolites in the embryo-larval and adult life stages of fathead minnow

   - Can *in silico* life-stage specific TK models be used to predict the internal abundance of B[*a*]P metabolites in the embryo-larval and adult life stages of fathead minnow?

- Can measured abundances of B[*a*]P metabolites in the whole-body embryo-larval life stage or bile of adult life stage fathead minnows be used to validate TK model predictions?

  H03: In silico TK models cannot be used to accurately predict the internal abundance of B[a]P metabolites in the embryo-larval whole-body or bile of adult fathead minnows

Chapter 3:

To parameterize and optimize life-stage specific TK models for organic contaminants in the white sturgeon using life-stage specific measurements of B[*a*]P biotransformation and experimental and an experimental dataset of aqueous organic contaminant exposures in sub-adult white sturgeon from the literature

Sub-objectives:

4. To characterize the capacity of the embryo-larval life stage of white sturgeon to biotransform B[*a*]P using *in vitro* assays

   H04: No statistically significant difference in biotransformation capacity will be observed in the embryo-larval life stage of white sturgeon as a function of exposure to increasing concentrations of B[a]P

5. To parameterize *in silico* life-stage specific TK models that describe the kinetics of B[*a*]P in the embryo-larval life stage and organic contaminants in the sub-adult life stage of white sturgeon

6. To use *in silico* life-stage specific TK models to predict the internal abundance of B[*a*]P metabolites in the embryo-larval life stage and the tissue-specific internal concentrations of organic contaminants in the sub-adult life stages of white sturgeon

   - Can *in silico* life-stage specific TK models be used to predict the internal abundance of B[*a*]P metabolites in the embryo-larval life stage and the tissue-specific internal concentrations of organic contaminants in the sub-adult life stages of white sturgeon?

- Can measured abundances of B[*a*]P metabolites in the embryo-larval life stage and a literature derived experimental dataset of internal organic contaminant concentrations in the adult life stage of white sturgeon be used to validate TK model predictions?

H05: In silico TK models cannot be used to accurately predict the internal abundance of B[a]P metabolites in the whole-body of embryo-larval white sturgeon and the internal concentrations of organic contaminants in the specific tissues of sub-adult white sturgeon

CHAPTER 2: *IN VITRO-IN VIVO* AND CROSS-LIFE STAGE EXTRAPOLATION OF UPTAKE AND BIOTRANSFORMATION OF BENZO[*A*]PYRENE IN THE FATHEAD MINNOW (*PIMEPHALES PROMELAS*)

PREFACE

The main objective of Chapter 2 was to integrate biotransformation of B[*a*]P into life-stage specific *in silico* TK models for fathead minnow. This objective was met by characterizing biotransformation of B[*a*]P and measuring the abundances of B[*a*]P metabolites in the embryo-larval and adult life stages of fathead minnow aqueously exposed to graded concentrations of B[*a*]P. The data generated from these exposures were used to parameterize an embryo-larval one-compartment model and a multi-compartment adult model. Chapter 2 was prepared in manuscript style and was published in the peer-reviewed scientific journal *Aquatic Toxicology*:

Grimard, C., Mangold-Döring, A., Schmitz, M., Alharbi, H., Jones, P. D., Giesy, J. P., Hecker, M. & Brinkmann, M. (2020). *In vitro-in vivo* and cross-life stage extrapolation of uptake and biotransformation of benzo [a] pyrene in the fathead minnow (*Pimephales promelas*). *Aquatic Toxicology*, *228*, 105616.

Author contributions:

Chelsea Grimard (University of Saskatchewan) helped design and performed embryo-larval and adult exposures, organized and helped with tissue sampling, generated and analyzed data, prepared figures and tables, and drafted the manuscript.

Annika Mangold-Döring (Wageningen University) helped with design, coding, and implementation of toxicokinetic models into Jupyter Notebook, as well as provided comments and edits on the manuscript.

Markus Schmitz (Goethe University Frankfurt) helped with set up and maintenance of adult exposure, helped with adult tissue sampling, and generated EROD and GST data from embryo-larval and adult tissue samples, as well as provided comments and edits on the manuscript.

2.1 Abstract

Understanding internal dose metrics is integral to adequately assess the effects that environmental contaminants might have on aquatic wildlife, including fish. *In silico* toxicokinetic (TK) models are a leading approach for quantifying internal exposure metrics for fishes; however, they often do not adequately consider chemicals that are actively biotransformed and have not been validated against early-life stages (ELS) that are often considered the most sensitive to the exposure to contaminants. To address these uncertainties, TK models were parameterized for the rapidly biotransformed chemical benzo[*a*]pyrene (B[*a*]P) in embryo-larval and adult life stages of fathead minnows. Biotransformation of B[*a*]P was determined through measurements of *in vitro* clearance. Using *in vitro-in vivo* extrapolation, *in vitro* clearance was integrated into a multi-compartment TK model for adult fish and a one-compartment model for ELS. Model predictions were validated using measurements of B[*a*]P metabolites from *in vivo* flow-through exposures to graded concentrations of water-borne B[*a*]P. Significantly greater amounts of B[*a*]P metabolites were observed with exposure to greater concentrations of parent compound in both life stages. However, when assessing biotransformation capacity, no differences in phase I or phase II biotransformation were observed with greater exposures to B[*a*]P. Results of modelling suggested that biotransformation of B[*a*]P can be successfully implemented into *in silico* models to accurately predict life stage-specific abundances of B[*a*]P metabolites in either whole-body larvae or the bile of adult fish. Models developed increase the scope of applications in which TK models can be used to support ecological risk assessments.
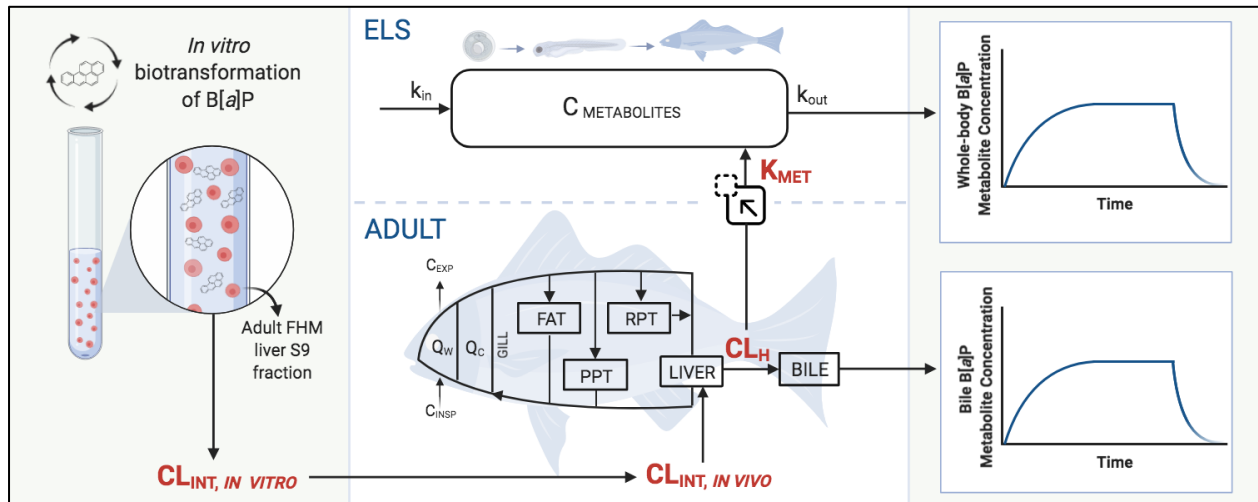
Figure 2.1. Graphical representation of the methodology in regard to the content encompassed in Chapter 2; $CL_{int,\ in\ vitro}$ = *in vitro* intrinsic clearance; $CL_{int,\ in\ vivo}$ = *in vivo* intrinsic clearance; CL_H = hepatic clearance; K_{MET} = whole-body metabolism rate. Graphic created with BioRender.com.

2.2 Introduction

Assessments of bioaccumulation are regularly used by toxicologists and environmental professionals to determine risks that water-borne contaminants could pose to aquatic life. While accumulation of a particular chemical might not be an immediate cause for concern, this information is critical for relating the amount of chemical in the exposure medium to that which needs to reach the toxic site of action to elicit adverse responses. Toxicokinetic (TK) *in silico* models allow predicting and quantifying bioaccumulation of chemicals (Nichols et al., 1990; Arnot & Gobas, 2004; Stadnicka et al., 2012; Brinkmann et al., 2016). While traditional TK models are accurate for persistent, neutral, organic chemicals, they do not usually account for biotransformation, which is an essential consideration when determining accumulation of some chemicals as it reduces the overall internal doses of parent materials in bodies of aquatic organisms (McElroy et al., 2011; Carrasco-Naavarro et al., 2015; Strobel et al., 2015). The degree of biotransformation is dependent on several biochemical and physiological parameters and, as a result, will naturally differ among life stages and species of fishes.

In vitro techniques have been the predominant methods used for assessing qualitative and quantitative differences in biotransformation of environmental contaminants by characterizing phase I and phase II biotransformation capacity in biological systems (Schlenk et al., 2008; Strobel et al., 2015; Franco & Lavado, 2019). Some of these *in vitro* systems make use of isolated sub-cellular fractions of liver, including microsomes or the post-mitochondrial supernatant fraction (S9), to measure the specificity of substrates and activities relating to a specific phase I or II enzymes under conditions of enzyme saturation (Han et al., 2009; Lee et al., 2014b; Lo et al., 2015). These subcellular fractions can also be used to determine rates of biotransformation under first-order conditions, in relation to a specific substrate (Nichols et al., 2007; Lo et al., 2015; Fay et al., 2017). From these rate constants, *in vitro* intrinsic clearance, which is defined as the volume of blood cleared entirely of a chemical per unit time, can be determined. Recently, the Organisation for Economic Co-operation and Development (OECD) adopted a method for measuring intrinsic clearance using *in vitro* metabolizing systems (OECD 319B; OECD, 2018), which is based on the approach described by Nichols et al. (2006). In combination with *in vivo-in vitro* extrapolation (IVIVE) methods described by Nichols et al. (2013b), the existing *in silico* modeling approaches for bioaccumulation of chemicals in fish could be significantly improved in this way and provide a means of obtaining estimates of hepatic clearance specific to species and chemicals of interest.

Most TK models have been established for adult fishes, while few exist that focus explicitly on early life-stages (ELS) (Foekema et al., 2012). ELS are often considered more sensitive to effects of exposure to some contaminants than their adult counterparts, and are increasingly being used in alternative testing approaches (Embry et al., 2010; Sloman et al., 2010; EFSA, 2015). Understanding life stage-specific TK properties affecting accumulation of chemicals will be critical to determining and understanding the differences in life stage-specific sensitivity to contaminants. This is particularly relevant for rapidly biotransformed chemicals since biotransformation can act to either detoxify and/or activate a compound. Because ELS fish have been shown to have reduced biotransformation capacity (Knöbel et al., 2012) and use a different proportion of biotransformation pathways (Le Fol et al., 2017) compared to adults, these differences might be of benefit or detriment to the organism. The potential for different outcomes between life stages as a result of differences in chemical biotransformation emphasizes the importance of understanding life stage-specific bioactivation processes. However, even though ELS are shown to be capable of biotransformation at the onset of gastrulation (Otte et al., 2010), due to their small size, obtaining estimates of hepatic clearance directly from the livers of ELS fish is not possible. To address this shortcoming, this study used allometric scaling to obtain estimates of whole-body biotransformation (k_{met}) from measurements of adult hepatic clearance that can be integrated into corresponding TK models.

This study focused on the model chemical, benzo[*a*]pyrene (B[*a*]P), a polycyclic aromatic hydrocarbon (PAH), and a ubiquitous environmental pollutant (U.S. EPA, 2017). B[*a*]P is a known ligand of the aryl hydrocarbon receptor (AhR), and exposure of fish to B[*a*]P has been shown to result in a multitude of effects. B[*a*]P is biotransformed by the enzyme cytochrome P450 1A (CYP1A). CYP1A most often catalyzes detoxification of the parent compound; however, it can also, by reacting with the primary metabolite, generate the highly reactive genotoxic metabolite B[*a*]P-7,8-diol-9,10-epoxide (BPDE), which can form adducts with DNA and ultimately, result in carcinogenesis (Gelboin, 1980; Hawkins et al., 1990; Stegeman & Lech, 1991; Wang et al., 2010; Yuan et al., 2017). Due to its well-defined biotransformation pathways, B[*a*]P acts as an optimal model compound for evaluation of IVIVE and integration of biotransformation into *in silico* modeling approaches. While a few TK models for B[*a*]P exist for mammals (Crowell et al., 2011; Heredia-Ortiz et al., 2011), the compound has yet to be integrated into an *in silico* TK model for fish.

To add to the existing database of TK models, the one-compartment bioaccumulation model from Arnot and Gobas (2004) and the multi-compartment physiologically based TK (PBTK) model described by Stadnicka et al. (2012) were adapted to predict accumulation of parent B[*a*]P and production of associated metabolites in embryo-larval and adult life stages of fathead minnows (*Pimephales promelas*), respectively. While *in vitro* clearance of B[*a*]P has been measured in several fishes as listed in the Fish *In vitro* Biotransformation Database of the European Union Reference Laboratory for Alternatives to Animal Testing (EURL ECVAM) (European Commission, 2018), no values have been reported for fathead minnows. Fathead minnows are one of the most commonly used model species to characterize toxicities of chemicals to both embryo-larval and adult life stages, in addition to having ecological importance (Ankley & Villeneuve, 2006). As such, it is an important target species for development of TK models.

Specific objectives of the present study were to: (a) characterize and compare the *in vitro* transformation kinetics of B[*a*]P at early and adult life stages of the fathead minnow, (b) measure the life stage-dependent relative abundances of B[*a*]P metabolites, (c) apply TK models to extrapolate biotransformation from *in vitro* to *in vivo,* and (d) validate model predictions using data from *in vivo* flow-through exposures to graded concentrations of water-borne B[*a*]P.

2.3 Materials and methods

2.3.1 Test organisms

Adult fathead minnows were obtained from an in-house culture originally established from a commercial supplier (Aquatic Research Organisms Inc., Hampton, USA). Fathead minnow embryos were obtained from the same in-house fathead minnow breeding colony. Fish populations were maintained at the Aquatic Toxicology Research Facility (ATRF) at the University of Saskatchewan (Saskatoon, SK, CAN). Husbandry and maintenance details are described in Appendix A.1. All fish culture protocols and experimental procedures for both embryo-larval and adult exposures were approved by the Animal Research Ethics Board at the University of Saskatchewan (Protocols #20180052 and #20160090).

2.3.2 Waterborne B[*a*]P exposures

Waterborne chronic exposures to B[*a*]P were conducted to evaluate uptake by and biotransformation of B[*a*]P in the embryo-larval and adult life stages of fathead minnows. Nominal

concentrations for both exposures were 1.3, 4.0 or 12.0 µg B[*a*]P/L (benzo[*a*]pyrene, Sigma-Aldrich, Oakville, ON, CAN) using 0.02% DMSO ($\geq$ 99.9% dimethyl sulfoxide, Fisher Scientific Co., Ottawa, ON, CAN) as the carrier solvent, or 0.02% DMSO only as the solvent control. The embryo-larval exposure also included de-chlorinated ATRF water as the water control. Due to space limitations and size of the exposure experiment, a water control was not included in the adult fathead minnow experiment. The exposure concentrations were chosen to represent both an environmentally relevant exposure concentration below the water solubility threshold (i.e. 3.8 µg B[a]P/L) (Miller et al., 1985), as well as concentrations above water solubility that would induce a response (i.e., changes enzyme activity, gene expression, morphometrics, behavior, and survival) (Gravato et al., 2009; Costa et al., 2013; Lee et al., 2014a, Booc et al., 2014). In the first experiment, fathead minnow embryos (<10 hours post-fertilization) were exposed for 32 days. Whole-body samples were taken after three, seven, 14 and 32 days of exposure. In the second experiment, adult fathead minnow breeding groups consisting of two males and three females were exposed for 21 days. Whole liver and gall bladder (bile) samples were taken after four, seven, 14 and 21 days of exposure. Sampling points were chosen to characterize the uptake of B[*a*]P, and in the case of the embryo-larval exposure, sampling points also characterized important developmental stages, i.e., the egg, 0-3 days post fertilization (dpf), the yolk-sac, 3-7 dpf, and the free-feeding stage, 7-32 dpf. In both experiments, respective samples were also taken after a seven-day depuration period to characterize the elimination of B[*a*]P. Exposure details are provided in Appendix B.1.

2.3.3 Sample collection

Whole-body larvae were sampled on days three, seven, 14 and 32 of exposure, as well as after the depuration period. The sampling times were chosen to represent the critical development stages of the embryo-larval fathead minnow (i.e., zero to three days = egg stage; three to seven days = yolk-sac stage; seven to 32 days = free-feeding stage). Larval samples were taken on days three (20 larvae; *n*=2 per treatment/endpoint) and seven (10 larvae; *n*=2 per treatment/endpoint), and were pooled to increase tissue mass for biochemical assays. Samples on day 14 were taken in pooled groups of two individuals for biochemical (*n*=3 per treatment), chemical (*n*=2 per treatment) and lipid analysis (*n*=2 per treatment). On day 32 and after the depuration period, larvae were sampled in pooled groups of five or three larvae, respectively, for biochemical (*n*=5 per treatment),

chemical (*n*=5 per treatment) and lipid analysis (*n*=5 per treatment). At each sampling point, wet mass was recorded. Samples were immediately flash-frozen in liquid nitrogen and stored at -80 °C until further analysis.

Adult fish were euthanized by blunt force on day four (*n*=5 per treatment), seven (*n*=2 per treatment), 14 (*n*=2 per treatment), and 21 (*n*=5 per treatment) of exposure, as well as after the depuration period (*n*=2 per treatment). Exposure length was based on OECD 229: Fish Short-Term Reproduction Assay (OECD, 2012), and sampling times were chosen to characterize the uptake of B[*a*]P over time. The wet mass was recorded for each fish. Liver samples were taken for biochemical analysis and gall bladder (bile) for chemical analysis of B[*a*]P metabolites. Samples were immediately flash-frozen in liquid nitrogen and stored at -80 °C until analysis.

2.3.4 Analytical analysis of waterborne B[*a*]P and B[*a*]P metabolites

Samples of aqueous B[*a*]P were collected on day one, 15, and 30 of the embryo larval exposure, and on days two, 11 and 20 of the adult exposure. Sample times were chosen to assess aqueous B[a]P concentrations at the start, middle and end of exposures. Water samples (1 L) were sent to SGSS AXYS Analytical Services Ltd. (Sydney, BC, CAN) for quantification of B[*a*]P (SGS AXYS method MLA-021) using gas chromatography-mass spectrometry (GC-MS) following C18 solid-phase extraction (SPE). B[*a*]P d-12 was used as an internal standard with a recovery of 39-81%. Matrix spike samples exhibited recoveries of 101-102%. Lab blanks did not test positive for B[*a*]P.

The protein precipitation method described by Nacalai Tesque, Inc. (2017) was used to quantify metabolites of B[*a*]P. Whole-body embryos were homogenized in HPLC grade acetonitrile (ACN, Fisher Scientific Co., Ottawa, ON, CAN) for 20 seconds at a ratio of 1:10 (m/v), while gall bladder (bile) samples were homogenized in ACN for 20 seconds at a ratio of 1:100 (m/v). Samples were incubated on ice for 15 minutes and then centrifuged at 1,700×g for 15 minutes. The supernatant was subsequently sampled for quantification of metabolites.

The major metabolites 3-hydroxy-benzo[*a*]pyrene (OH-B[*a*]P) and 3-hydroxy-benzo[*a*]pyrene *O*-glucuronide (gluc-B[*a*]P) were quantified using ultra-high-performance liquid chromatography high-resolution mass spectrometry (UPLC-HRMS) by use of a modified method described by Beach et al. (2000), Zhu et al. (2008), Lu et al., (2011), and Tang et al. (2016). Metabolite analysis was conducted using a Vanquish UHPLC and Q-Exactive™ HF Quadrupole-

Orbitrap[TM] mass spectrometer (Thermo-Fisher, Waltham, MA, USA). Samples were ionized in negative mode heated electrospray ionization (HESI) followed by a full MS/parallel reaction monitoring (PRM) method. Concentrations of OH-B[a]P were quantified directly using analytical standards and external calibration. To quantify gluc-B[a]P, a semi-quantitative method was used in which peak areas of from the OH-B[a]P standard curve were converted to gluc-B[a]P peak areas using response factors. The detailed method is described in Appendix C.

Final concentrations of B[a]P metabolites, reported as ng/mg whole body larvae or bile, were calculated from the volume of solvent used for extraction and specific bile mass. B[a]P equivalents, i.e., mass concentrations that are independent of differences in molecular mass of the parent compound and the two metabolites, were calculated from the obtained metabolite concentrations for use in subsequent analyses and to match model output units.

2.3.5 Measurement of intrinsic clearance

Intrinsic clearance ($n=2$) in fathead minnow liver tissue was measured using an adaptation of OECD 319B: Determination of *in vitro* clearance using rainbow trout liver S9 sub-cellular fraction (RT-S9) (OECD, 2018). Pooled liver tissue was homogenized in 5 µL homogenization buffer per mg tissue and centrifuged at 9,000 × g for 20 minutes. The supernatant (S9) was sampled for use in the *in vitro* clearance assay. Assay details are described in Appendix D. Depletion of parent B[a]P from the S9 was measured at 0, 20, 40, 60, 80, 100 and 120 minutes by use of synchronous fluorescence spectrophotometry in a quartz cuvette (Lumina, Thermo Fisher Scientific, Ottawa, ON, CAN). Parent B[a]P fluoresces between 400-440 nm and the B[a]P metabolites between 420-480 nm, measured and validated using neat B[a]P and OH-B[a]P standards. Concentrations of B[a]P at each time point were determined from a standard curve and concentrations were plotted as a function of time. The depletion curve was *log*-transformed, and the first-order depletion rate constant (k) was determined by multiplying the slope of the line by -2.3. Intrinsic clearance (Cl$_{int, in vitro}$) was calculated (Eq. 1):

$$Cl_{int,in\ vitro}(mL\ h^{-1}mg^{-1}) = \frac{k(h^{-1}) \cdot volume\ of\ the\ reaction\ (mL)}{reaction\ protein\ concentration\ (mg\ L^{-1})} \qquad (1)$$

2.3.6 Biochemical analysis

EROD (7-ethoxyresorufin *O*-deethylase) and GST (glutathione-*S*-transferase) activities were measured to characterize phase I and II biotransformation as described by Kennedy and Jones (1994) and Habig et al. (1974), respectively, with modifications. For both assays, the post-mitochondrial supernatant fraction was generated from whole-body larval and adult liver samples following a modified OECD 319B protocol (OECD, 2018). Tissue was homogenized in homogenization buffer at a ratio of 20 µL buffer: 1 mg tissue then centrifuged at 10,000 × g. The supernatant was subsequently taken for use in biochemical assays. EROD activity (pmol/mg protein/min; *n*=5) was measured through fluorescent measurements of resorufin (570 nm excitation/ 630 nm emission) and protein (365 nm excitation/ 480 nm emission). GST activity (nmol/mg/min; *n*=5) was measured through a kinetic measurement of CDNB (1-Chloro-2,4-dinitrobenzene; 340nm emission). Assays are described in detail in Appendix E and F.

2.3.7 Lipid analysis

Total whole-body lipid content in both life stages was quantified using a modification of the microcolorimetric sulfophosphovanillin (SPV) method described by Lu et al. (2008). Lipids (*n*=5) were extracted using whole-body fish (embryo-larval, 10-50 mg wet mass; adult, 10-50 mg homogenized sub-sample). Lipid extracts were quantified by the addition of sulphuric acid and SPV reagent. Lipid content (mg) was determined through measurements of absorbance and lipid percent was subsequently calculated. Additional assay details are provided in Appendix G.

2.3.8 Estimation of embryo-larval cardiac output

Cardiac output was estimated for fathead minnow larvae to use in *in vitro-in vivo* scaling calculations of whole-body biotransformation rates using an Excel spreadsheet provided by Nichols et al. (2013b) for subsequent use in *in silico* models (summarized in Appendix I). Adult fish cardiac output was not measured since previously it has been calculated (Stadnicka et al., 2012). Cardiac output was measured at three, seven, and approximately 32 days post fertilization (dpf) by use of methods described by Schwerte et al. (2005). Larvae (*n*=5) were anesthetized by use of Aquacalm™ (approximately 200 µg/L, Syndel; Nanaimo, BC, CAN). Heart rate (beats per minute) were manually counted for two minutes and estimates of the length and width of the ventricle were recorded four times for both the diastole and systole phases using digital microscopy

(ZEISS Observer Z.1 equipped with Axiocam 105, Carl Zeiss Canada, Toronto, ON). Heart rates can be visually/microscopely observed due to transparency of larvae. Estimates of the ventricular volume for each phase was calculated, assuming a spherical shape of the larval hearts (4/3 * π * length * width^2), and was used to determine stroke volume (diastole volume – systole volume) and cardiac output (stroke volume * heart rate).

2.3.9 TK models

The current study provided parameters to be used in an embryo-larval one-compartment TK and adult multi-compartment TK model for fathead minnows (detailed in Appendix I and J). For the embryo-larval model, the whole-body biotransformation rate was calculated by scaling adult *in vivo* intrinsic clearance by use of measurements of embryo-larval cardiac output. The adult model used the *in vivo* intrinsic clearance directly to calculate hepatic clearance, which was applied to determine metabolite abundance in the bile. Both models used measurements of wet mass and whole-body lipid content as inputs. Additionally, the adult model used measurements of bile mass. The models were used to make predictions of metabolite abundance, in either the whole-body (embryo-larval) or the bile (adult), which were compared to results determined by the chemical analysis of whole-body or bile metabolite abundance, respectively. Model outputs for all compartments, including the bile, were produced as parent B[*a*]P concentration units. Therefore, for the purpose of evaluating model accuracy and to replicate model units, the measured concentrations of B[*a*]P metabolites, OH-B[*a*]P and gluc-B[*a*]P, were converted to B[*a*]P equivalents and summed (ng/mg whole body tissue, ng/mg bile).

2.3.10 Statistical analysis

A parametric analysis consisting of a 2-way ANOVA followed by Tukey's HSD post hoc test was used to determine if differences existed among treatment groups and time of exposure for chemical analysis of B[*a*]P metabolites, EROD, and GST activity. The two-sided Iglewicz and Hoaglin's robust outlier test (Z=3.5) was used to remove 28 data points from the adult data set, determined to be outliers (Contchart online calculator; Contchart Software, 2018). Data were log-transformed when necessary to meet heteroscedasticity (Spearman's test for heteroscedasticity) and normality assumptions. A Wilcoxon sign test was performed to determine if differences existed between measured and predicted B[*a*]P equivalent values. Significant differences were defined by $p \leq 0.05$.

All statistical tests were performed using GraphPad Prism 8® (GraphPad Software, Inc., San Diego, CA, USA). Additionally, RMSE (root mean square error) calculations were performed to analyze model accuracy. All RMSE calculations were performed by use of Microsoft® Excel 16.30 (Microsoft Co., Redmond, WA, USA).

2.4 Results

2.4.1 B[*a*]P concentrations

Mean (± S.D.), measured aqueous concentrations of B[*a*]P for the embryo-larval exposure were 0.16 (± 0.15), 0.85 (± 0.70) and 4.55 (± 3.18) µg B[*a*]P/L. For the adult life stage exposure, mean, measured aqueous concentrations of B[*a*]P (± S.D.) were 0.03 (± 0.01), 0.08 (± 0.02) and 1.34 (± 0.70) µg B[*a*]P/L. Time-resolved concentrations are stated in Table B.1. The measured concentrations were considerably lower than nominal concentrations. Losses of B[*a*]P are likely a result of sorption to the exposure aquaria and particulates (i.e., food and algae), incomplete solubility, and degradation. At these measured concentrations, no significant effect on growth, reproduction or survival were observed.

2.4.2 Chemical analysis of B[*a*]P metabolites

A significant interaction occurred between duration and magnitude of exposure to B[*a*]P for concentrations of OH-B[*a*]P metabolite in both the embryo-larval (2-way ANOVA, df=16, $F_{16,45}$=6.294, p<0.0001) and adult life stage (2-way ANOVA, df=12, $F_{12,40}$=9.916, p<0.0001) (Figure 2.2). Likewise, a significant interaction also occurred for gluc-B[*a*]P between concentration and duration of exposure in both the embryo-larval (2-way ANOVA, df=16, $F_{16,47}$=6.811, p<0.0001) and the adult life stage (2-way ANOVA, df=12, $F_{12,40}$= 9.119, p<0.0001) (Figure 2.2). In the embryo-larval stage significant differences among durations of exposure suggested an increase in the abundance of both OH-B[*a*]P and Gluc-B[*a*]P with increasing exposure time. A slight decrease in both metabolites, however, was observed after 14 days of exposure. This trend was less apparent in the adult life stage, in which differences in abundances of OH-B[*a*]P varied among exposure times in the 0.03 and 0.08 µg B[*a*]P/L treatments. Similar to the embryo-larval stage, an increasing trend in the abundance of OH-B[*a*]P among exposure time was observed in the highest exposure treatment (1.34 µg B[*a*]P/L). Differences in the abundances

of Gluc-B[*a*]P, however, varied among all exposure times for all B[*a*]P treatments in the adult exposure.

Abundances of B[*a*]P equivalents (mass concentrations that are independent of differences in molecular mass of the parent B[*a*]P and the two metabolites) used for evaluating model accuracy are shown in the Figure C.1.
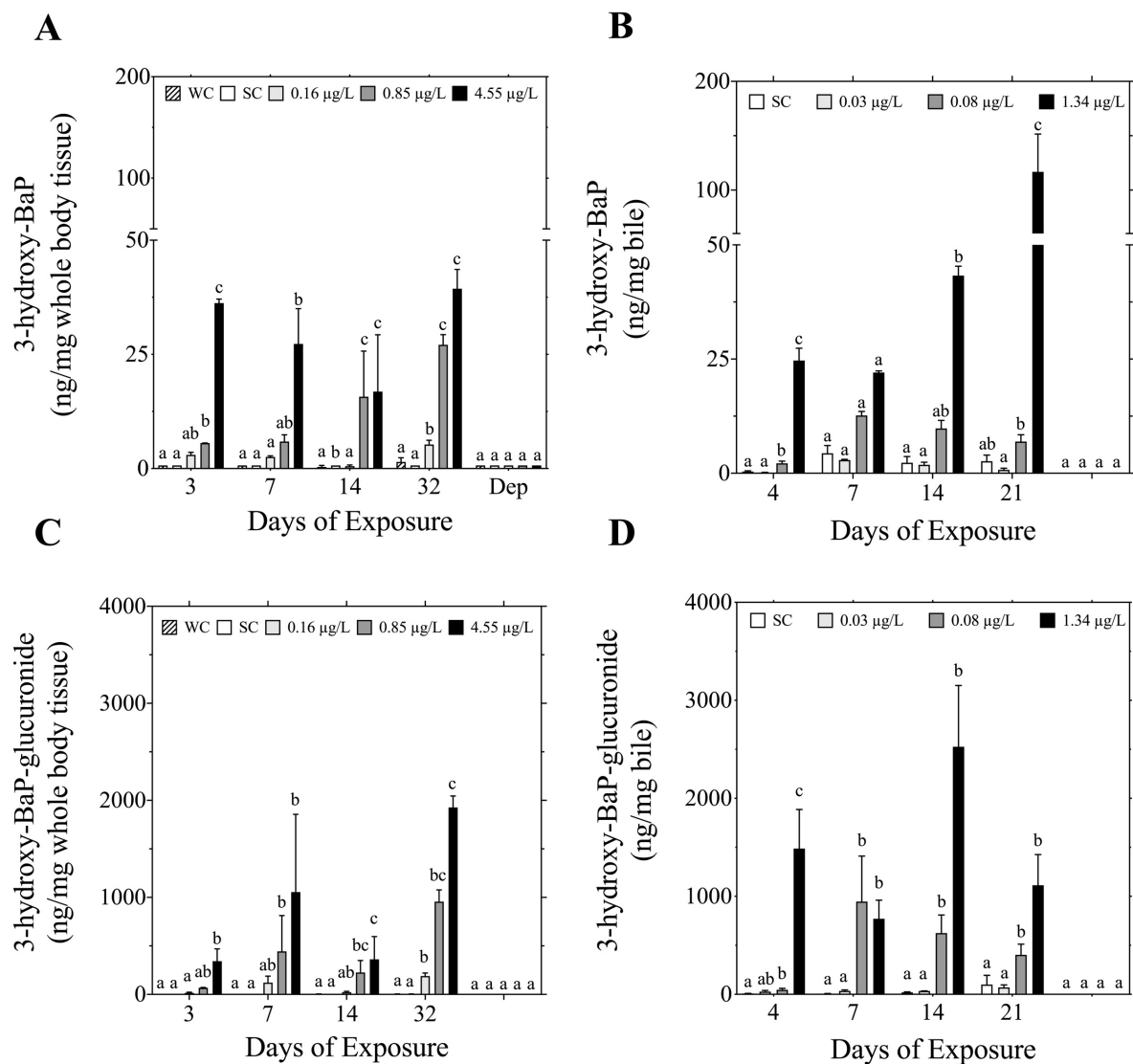
Figure 2.2. Abundances of 3-hydroxy-B[*a*]P and 3-hydroxy-B[*a*]P glucuronide (ng/mg whole body tissue or ng/mg bile) in whole body embryo-larval (A, C) or the bile of adult (B, D) fathead minnows after three, seven, 14 and 32 or four, seven, 14 and 21 days of exposure to increasing concentrations of B[*a*]P as well as water control (WC) and solvent control (SC), respectively. Data is expressed as mean ± standard error of the mean (S.E.M.). Different letters denote a significant difference in B[*a*]P metabolites among treatment groups within each respective time point (2-way ANOVA with Tukey's HSD, $\alpha = 0.05$).

2.4.3 Enzyme activity analysis

No significant differences in EROD activity occurred among treatment groups for either life stage. There was, however, a significant difference in EROD activity among exposure days for both the embryo-larval (2-way ANOVA, df=2, $F_{2,40}$ = 81.00, p<0.001; Figure 2.3A) and adult life stage (2-way ANOVA, df=2, $F_{2,58}$ = 8.565, p=0.0006; Figure 2.3B). In the embryo-larval stage the difference among exposure times indicated a decrease in EROD activity ,while in the adult stage, differences among treatments suggest a slight increase in EROD activity over the duration of the exposure.

Similarly, there were no significant differences in GST activity in the embryo-larval stage among exposure concentrations, but a significant difference among durations of exposure was observed (2-way ANOVA, df=2, $F_{2,40}$ = 81.00, p<0.0001; Figure 2.4A). These differences suggest an increase in GST activity in the embryo-larval stage over the duration of the exposure. In the adult life stage, a significant interaction for GST activity occurred between magnitude and duration of exposure to B[a]P (2-way ANOVA, df=6, $F_{6,60}$ = 2.582, p=0.0272; Figure 2.4B). The differences in the adult stage, however, were highly variable and did not indicate either induction or inhibition of GST activity with B[a]P exposure.
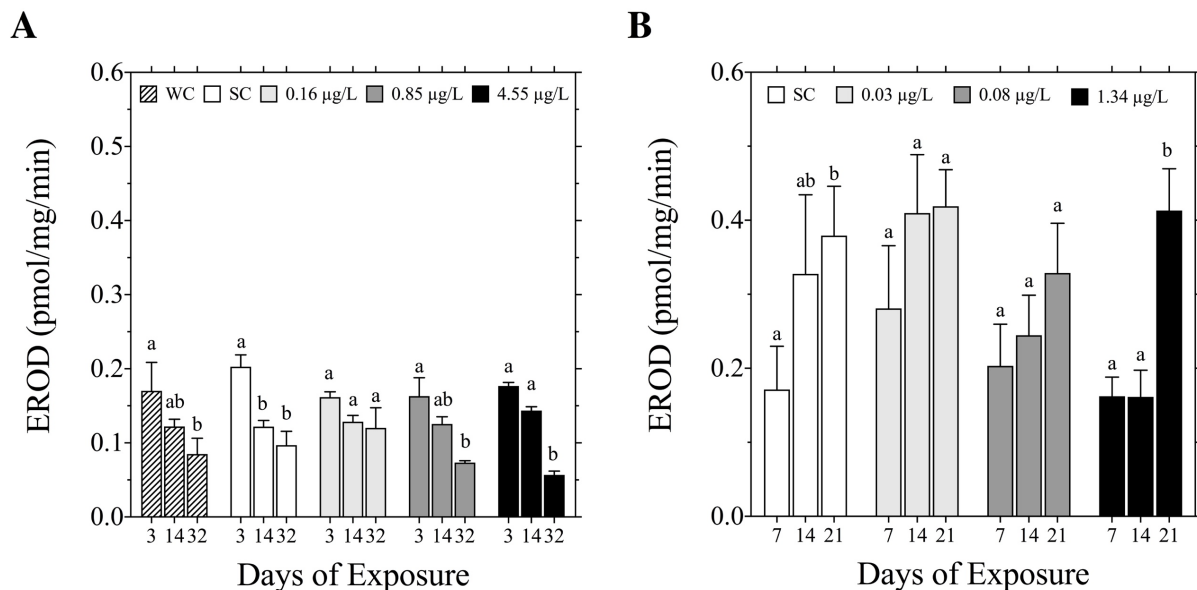
Figure 2.3. EROD activity (pmol/mg/min) for whole body embryo-larval (A) or liver of adult (B) fathead minnows after three, 14, and 32 or seven, 14 and 21 days of exposure to increasing concentrations of B[*a*]P as well as water control (WC) and solvent control (SC), respectively. Data is expressed as mean ± S.E.M. Different letters denote a significant difference in EROD activity among time points within each respective treatment group (2-way ANOVA, $\alpha = 0.05$). No significant differences existed among treatment groups within each respective time point.
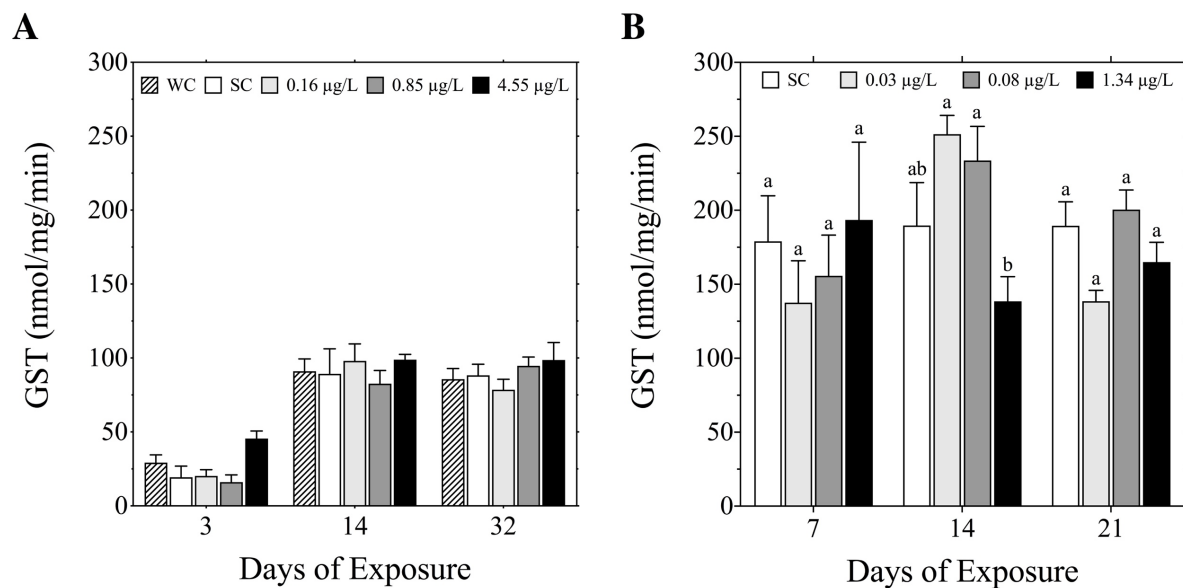
Figure 2.4. GST activity (nmol/mg/min) for whole body embryo-larval (A) or liver of adult (B) fathead minnows after three, 14, and 32 or seven, 14 and 21 days of exposure to increasing concentrations of B[*a*]P as well as water control (WC) and solvent control (SC), respectively. Data is expressed as mean ± S.E.M. Different letters denote a significant difference in GST activity among treatment groups within each respective time point (2-way ANOVA, $\alpha = 0.05$). No significant differences existed in the embryo-larval life stage among treatment groups for each respective time point.

2.4.4 TK model parameters and outputs

Parameters specific to exposures are summarized (Table 2.1). Additional model parameter values are defined in the appendices (Table I.1, Table I.2, Table J.2, Table J.3). A significant correlation between predicted and measured internal concentrations of B[*a*]P equivalents was observed for both the embryo-larval and adult models (Figure 2.5). Model outputs were within approximately one order of magnitude of the measured values (Figure 2.5, Figure 2.6). No significant differences were observed between predicted and measured values for either model (embryo-larval one-compartment, Wilcoxon Signed Rank test; $p=0.3013$; Adult multi-compartment, Wilcoxon Signed Rank test; $p=0.9697$). The adult model, however, had a slightly smaller RMSE of 0.6010 log units, compared to the embryo-larval one-compartment model with an RMSE of 0.6371 log units.

Table 2 1. Measured input parameters for embryo-larval (ELS) one-compartment and adult multi-compartment models.

Life stage	Wet mass (mg ± S.D.)	Bile volume (mg ± S.D.)	$Cl_{int, in\ vitro}$[b] (ml/h/mg)	Lipid (%)	Cardiac output (nl/min ± S.D.)	K_{MET}[c] (1/d)
ELS 3 dpf[a]	1.22 ± 0.17	---	---	1.84 ± 0.52	29.64 ± 9.62	1.325
ELS 7 dpf	0.79 ± 0.11	---	---	1.70 ± 0.41	60.82 ± 18.71	2.748
ELS14 dpf	3.60 ± 1.76	---	---	2.30 ± 0.84	Interpolated[e]	Interpolated[e]
ELS 32 dpf	35.00 ± 8.00	---	---	2.84 ± 1.16	955.25 ± 168.96	0.905
Adult day 4	2,248 ± 1386	6.23 ± 3.81	0.742 ± 0.061	---	calculated[d]	---
Adult day 7	2,337 ± 1440	4.74 ± 2.73	0.742 ± 0.061	---	calculated[d]	---
Adult day 14	2,396 ± 1418	4.27 ± 2.56	0.742 ± 0.061	---	calculated[d]	---
Adult day 21	2,481 ± 1421	4.12 ± 2.60	0.742 ± 0.061	---	calculated[d]	---

[a] days post fertilization (dpf)
[b] intrinsic *in vitro* clearance ($Cl_{int, in\ vitro}$)
[c] whole body biotransformation rate (K_{MET})
[d] value as determined from fathead minnow TK model outlined in Stadnicka et al. (2012)
[e] interpolated using ELS one-compartment model
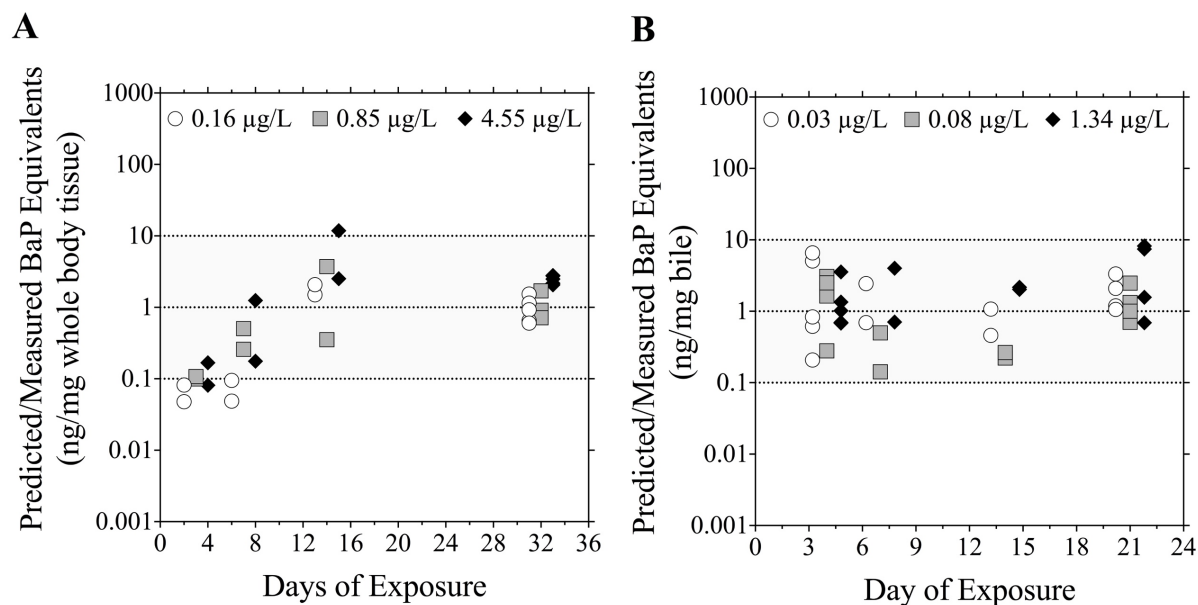
Figure 2.5. Relationships between predicted and measured concentrations of B[*a*]P equivalents from the embryo-larval one compartment (A) and adult multi-compartment (B) model outputs with linear regression (blue) and associated 95% confidence intervals (grey), equality line (dashed red) and ± 10-fold deviation from equality (dashed black). Error bars for the adult multi-compartment model points indicate range of predictions in the last eight hours of simulation to depict bile dynamics. Predicted B[*a*]P equivalents were obtained directly from model outputs. Measured B[*a*]P equivalents were calculated as mass concentrations that are independent of differences in molecular mass of the parent B[*a*]P and the two metabolites, OH-B[*a*]P and gluc-B[*a*]P, from measured metabolite concentrations in order to match model output units. RMSE, root mean squared error.
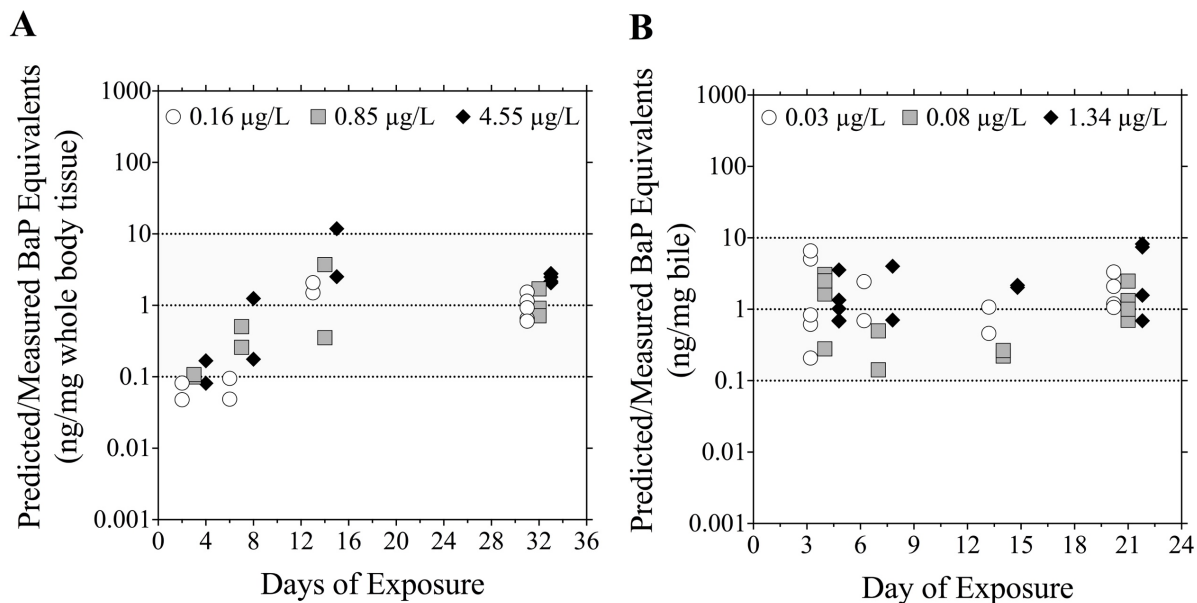
Figure 2.6. Relationships between predicted and measured concentrations of B[*a*]P equivalents from the embryo-larval one compartment (A) and adult multi-compartment (B) model outputs relative to the day of exposure with ± 10-fold error from equality (grey). Predicted B[*a*]P equivalents were obtained directly from model outputs. Measured B[*a*]P equivalents were calculated as mass concentrations that are independent of differences in molecular mass of the parent B[*a*]P and the two metabolites, OH-B[*a*]P and gluc-B[*a*]P, from measured metabolite concentrations in order to match model output units.

2.5 Discussion

Using *in silico* models is a promising approach that enables prediction of the internal dose metrics for a growing number of fish species, chemicals, and exposure scenarios. In this study, we investigated the biotransformation characteristics and capacity in embryo-larval and adult life stages of fathead minnow exposed to water-borne B[*a*]P. These data were further integrated into pre-existing models. Results showed that the resulting models were successful in predicting the life-stage specific abundances of B[*a*]P metabolites in both the embryo-larval and adult life stages of fathead minnow.

2.5.1 Integration of biotransformation into TK models

The finding of no differences in either phase I (CYP1A; EROD) or phase II (glutathione; GST) enzyme activities observed among treatments for both life stages of fathead minnow (Figure 2.3, Figure 2.4) is consistent with data published from previous aqueous B[*a*]P studies in other fishes, which revealed that induction of these responses is not commonly found in fish unless exposed to B[*a*]P concentrations of 10 μg B[*a*]P/L or greater (Sandvik et al., 1997; Peters et al., 1997; Ortiz-Delgado et al., 2007; Costa et al. 2011). Measured, aqueous B[*a*]P concentrations from this study were substantially lesser. Additionally, it has been suggested that cyprinids, such as the fathead minnow, exhibit lesser CYP1A activity and inducibility compared to other species, and accordingly show fewer effects such as carcinogenesis (Hawkins et al., 1991, van den Hurk et al., 2017). However, given these results, the *in vitro* clearance of B[*a*]P in fathead minnow (Table 2.1) was within the range of values that have previously been measured in other species such as *Oncorhynchus mykiss* (rainbow trout) and *Lepomis macrochirus* (bluegill sunfish) as listed in EURL ECVAM *In vitro* Biotransformation database (European Commission, 2018).

Biotransformation of substrates typically follows the Michaelis-Menten model, which contains a first-order and a quasi zero-order, i.e., saturation phase. It is important to consider the possibility of saturation kinetics when integrating biotransformation into TK models as it could have a substantial impact on their scaling, and subsequently, model outputs. The concept of enzyme saturation regarding B[*a*]P exposure was explored by Nichols et al. (2013a). However, it was concluded that, in contrast with other chemicals, at a high exposure concentration (0.98 μM) saturation was unlikely, and would have little or no impact on hepatic clearance of B[*a*]P, but

rather hepatic clearance was more sensitive to liver perfusion rates due to the high extraction ratio of B[*a*]P.

The information provided by Nichols et al. (2013), along with the insignificant differences we observed in phase I and II biotransformation, provided a basis for the assumption that all exposure concentrations occurred within the first-order portion of the Michaelis-Menten model. This assumption meant that biotransformation would increase proportionally with our increase in exposure concentrations. Therefore, we were able to apply a single biotransformation parameter for all exposure simulations and did not account for saturation kinetics. In exposure scenarios where saturation kinetics could occur, a series of clearance studies would need to be performed as described by Nichols et al. (2013a).

2.5.2 Model performance and predictive power

Integration of biotransformation into pre-existing TK models produced accurate predictions within 10-fold of measured concentrations for both the embryo-larval and adult life stages of fathead minnow (Figure 2.5). The one-compartment embryo-larval model showed slightly lesser predictive power compared to the multi-compartment adult model. This result is consistent with previously published results for when these two model types were compared (Nichols et al., 2007, Stadnicka et al., 2012). Inaccuracies in model predictions from the one-compartment model occurred specifically during the first two phases of development, i.e. the egg stage (0-3 dpf) and yolk sack stage (3-7 dpf) and became less prevalent as the model progressed into the free-feeding stages (7-32 dpf) (Figure 2.6A). These inaccuracies are potentially a result of estimates of biotransformation for the embryo-larval fish that was allometrically scaled from measurements of adult *in vitro* clearance rates using measurements of cardiac output. Measurements of embryo-larval stage-specific *in vitro* clearance were attempted using the methods described in OECD 319B (OECD, 2018); however, the assay was not optimized for use with whole-body samples and measurements could not be obtained due to insufficient sensitivity. This was likely a result of enzyme protein dilution within the whole-body larvae, and therefore, a sufficient concentration of enzymes could not be isolated for proper performance in the assay.

Few studies have been conducted in which embryo-larval biotransformation was compared to adults. Studies conducted with embryo-larval zebrafish have shown that biotransformation can begin as early as the gastrulation stage of development (Otte et al., 2010), and that larvae are

capable of extensive phase II biotransformation as soon as 3 dpf (Le Fol., 2017). Therefore, these results suggest that the embryo-larval fish have a higher capacity for biotransformation than we calculated during the initial stages of embryo-larval development. This conclusion is supported by the observed linear relationship between whole-body biotransformation (k_{met}) and B[a]P equivalent concentrations (Figure K.1C). The positive relationship indicates that increases in k_{met} will generate increases in B[a]P equivalents. Additional research pertaining to the optimization of *in vitro* clearance assays for embryo-larval stages of fish would provide more accurate estimates of biotransformation to be used in embryo-larval stage TK models.

Performance of the adult multi-compartment model, with an RMSE of 0.60 *log* units (Figure 2.5B), were comparable to previously published results when the model was used for exposure simulations across numerous other chemicals in the fathead minnow, which showed an RMSE of 0.66 *log* units (Stadnicka et al., 2012; Brinkmann et al., 2016). Advances to the existing TK model for fathead minnows were made by the addition of a bile compartment, which included the parameters bile flow, volume, and purge time, to depict bile dynamics and include biotransformation. A similar TK model including bile dynamics for rainbow trout has been described by Brinkmann et al. (2014). Additionally, we were able to make bile-specific predictions of metabolites, allowing for a simple quantification method of B[a]P metabolites in the bile to act as a validation data set. Some assumptions needed to be made regarding the bile specific parameters as literature values and measurement techniques were not available. Changes in these parameters were shown to influence the abundance of metabolites predicted, and therefore, species-specific measurements of these parameters could change model performance (Figure K.1E,F).

An additional assumption implemented into the adult multi-compartment model was that only 60% of the metabolites predicted would represent OH-B[a]P and gluc-B[a]P. This assumption was made based on studies conducted with mummichog (*Fundulus heteroclitus*) in which the abundance of OH-B[a]P and the associated glucuronide was determined to be between 58-66% of total metabolites produced (Zhu et al., 2008). Measuring the specific concentrations of all B[a]P metabolite fractions produced by fathead minnows could further improve model performance. In the embryo-larval model, 100% of the predicted metabolites were assumed to be the OH-B[a]P and associated glucuronide as studies conducted with zebrafish larvae suggest that embryo-larval biotransformation occurs predominately through the glucuronide pathway opposed

to a combination of other pathways such as sulfation (Le Fol et al., 2017). In both life-stages, however, it should be noted that other pathways of B[*a*]P biotransformation might exist. These pathways include hydrolysis *via* the epoxide pathway to form the genotoxic metabolite BPDE, conjugation *via* GST, and the formation of diols, diones, tetrols, triols, phenols and quinones (Gelboin, 1980; Kennedy et al., 2008; Zhu et al., 2008; Liu et al., 2014, Strobel et al., 2015).

Biotransformation was also shown to affect abundances of B[*a*]P metabolites produced (Figure K.1D). However, at greater rates of biotransformation, the sensitivity of the parameter was shown to decrease. This further indicates that the extent of metabolites produced from hepatic clearance of rapidly metabolized chemicals is largely influenced by liver perfusion rather than binding to CYP proteins and enzyme activity. Studies conducted with isolated perfused rainbow trout livers showed similar findings (Nichols et al., 2009; Nichols et al., 2013). In these studies, the effect of increasing BSA concentration in the liver perfusate on hepatic clearance was evaluated. For chemicals with high extraction ratios, such as B[*a*]P and pyrene, changes in protein concentration had little effect on hepatic clearance. No evidence of enzyme saturation was observed, and therefore, biotransformation capacity was determined to be relative to rate of liver perfusion (Nichols et al., 2013). However, for the chemicals naphthalene, fluorene, anthracene, phenanthrene (Nichols et al., 2013) and 7-ethoxycoumarin (Nichols et al., 2009), decreases in BSA concentration resulted in increases in hepatic clearance suggesting that protein binding has greater influence on hepatic clearance for these compounds. These differences among chemicals are attributed to their respective log K_{ow} values, as log K_{ow} was shown to have a positive correlation with *in vitro* clearance (Nichols et al., 2013). In mammals, it has been shown that CYP1A enzymes have a higher affinity for hydrophobic compounds (Long & Walker, 2005). Therefore, it is likely that the greater the hydrophilicity of a chemical (i.e., naphthalene, fluorene, anthracene, phenanthrene, and 7-ethoxycoumarin) the greater its affinity for non-CYP proteins. As protein content decreases the availability for these chemicals to bind to CYP enzymes increases, resulting in increased *in vitro* clearance. For more hydrophobic chemicals such as B[*a*]P and pyrene, there is a higher affinity for CYP enzymes compared to non-CYP proteins, and changes in protein content have no effect on *in vitro* clearance.

2.5.3 Differences between life stages

Differences in the biotransformation characteristics between life stages were observed. The embryo-larval life stage exhibited lesser formation of B[*a*]P metabolites compared to the adult life stage (Figure 2.2). This difference, however, was difficult to quantify based on results of this study, as B[*a*]P equivalents were measured in the whole body of the embryo-larval stage while in the adult stage they were assessed in bile. Therefore, some dilution of metabolites likely occurred in the whole-body embryo-larval samples corresponding to the reduced abundance of B[*a*]P metabolites. The same conclusion can be drawn for the differences in EROD and GST activity between life stages (Figure 2.3, Figure 2.4). However, differences in metabolic capacity between life stages of fish have been observed previously. Knöbel et al. (2012) found that when embryo-larval and adult zebrafish were exposed to allyl alcohol, a chemical for which biotransformation is responsible for the associated toxicity, embryo-larval fish exhibited a LC_{50} value 1059-fold greater than the adult fish. This difference was attributed to a lack in the biotransformation capacity at the embryo-larval stage, and as a result a lesser concentration of toxic metabolites was produced compared to adult fish. Le Fol et al. (2017) also demonstrated life stage-specific differences in metabolic capacity when embryo-larval and adult zebrafish were exposed to benzophenone-2 (BP2) and bisphenol S (BPS). Overall, the adult life stage showed a greater capacity of biotransformation for both chemicals. Additionally, for BP2, life stage differences in metabolic pathways were observed. Glucuronidation was the predominant pathway in the embryo-larval stage while sulfation predominated in the adult life stage. Understanding these life stage differences is critical when assessing toxicity for chemicals that are activated by biotransformation. If life stage-specific biotransformation is not considered, researchers and risk assessors might underestimate the toxic effects of such chemicals.

The concentration of a chemical that can reach the target site of action is known to be influenced directly by biotransformation activity (McElroy et al., 2011; Carrasco-Naavarro et al., 2015; Strobel et al., 2015). B[*a*]P is a known ligand for the AhR, inducing the transcription of target genes, and ultimately the CYP1A and CYP1B proteins responsible for biotransformation of parent B[*a*]P into toxic metabolites (Gelboin, 1980). The results of this study suggest that the embryo-larval stage will be less affected by genotoxicity from biotransformation of B[*a*]P compared to the adult life stage. However, the embryo-larval stage, in turn, might be more susceptible to other effects associated with binding of the AhR such as teratogenicity (Jönsson et

al., 2007; Schiwy et al., 2015). Developmental effects, likely associated with AhR ligand binding in the embryo-larval stage, have been shown to be directly related to increases in aqueous B[a]P exposure concentrations (Gravato et al., 2009). These results emphasize the importance of life stage-specific models parameterized for chemicals that are rapidly biotransformed for accurate risk assessments for fish.

The use of ELS of fish in support of toxicity studies and hazard assessments is increasing. ELS are often considered to be more sensitive to contaminants than adults. However, as discussed above, ELS might be less sensitive to exposure to some chemicals in which biotransformation elicits toxicity, as the ELS were shown to have less extensive biotransformation capacity compared to the adult life stage. Therefore, a greater understanding of contaminant effects on ELS is important in terms of protection of species survival and ecosystem homeostasis. Additionally, the embryo-larval stage is currently being considered as a replacement and refinement method to live animal testing (EFSA, 2005). Thus, a better understanding of life-stage specific differences in toxicokinetic processes is essential in advancing these developments. Research initiatives such as the fish embryo test (FET) (Lammer et al., 2009; Embry et al., 2010; Knöbel et al., 2012; OECD, 2013; Kais et al., 2017), the embryo test with the Zebrafish *Danio rerio* (DarT) (Nagel, 2002), and the EcoToxChip project focusing on fish, amphibian and bird embryo testing (Basu et al., 2019) are currently using embryo-based approaches as a replacement for juvenile or adult organisms. Additionally, ELS tests as well as *in silico* approaches are considered new approach methodologies (NAM) that hold promise for being used by governments, regulators, and businesses in support of more ethical risk assessment approaches (Mondou et al., 2019).

2.5.4 Conclusions and further directions

This study showed that biotransformation of B[a]P can be successfully implemented into TK models to predict the abundances of B[a]P metabolites in both the embryo-larval and adult life stages of the fathead minnow. The multi-compartment adult model had slightly better predictive power compared to the embryo-larval one-compartment model. However, both models could be improved through measurements of further model parameters, specifically biotransformation in the embryo-larval developmental stages and bile dynamics in the adult life stage. Additionally, integrating saturation kinetics could increase model applications. Increasing a model's scope and applications is an important development for the use of TK in ecological risk assessment, as it

provides a means of estimating impacts of chemical accumulation, as well as reverse dosimetry. This allows for a system to be developed in which chemicals can be prioritized for more extensive *in vivo* testing as suggested by Nichols et al. (2013a). Future work should be focused on parameterizing the current TK models to be extrapolated to other species and biotransformed chemicals.

2.6 Acknowledgements

CHAPTER 3: CROSS LIFE-STAGE TOXICOKINETIC MODELS FOR THE UPTAKE AND BIOTRANSFORMATION OF ORGANIC CONTAMINANTS IN WHITE STURGEON (*ACIPENSER TRANSMONTANUS*)

PREFACE

The main objective of Chapter 3 was to develop life-stage specific *in silico* toxicokinetic models to predict the bioaccumulation of organic contaminants in embryo-larval and sub-adult white sturgeon. The methods for model parameterization and characterization of biotransformation and the TK model structures used in Chapter 3 were adapted from the methods and TK models described in Chapter 2. The main objective was met by measuring various physiological parameters in the embryo-larval and sub-adult life stages, and generating validation sets from aqueous exposure to graded concentrations of B[*a*]P for the embryo-larval life stage, and compiling an experimental dataset of aqueous organic contaminant exposures from the literature for the sub-adult life stage. The data generated were used to parameterize an embryo-larval one-compartment model and a multi-compartment PBTK adult model. Chapter 3 was prepared in manuscript style and was submitted for publication in the peer-reviewed scientific journal *Environmental Science and Technology:*

Grimard, C., Mangold-Döring, A., Alharbi, H., Weber, L., Hogan, N., Jones, P. D., Giesy, J. P., Hecker, M., & Brinkmann, M. (2021). Cross life-stage toxicokinetic models for the uptake and biotransformation of organic contaminants in white sturgeon (*Acipenser transmontanus*). *Environmental Science and Technology.*

Author Contributions:

Chelsea Grimard (University of Saskatchewan) helped with designing and performing embryo-larval exposures, performed all tissue sampling and data generation for the embryo-larval exposure, generated data for adult sturgeon model, implemented data into toxicokinetic models, performed data analysis, prepared figures and tables, and drafted the manuscript.

3.1 Abstract

The white sturgeon (*Acipenser transmontanus*) is an endangered ancient fish species that is known to be particularly sensitive to certain environmental contaminants, partly because of the accumulation and subsequent toxicity of lipophilic and bioaccumulative pollutants as a result of their high lipid content. To better understand the bioaccumulation of organic contaminants in this species, toxicokinetic (TK) models were developed for the embryo-larval and sub-adult life stages. The embryo-larval model was designed as a one-compartment model and validated using whole-body measurements of benzo[*a*]pyrene (B[*a*]P) metabolites from a waterborne exposure to B[*a*]P. A multi-compartment physiologically based TK (PBTK) model was used for the sub-adult model. The predictive power of the sub-adult model was validated with an experimental data set of four chemicals with *log n*-octanol-water partitioning coefficients ranging from $0.53 - 4.40$. Results showed that the TK models could accurately predict the accumulation of organic contaminants for both life stages of white sturgeon within one order of magnitude of measured values. These models provide a tool to better understand the impact of environmental contaminants on the health and survival of endangered white sturgeon populations.

3.2. Introduction

The white sturgeon (*Acipenser transmontanus*) is an ancient fish species native to the western regions of North America. Presently, as a result natural recruitment failure from habitat degradation (McAdam et al., 2005; Paragamian et al., 2009; McAdam, 2011) and pollution (Fiest et al., 2005; Greenfield et al., 2005; Gunderson et al., 2008; MacDonald 2009., Gunderson et al., 2017), some white sturgeon populations from northwestern rivers in the United States (U.S.) and British Columbia, Canada have been classified as endangered (U.S Fish and Wildlife Service, 1999; COSEWIC, 2012). The endangered status of these populations has resulted in an increasing number of ecological risk assessments conducted for this species to ensure its protection and long-term sustainability. Exact causes of recruitment failure are unknown and complex; however, it is known that in certain habitats the failure is attributed to poor offspring survival (Gross et al., 2002; McAdam, 2011), rather than a lack of spawning (McAdam et al., 2005). Habitat degradation, in both quality and quantity, as a result of anthropogenic activity, is the primary cause under investigation. These habitat changes disrupt bed substrates and water flow regulation, which are critical components to offspring hatchability and survival (McAdam et al., 2005; Paragamian et al., 2009; McAdam, 2011). In addition to habitat changes, industrial impacts on water quality and the release of pollutants also pose chronic threats to white sturgeon populations as white sturgeon have been shown to be more sensitive to some contaminants compared to other species (Bennet & Farrell, 1993; Vardy et al., 2011; Vardy et al., 2013; Doering et al., 2015). Therefore, bioaccumulation of contaminants, resulting in adverse effects and ultimately mortality, might be one of the causes hindering successful population recruitment in this species.

White sturgeon are unique in their physiology as they have a higher lipid content relative to other freshwater fishes (Birstein, 1993). They are bottom dwellers and live near the sediment. As a result of their benthic lifestyle and high lipid content, there is increased potential for exposure to and subsequent toxicity of lipophilic bioaccumulative contaminants from both direct exposure and leaching from sediments (Birstein, 1993). Accordingly, elevated levels of organic contaminants such as polychlorinated biphenyls, polybrominated diphenyl ethers, polychlorinated dibenzo-*p*-dioxins, polychlorinated dibenzofurans, and organochlorine pesticides have been reported in wild-caught white sturgeon from northwestern U.S. and Canadian freshwater systems (Fiest et al., 2005; Greenfield et al., 2005; Gunderson et al., 2008; MacDonald 2009., Gunderson et al., 2017). Exposure to polycyclic aromatic hydrocarbons, such as benzo[*a*]pyrene (B[*a*]P), is likely also a concern as the habitats of vulnerable white sturgeon populations overlap with areas that rely on fossil fuels for industrial usage (Yunker et al., 2002; Oros et al., 2007). Previous studies have shown that white sturgeon might be more sensitive to the adverse effects of dioxin-like

compounds (DLCs) due to the structure of their aryl hydrocarbon receptors (AhR) that drive DLC toxicity (Doering et al., 2014), thus, emphasizing the importance of better understanding the bioaccumulation of such compounds.

Knowledge of the extent of bioaccumulation of organic contaminants is essential to better understand the effects that pollutants have on white sturgeon fitness, health, and recruitment. This information, however, can be difficult and often impractical to generate as white sturgeon individuals are often required for restocking programs, necessitate a large space, and require special permits for use in research. Furthermore, there are ethical limitations when conducting research with endangered species, as the contribution of the research to species conservation must justify the environmental impact, i.e., disruption to habitat and population (Bennet et al., 2016; Sloman et al., 2019). The use of toxicokinetic (TK) models, an *in silico* approach, can be a powerful alternative to *in vivo* studies with endangered species to relate internal chemical concentrations to external exposure scenarios (Grech et al., 2017). For early-life stages (ELS), empirically-based one-compartment models are useful to obtain estimates of whole-body internal concentrations in the egg, yolk, and free-feeding stages (Foekema et al., 2012; Grimard et al., 2020). For the sub-adult and adult life stages, a more complex mechanistic model, i.e., a physiologically based toxicokinetic (PBTK) model, can be used to obtain estimates of internal concentrations in the whole fish and specific tissues during the time course of an exposure (Nichols et al., 1990; Stadnicka et al., 2012). PBTK models use the physiological parameters cardiac output, oxygen consumption rate, and effective respiratory volume, and characterize individual tissues by volume, total lipid content, total water content, and tissue perfusion rates (Nichols et al., 1990) Both model types can be integrated with parameters specific to biotransformation of an organic contaminant when applicable (Nichols et al., 2007; Nichols et al., 2013; Grimard et al., 2020). Additionally, the TK model framework allows for interpolation and extrapolation in relation to life-stage, intraspecies and interspecies differences in bioaccumulation, and thus, a better understanding of these differences can be obtained.

To our knowledge, there are currently no TK models developed for white sturgeon. Additionally, there is a limited number of toxicity studies focusing to the developmental stages of white sturgeon, none of which pertain to TK. TK models developed for white sturgeon would provide a tool to better understand the bioaccumulation of contaminants in this species and the potential risks accumulation of chemicals may pose to its survival. The research goals of the present study were to: (a) develop TK models for bioaccumulation of organic chemicals in the embryo-larval and adult life stages of white sturgeon; (b) integrate life-stage specific biotransformation into the corresponding models; (c) make predictions of internal concentrations

for each respective life stage; and (d) validate model predictions using measurements of B[*a*]P metabolites from exposure to graded concentrations of waterborne B[*a*]P in the embryo-larval stage and published data sets of internal organic contaminant concentrations in adult fish.

3.3. Materials and methods

3.3.1 Study design

This current study was designed to provide species-specific model parameters to be integrated into a one-compartment embryo-larval model and a multi-compartment PBTK sub-adult model. The one-compartment embryo-larval model is a re-parameterization of the bioaccumulation model described by Arnot and Gobas (2004), which allows for predictions of the accumulation of B[*a*]P metabolites throughout developmental stages, i.e., eggs, yolk-sac larvae, and free-feeding stages of white sturgeon.

The sub-adult PBTK model is a re-parameterization of the PBTK model originally designed for rainbow trout (*Oncorhynchus mykiss*) (Nichols et al., 1990) and subsequently re-parameterized for a multitude of other species (Stadnicka et al., 2012; Brinkmann et al., 2016; Grimard et al., 2020). This model was modified to include stochasticity, allowing for Monte Carlo-like simulations to be performed (U.S. EPA, 2006; Chiu et al., 2007). Model performance was assessed by comparing predictions to a sub-set of experimental values obtained from the literature.

3.3.2 Test organisms

White sturgeon embryos were obtained from the Nechako White Sturgeon Conservation Centre (Vanderhoof, BC, CAN) in 2018 under the Species at Risk Act (SARA) permit 16-PPAC-00002. Embryos less than 24 hours post fertilization were directly used in exposure experiments. Sub-adult white sturgeons were raised in the Aquatic Toxicology Research Facility (ATRF) at the University of Saskatchewan from embryos originally obtained from the Nechako White Sturgeon Conservation Centre in 2013 under the SARA permit XRSF-20-2013. All fish culture protocols and experimental procedures for both the embryo-larval and sub-adult experiments were approved by the Animal Research Ethics Board at the University of Saskatchewan (Protocol #20070049).

3.3.3 Embryo-larval waterborne B[*a*]P exposure

A chronic waterborne B[*a*]P exposure was conducted for 49 days to evaluate the uptake and biotransformation of B[*a*]P during the egg, yolk, and free-feeding developmental stages of the white sturgeon. Nominal exposure concentrations were 1.3, 4.0 and 12.0 µg B[*a*]P/L (Sigma-Aldrich, Oakville, ON, CAN) using 0.02% DMSO (≥ 99.9% dimethyl sulfoxide, Fisher Scientific

Co., Ottawa, ON, CAN) as the solvent carrier, or 0.02% DMSO only as the solvent control, or de-chlorinated ATRF water as the water control ($n=4$ replicate tanks per treatment). Exposure details are described in Appendix B.2.

Five whole-body larvae were euthanized using buffered tricaine methanesulfonate (MS222; Acros Chemicals) on days seven, 14, 21, 28, 35, 42, and 49 of exposure, as well as after a seven day depuration period. One larval fish ($n=4$ per treatment/endpoint/sample day) was taken for biochemical and lipid analysis, as well as for analytical metabolite profiling. At each sampling point, the wet mass was recorded. The length was also recorded starting at day 21 of exposure. Samples were immediately flash-frozen in liquid nitrogen and stored at -80°C until further analysis.

3.3.4 Biochemical analysis

Phase I and II activity was determined through measurements of EROD (7-ethoxyresorufin-*O*-deethylase) and GST (glutathione-*S*-transferase) activity, respectively. Whole-body embryo-larval tissue (n=3; one larva per treatment/sample day) was homogenized at 1 mg tissue: 20 μL homogenization buffer to generate the post-mitochondrial supernatant fraction using a modification of the protocol described by OECD319B (2018). Fluorescent measurements of resorufin (570 nm excitation/ 630 nm emission) and protein (365 nm excitation/ 480 nm emission) were used to determine EROD activity (nmol/mg/min) using a modification of the protocol described by Kennedy & Jones (1994), and a kinetic measurement of CDNB (1-Chloro-2,4-dinitrobenzene; 340nm emission) was used to determine GST activity using a modification of the protocol described by Habig et al. (1974). Assay details and results are summarized in Appendix E and F.

3.3.5 Analytical confirmation of aqueous B[*a*]P and B[*a*]P metabolites

Aqueous B[*a*]P samples (15 mL) were taken on days seven, 14, 21, 28, 35 and 49 of exposure by pooling 3.75 mL of water from replicate tanks ($n=1$ per treatment) . Internal standards (Acenaphthene-d$_{10}$, Chrysene-d$_{12}$, and Phenanthrene-d$_{10}$; Sigma Aldrich; 0.5 μg each) were added to the samples. The samples were then liquid-liquid extracted by vortexing-mixing with 5 mL dichloromethane (DCM; Sigma-Aldrich) and removing the solvent layer into a glass vial. This process was repeated three times for each sample. The solvent extracts were reduced to almost complete dryness with a gentle stream of nitrogen gas and reconstituted in 150 μL nonane (Sigma-Aldrich). Samples were analyzed using gas chromatography-mass spectrometry (GC-MS) on a 7890A gas chromatograph with an Agilent DB-5ms (60 m x 250 μm ID, film thickness 0.1 μm)

fused silica capillary column equipped with a 5975C quadrupole mass detector (Agilent Technologies). A 6-point external calibration standard curve (0.1, 0.3, 0.6, 1.3, 2.5, and 5.0 µg/mL; r^2=0.994) was used to interpolate B[*a*]P concentrations.

The major B[*a*]P metabolites, OH-B[*a*]P and gluc-B[*a*]P, were quantified with ultra-high-performance liquid chromatography high-resolution mass spectrometry (UHPLC-HRMS) in whole-body embryos using the method described by Grimard et al. (2020). Briefly, whole-body embryo samples (*n*=3; one larva per treatment/sample day) were homogenized in HPLC grade acetonitrile (ACN, Fisher Scientific Co., Ottawa, ON, CAN) at a ratio of 1:10 (w/v) for 20 seconds. Samples were centrifuged at 1,700 × g for 15 minutes, and the supernatant subsequently sampled for quantification of metabolites. Metabolites were analyzed using a Vanquish UHPLC and Q-Exactive™ HF Quadrupole-Orbitrap™ mass spectrometer (Thermo-Fisher, Waltham, MA, USA), followed by ionization in negative mode heated electrospray ionization and a full MS/parallel reaction monitoring (PRM) method. OH-B[*a*]P concentrations were quantified with an analytical standard and external calibration, and a semi-quantitative method was used to quantify gluc-B[*a*]P in which a response factor was used to convert peak areas of OH-B[*a*]P to peak areas of gluc-B[*a*]P.

Final B[*a*]P metabolite concentrations (ng/mg whole body larvae) were calculated from the volume of solvent used for extraction. To evaluate model performance and to replicate model outputs, B[*a*]P equivalents, i.e., mass concentrations that are independent of differences in molecular mass of the parent compound and the two metabolites, were calculated from the obtained metabolite concentrations.

3.3.6 Model parameterization

The parameterization of the embryo-larval model (Table 3.1, Table I.2) included experimental values for wet mass, whole-body total lipid content, and whole-body biotransformation rate (k_{MET}). The more complex sub-adult PBTK model (Table 3.2, Table J.3) required parameterization of tissue volume, lipid, and moisture content for each model compartment, i.e., fat, liver, poorly perfused tissues and richly perfused tissues, in addition to the parametrization of the physiological components; cardiac output, oxygen consumption, and effective respiratory volume.

3.3.6.1 Embryo-larval whole-body biotransformation of B[*a*]P

Even though measurable levels of B[*a*]P metabolites were present in the embryo-larval white sturgeon, we were unable to accurately scale embryo-larval k_{MET} from the measurements of adult *in vitro* clearance, as done in previous studies (Grimard et al., 2020), as the embryo-larval

stage showed very low biotransformation activity. Therefore, the value for k_{MET} in the embryo-larval stage was calibrated using the measured B[a]P metabolite abundances. Using 42 data points, a train-test split was generated in Microsoft® Excel 16.30 (Microsoft Co., Redmond, WA, USA). Values for k_{MET} were adjusted in the embryo-larval model until the highest achievable number of predictions were within one order of magnitude of the training set of measured values (Figure I.1). The test values for k_{MET} were obtained by adjusting values of *in vitro* clearance in an *in vitro-in vivo* extrapolation (IVIVE) equation (Table I.1) that uses estimates of cardiac output to calculate whole-body biotransformation. Since we were unable to directly measure cardiac output in the embryo-larval white sturgeon, we used estimates of cardiac output from embryo-larval fathead minnow (*Pimephales promelas*) (Grimard et al., 2020). Equations used for determination of k_{MET} were obtained from Nichols et al. (2007) and are summarized in Appendix I (Table I.1).

3.3.6.2 Lipid contents

Total whole-body lipid content in both life stages was quantified using a modification of the microcolorimetric sulfophosphovanillin (SPV) protocol described by Lu et al. (2008). Lipids were extracted from whole-body embryo-larval fish (*n*=4; one larva per treatment/sampling point) and each sampled tissue in the adult fish (*n*=11 individuals). Lipid extracts were quantified by the addition of sulphuric acid and SPV reagent. Lipid content (mg) was determined through measurements of absorbance using cod liver oil as the standard, and the lipid fraction was subsequently calculated. Additional assay details are defined in Appendix G.

3.3.6.3 Sub-adult tissue volumes and moisture content

Volumes of eight tissues from the sub-adult white sturgeon were determined in a total of 11 fish. The sampled tissues consisted of liver, kidney, spleen, muscle, brain, gills, viscera, and carcass, i.e., the tissue remaining after all other tissues had been sampled. The tissues were weighed, and volumes were estimated from the wet mass by assuming all tissues had a specific density of 1.0 g mL^{-1}. Tissues were stored at -20°C until further analysis of lipid and moisture content. A sub-sample of the tissue samples was dried in an oven at 105°C for 24 hours to determine total moisture content (%) for each sampled tissue of the sub-adult fish (*n*=11 individuals).

3.3.6.4 Sub-adult tissue perfusion and cardiac output

Cardiac output and tissue perfusion rates were measured in four sub-adult white sturgeon. First, the fish were anesthetized with a 10 mg/L solution of Aquacalm (Syndel; Nanaimo, BC, CAN). A continual flow of aerated water at 13 °C containing the same anesthetic solution was dispensed

through the mouth of the fish to maintain anesthesia and oxygenation throughout the duration of the procedures.

Cardiac output (n=4 individuals) was measured using the protocol described by Pettem et al. (2018), using a Vevo3100 ultrasound system (FujiFilm VisualSonics, Toronto, ON, Canada) with an MX250 transducer capable of pulse-wave Doppler and B-mode imaging. The fish were restrained ventral side up in a foam holder for imaging of the cardiac area. Measurements of systolic and diastolic volume were used to determine ventricular stroke volume (V_S), and measurements of ventricular contractile rates (f_H) were manually counted (bpm). Cardiac output was calculated as $f_H \times V_S$.

Tissue perfusion rates (n=4 per tissue) were measured using fluorescently-labeled microspheres. A heparinized catheter was used to cannulate the dorsal aorta in the roof of the mouth. The catheter was injected at a volume of 1 mL per kg fish with a saline solution containing a nominal count of 500,000 pink NuFlow Hydro-Coat™ microspheres (15.5 ± 1.1 µm diameter, NuFlow Microspheres, Smithville, MO, USA), and 30 minutes was allotted for microsphere tissue distribution. After 30 minutes, the fish were euthanized with an overdose of metomidate (Syndel, Ferndal, WA, USA), and the liver, spleen, muscle, brain, gills, viscera, and carcass were dissected. Microspheres were extracted using the NuFLOW™ Fluorescent Microsphere Extraction Protocol with yellow NuFlow Hydro-Coat™ microspheres as the recovery standard. Using an Accuri C6 flow cytometer (BD Bioscience, San Jose, CA, USA), microspheres were counted. The number of recovery microspheres (yellow) was used to correct for the number of target microspheres (pink), which were further scaled to total tissue volume, and tissue perfusion was calculated as a fraction of cardiac output.

3.3.6.5 Sub-adult oxygen consumption rate and effective respiratory volume

A data set for oxygen consumption rate (n=4 individuals) was generated from active fish values listed in the metabolism table of the FishBase database (www.fishbase.org) (Froese, 2019) for white sturgeon. Effective respiratory volume was calculated using the equation described in a previously published PBTK model for rainbow trout (Stadnicka et al., 2012).

3.3.7 TK model implementation and performance

All model parameters and equations are summarized in Appendix I and J. For the embryo-larval model, we implemented our measured wet mass, lipid contents, and calibrated k_{MET} values. The model was used to predict the abundance of B[a]P metabolites (output as B[a]P equivalents).

Embryo-larval model predictions were compared to measured abundances of B[*a*]P metabolites (converted to B[*a*]P equivalents; Figure C.2) from the embryo-larval B[*a*]P exposure.

For the sub-adult PBTK model, we implemented measured values for tissue volume, lipid content, moisture content, and tissue perfusion parameters. A bile compartment was integrated into the model to account for biotransformation, which can be parameterized with measurements of *in vitro* clearance. Because there is no information regarding *in vitro* clearance in white sturgeon for our test chemicals, biotransformation was set to zero. The parameters were implemented with stochasticity by providing the model with the average parameter value along with the standard deviation to represent the range in parameter values. Monte Carlo-like simulations (200 simulations per data point) were run in which a random combination of parameter values from each parameter distribution was chosen, assuming that the parameters are independent. The model outputs were compared to published data sets of internal concentrations or muscle concentrations for sturgeon that were exposed to the organic contaminants avermectin-B1 (Shen et al., 2005), molinate (Tjeerdema et al., 1988), sulfamethazine (SM_2) (Hou et al., 2003), or *p*-nitrophenol (PNP) (TenBrook et al., 2006). As experimental TK data are limited for white sturgeon, two of the experimental data sets (avermectin-B1 & SM_2) pertained to Chinese sturgeon, and we assumed that the two species would be physiologically similar.

3.3.8 Statistical analysis

A one-way ANOVA was used for parametric analysis, and the Kruskal-Wallis test was used for non-parametric analysis to determine if differences in B[*a*]P metabolite concentrations existed among treatment groups within time points from the embryo-larval B[*a*]P exposure. A t-test was used to determine if difference existed between the modelled and the measured or literature values for sub-adult cardiac output and oxygen consumption, respectively. Significant differences were defined by $p \leq 0.05$. All statistical tests were performed using GraphPad Prism 8® (GraphPad Software, Inc., San Diego, CA, USA). RMSE (root mean squared error) calculations were performed to evaluate model performance using Microsoft® Excel 16.30 (Microsoft Co.)

3.4 Results and Discussion

3.4.1 Embryo-larval B[*a*]P concentrations and B[*a*]P metabolites

Mean measured aqueous B[*a*]P concentrations (± SD) for the embryo-larval exposure were 2.08 (±1.59), 4.11 (±2.61) and 9.11 (±3.54) µg B[*a*]P/L. There were no observed effects on growth or mortality at these measured concentrations.

Results of B[*a*]P metabolite analysis showed an increasing trend in abundance of both the OH-B[*a*]P and Gluc-B[*a*]P with time and exposure concentration. A significant increase in OH-B[*a*]P was observed at 12 (chi-square=9.593, df=5, p=0.0207) and 49 (chi-square=10.78, df=5, p<0.0001) days of exposure (Figure 3.2A). Likewise, a significant increase was observed in gluc-B[*a*]P at 49 days of exposure (One-way ANOVA, F=60.02, p<0.0001; Figure 3.2B). The measured abundances of B[*a*]P metabolites were significantly less than what has been reported in fathead minnow larvae at the same life-stage (Grimard et al., 2020). Additionally, in the present study, no detectable abundance of gluc-B[*a*]P was measured on days seven, 12, or 21 of exposure, despite showing phase II (GST) activity during the early developmental stages (Figure F.2). Because the glucuronide is the primary metabolite of glucuronosyltransferase (UDPGT) (Gelboin et al., 1980), this observation may be indicative of absence or limitation in UDPGT activity during the first developmental phases of white sturgeon.

To our knowledge, there is no information regarding uptake and biotransformation of B[*a*]P in white sturgeon. White sturgeon are unique in physiology, as they are slow-growing and generally have higher lipid content, comparative to other species (Birstein, 1993). Lipid content is known to be a leading factor driving the uptake of lipophilic organic contaminants, such as B[*a*]P (McKim et al., 1985; Gelboin et al., 1980; McKim & Erickson, 1991). In the present study, the embryo-larval white sturgeon showed slightly higher whole-body lipid content during the egg and yolk-sac stages compared to other fish species (Foekema et al., 2012; Grimard et al., 2020); however, during the free-feeding stage, the whole-body lipid content decreased significantly (Table 3.1). Compared to other species at the free-feeding stage, such as fathead minnow (Grimard et al., 2020) and common sole (*Solea solea*) (Foekema et al., 2012), which had a whole-body lipid content averaging 2.84% and 2.45%, respectively, free-feeding white sturgeon in this study showed a substantially lower whole-body lipid content (0.25-1.38%). The decrease in lipid content is likely a result of a rapid increase in growth observed in the free-feeding stage and will contribute to a lesser uptake of B[*a*]P. Accordingly, a lesser uptake in B[*a*]P will result in less available parent compound for biotransformation. In addition, white sturgeon are shown to have slower rates of biotransformation compared to other species (Liu et al., 2012). Therefore, limited uptake in combination with slow rates of biotransformation likely contributed to the reduced B[*a*]P metabolite abundances. As a result, embryo-larval white sturgeon are more likely subject to the teratogenic (Jönsson et al., 2007; Schiwy et al., 2015) effects associated with AhR-binding when exposed to B[*a*]P, rather than the genotoxic effects associated with the formation of toxic metabolites (Wang et al., 2010; Yuan et al., 2017).
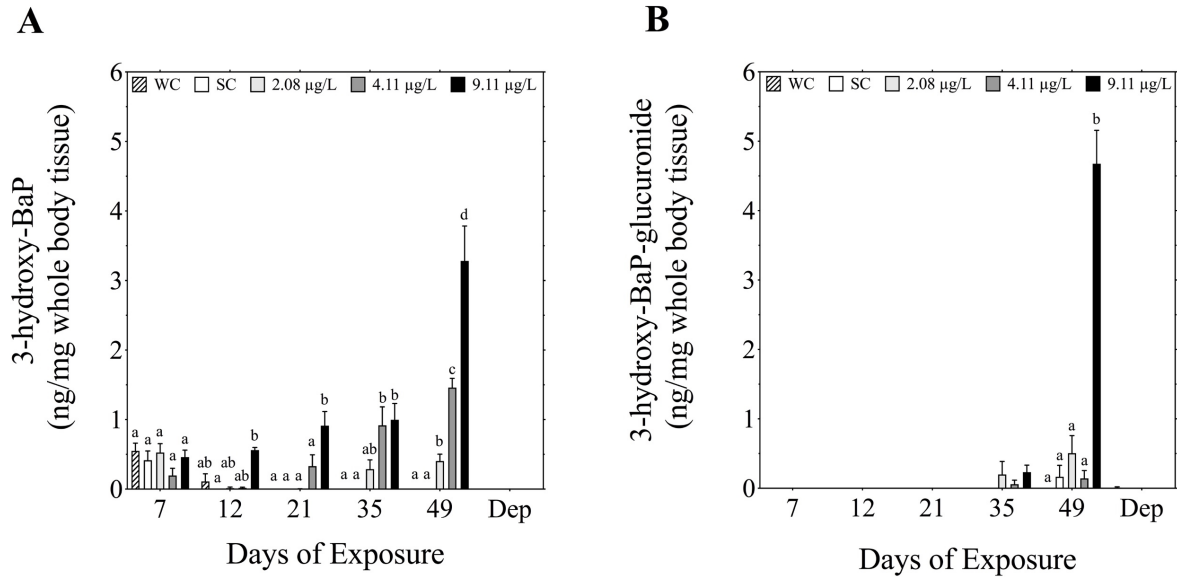
Figure 3.1. Abundance of 3-OH-B[*a*]P (A; ng/mg whole body tissue) and 3-OH-B[*a*]P - glucuronide (B; ng/mg whole body tissue) in whole-body embryo-larval white sturgeon after seven, 12, 21, 35 and 49 days of exposure to increasing concentrations of B[*a*]P as well as water control (WC) and solvent control (SC). Data are expressed as mean ± SEM Different letters denote a significant difference in B[*a*]P metabolites between treatment groups within each respective time point. No letters indicate no significant differences between treatment groups within the respective time point (Non-parametric analysis: Kruskal-Wallis with Dunn's multiple comparison test, α = 0.05; Parametric analysis: One-way ANOVA with Tukey's HSD, α = 0.05). No abundance of gluc-B[*a*]P was measured on day 7, 12, or 21 days of exposure.

3.4.2 Embryo-larval model parameterization and performance

Whole-body concentrations of B[a]P metabolites, represented as B[a]P equivalents, were predicted using the one-compartment embryo-larval model. The model was parameterized using direct measurements of wet mass and lipid content, and calibrated k_{MET} rates. Values for k_{MET} were scaled from an *in vitro* clearance value of 0.00078 mL/h/mg protein (Table 3.1).

A significant correlation was observed between the measured metabolite abundances and the predicted values from the one-compartment embryo-larval model. The model displayed good predictive power, with 62% of predictions deviating less than 5-fold of the measured values, and 81% of the predictions deviating less than 10-fold of the measured values. An RMSE of 0.92 *log* units was calculated, which is slightly higher than when this model was used to make predictions of B[a]P metabolites in embryo-larval fathead minnow (0.6371) (Grimard et al., 2020).

The major limitation to generating accurate predictions of B[a]P metabolites with the one-compartment embryo-larval model is accurately parameterizing k_{MET}. In the present study, when k_{MET} was allometrically scaled from *in vitro* intrinsic clearance measured directly from sub-adult white sturgeon livers (0.219 ± 0.070 mL/h/mg protein, Appendix D), model predictions were greatly over-estimated (>100-fold). Similarly, a large over-prediction was observed when k_{MET} was scaled using half the lowest observable detection (LOD) value for the *in vitro* clearance assay (0.05 mL/h/mg protein) (OECD, 2018). We could not attribute the over-predictions to differences in the fractional liver volume or blood flow parameters, used in the IVIVE equations, between the embryo-larval and sub-adult life stages. Therefore, k_{MET} was internally calibrated using half our measured metabolite abundance data points. The training data showed a greater number of predictions (86%) within one order of magnitude (Figure I.1) compared to the test data set (Figure 3.3). However, a smaller RMSE was calculated in the test data suggesting a better fit. In the test data set, the discrepancies were a result of two data points that were greatly over-predicted and two data points that were greatly under-predicted. These data points are likely a result of individual differences in uptake and biotransformation, and represent the extremes on both sides of the spectrum.

When the test data set was plotted against exposure time (Figure I.2), it was observed that discrepancies occurred particularly during the first two phases of development, i.e., the egg and yolk-sac stage. This result is comparable to what has been observed previously when this model was used to predict B[a]P metabolites in embryo-larval fathead minnow (Grimard et al., 2020). In fathead minnow, it was concluded that biotransformation was underestimated during the egg and yolk-sac stages of development as an underprediction of B[a]P metabolites was observed. Studies with zebrafish larvae show that extensive biotransformation can occur as soon as gastrulation (Otte

et al., 2010; LeFol et al., 2017); therefore, it is likely that biotransformation in the embryo-larval stage is greater at the onset of development than what was calculated. The observations in embryo-larval white sturgeon support this conclusion during the egg stage; however, a trend of over-predictions was observed during the yolk-sac stage. Because B[*a*]P toxicity can be elicited either by AhR binding and/or through the generation of toxic metabolites, the extent of biotransformation in the embryo-larval life stage must be better understood to make accurate conclusions of the cause of toxicity.

Table 3 1. Physiological parameters used in the one-compartment model for embryo-larval White sturgeon (*Acipenser transmontanus*).

Life stage (dpf[a])	Wet mass (mg ± SD)	Lipid (%)	K_{MET} (1/d)[b]
7	49.11 ± 10.61	2.85 ± 0.42	0.0016
12	32.30 ± 6.78	3.62 ± 0.91	0.0013
21	40.09 ± 6.45	2.99 ± 0.71	0.0015
35	49.38 ± 8.51	2.54 ± 1.48	0.0019
42	59.5 ± 15.83	1.38 ± 0.16	0.0033
49	82.60 ± 27.88	0.47 ± 0.32	0.0097
56	124.15 ± 36.63	0.25 ± 0.16	0.0183

[a] days post fertilization
[b] whole-body biotransformation; internally calibrated and calculated through allometric scaling
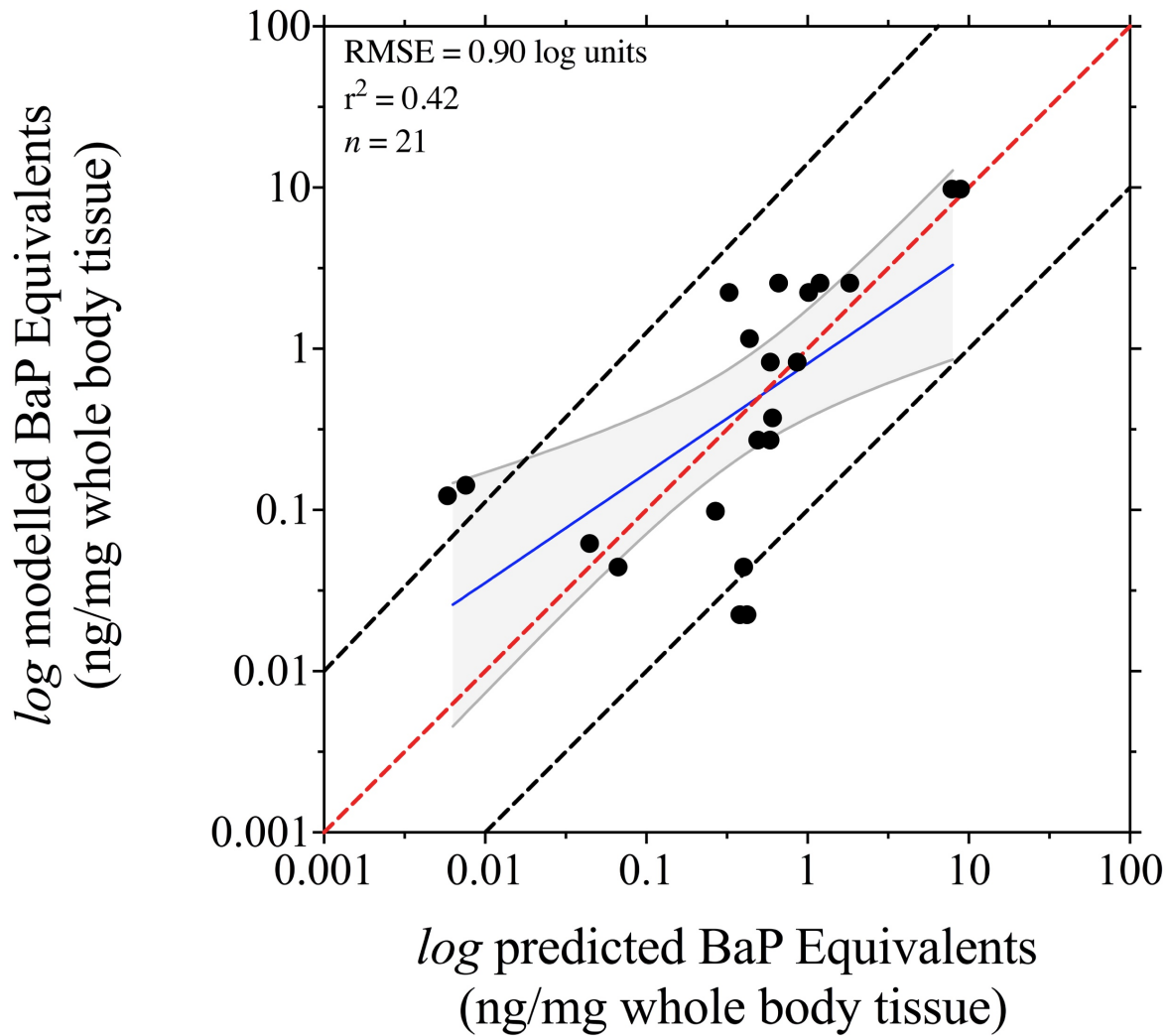
Figure 3.2. Relationship between predicted and measured concentrations of B[*a*]P equivalents using the test data set of 21 data points for validation. The red dashed line represents the equality line, the black dashed lines represent the ± 10-fold deviation from equality, and the solid blue line represents a linear regression with associated 95% confident intervals (grey). Predicted B[*a*]P equivalents were obtained directly from model outputs and measured B[*a*]P equivalents were calculated as mass concentrations that are independent of differences in molecular mass the parent B[*a*]P and the two measured metabolites, OH-B[*a*]P and gluc-B[*a*]P. RMSE, root mean squared error.

3.4.3 Sub-adult model parameterization and performance

A sub-adult PBTK model for white sturgeon was developed to predict the bioconcentration of organic contaminants. Parameterization of tissue volume, lipid content, and water content was determined experimentally, and the measured values were directly implemented in the model (Table 3.2). The modelled value for cardiac output and oxygen consumption did not significantly differ from the measured values (t-test, t_6=0.4067, p=0.6983). Likewise, the modelled value for oxygen consumption did not significantly differ from the literature values (t-test, t_6=0.9207, p=0.3927), which indicates that the scientific literature data was sufficient for model parameterization.

An experimental data set, comprised of 39 data points, was compiled for evaluation of the sub-adult white sturgeon model. This data set consisted of measured internal or muscle concentrations from white or Chinese sturgeon that were aqueously exposed to various organic contaminants ranging in log K_{ow}s from 0.53 to 4.40. Specific exposure conditions, i.e., chemical concentrations, temperature, dissolved oxygen, and fish mass, were also included (Table J.1). The sub-adult PBTK model showed relatively good performance with 59% of predicted values deviating less than 5-fold from the measured values, and 90% of predicted values deviating less than 10-fold from the measured values (Figure 3.4). Additionally, the model had an RMSE of 0.68 log units, and the r^2 was 0.81. The model performed equally well compared to models for other species of fishes (Stadnicka et al., 2012; Brinkmann et al., 2016; Grimard et al., 2020).

PNP (p-nitrophenol) and molinate showed the most accurate predictions with all data points deviating less than 5-fold from equality. The experimental data sets for both chemicals were specific to white sturgeon, and therefore, we have a satisfactory level of confidence that our model is accurately parameterized for this species. Sulfamethazine had relatively accurate predictions, except for one data point that was largely over-predicted, and avermectin-B1 showed consistent over-predictions of approximately 10-fold for all data points. Both of these data sets were obtained from the Chinese sturgeon. Therefore, slight interspecies differences in physiology might have contributed to the observed discrepancies.

Table 3.2. Physiological parameters used in the PBTK model for sub-adult White sturgeon (*Acipenser transmontanus*). Values were determined from n=11 3-year-old fish with a body length of 40.6 ± 2.74 cm and a wet mass of 510 ± 105 g.

Parameter	Description	Value (mean ± SD)
W	Body wet mass *(kg)*	model input
Q_c	Cardiac output *(L kg^{-1} h^{-1})*	calculated
VO_2	Oxygen consumption rate *(mg kg^{-1} h^{-1})*	calculated
Q_w	Effective respiratory volume *(L kg^{-1} h^{-1})*	calculated
Compartment volumes (liters)		
V_l	Volume of the liver compartment	0.029 ± 0.004
V_m	Volume of poorly perfused tissues	0.894 ± 0.013
V_r	Volume of richly perfused tissues	0.058 ± 0.010
V_f	Volume of the fat compartment	calculated
Arterial blood flow to compartments (fraction of cardiac output)		
Q_l	Arterial blood flow to liver compartment	0.071 ± 0.025
Q_m	Arterial blood flow to poorly perfused tissues	0.717 ± 0.175
Q_r	Arterial blood flow to richly perfused tissues	0.202 ± 0.156
Q_f	Arterial blood flow to fat compartment	0.010 (assumed)
Lipid content of tissue compartments (fraction of body wet mass)		
α_l	Lipid content of the liver compartment	0.306 ± 0.078
α_m	Lipid content of poorly perfused tissues	0.026 ± 0.009
α_r	Lipid content of richly perfused tissues	0.014 ± 0.007
α_f	Lipid content of the fat compartment	0.522 ± 0.168
Water content of tissue compartments (fraction of body wet mass)		
γ_l	Water content of the liver compartment	0.510 ± 0.057
γ_m	Water content of poorly perfused tissues	0.757 ± 0.022
γ_r	Water content of richly perfused tissues	0.848 ± 0.029
γ_f	Water content of the fat compartment	0.342 ± 0.217
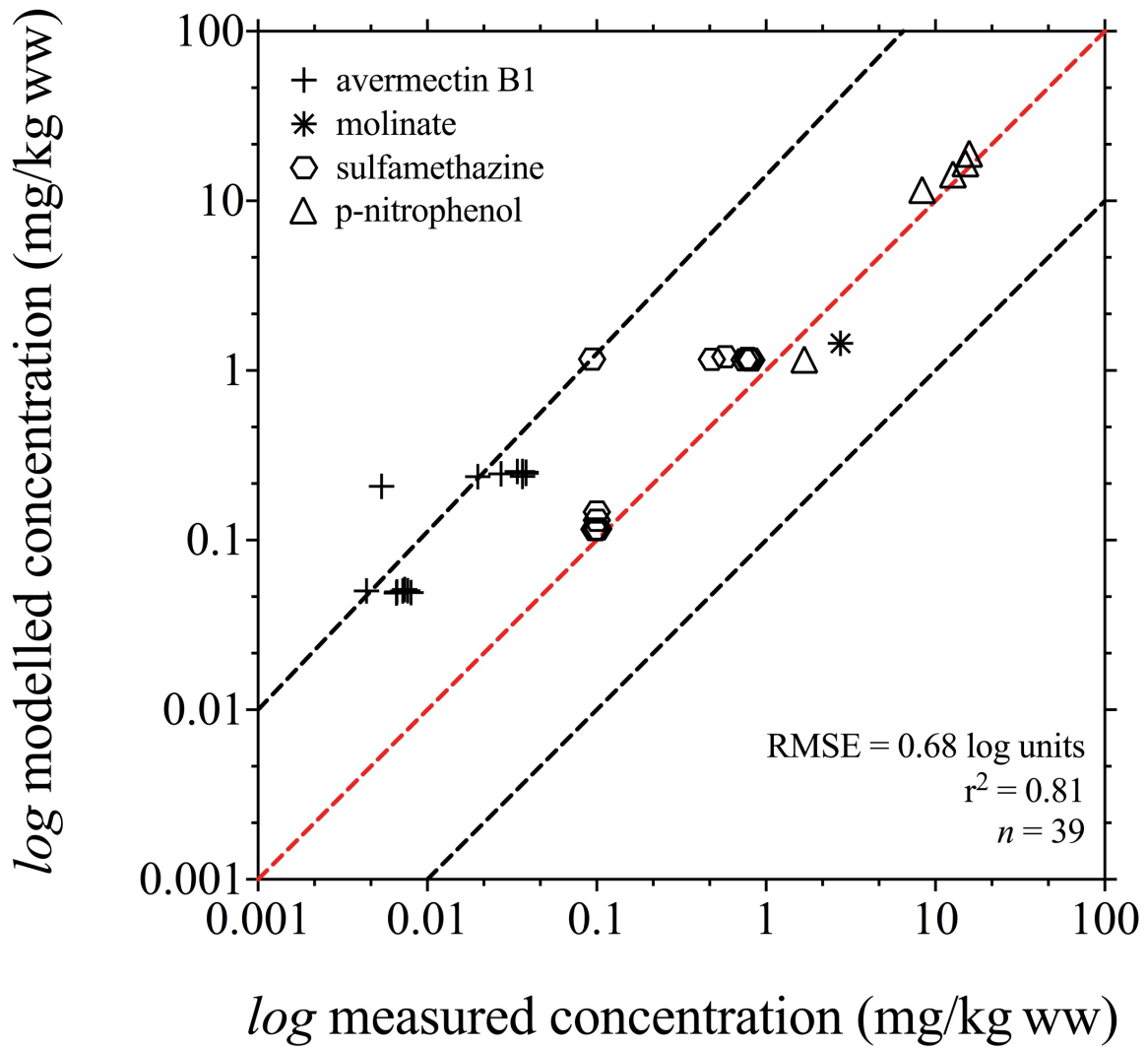
Figure 3.3. Relationship between measured and modelled internal concentrations of avermectin B1, molinate, sulfamethazine, and *p*-nitrophenol in sub-adult white sturgeon. The red dashed line represents the equality line, and the black dashed lines represent the ± 10-fold deviation from equality. RMSE, root mean squared error; ww, wet weight.

3.4.3.1 P-nitrophenol

PNP originates as a residue of organophosphates and elicits toxicity primarily through mitochondrial oxidative phosphorylation (TenBrook et al., 2006; Lam et al., 2013). While PNP can be actively biotransformed, it was observed that aquatic organisms, including white sturgeon, can depurate the majority of parent PNP unchanged. It was concluded, however, that extensive biotransformation is possible when required (TenBrook et al., 2006). In the present model, the biotransformation of PNP was not included. While the integration of biotransformation could improve model outputs in some PNP exposure scenarios, our data shows that it is not necessary in all cases.

3.4.3.2 Molinate

Molinate is a commonly used herbicide that is leached into groundwater and, subsequently, rivers and lakes (Tjeerdema et al., 1988; Cochran et al., 1997). Similar to B[a]P, molinate is actively biotransformed (Tjeerdema et al., 1987; Tjeerdema et al., 1988a; Tjeerdema et al., 1988b); however, biotransformation of molinate was not included in the model. The experimental data set provided only a single data point after 24 hours of depuration. Our data show that, for this exposure scenario, the PBTK model could accurately predict the depuration of the parent compound, and a biotransformation parameter was not needed. It is possible, as shown with other chemicals (Liu et al., 2012), that white sturgeon have limited biotransformation capacity for molinate. Integration of biotransformation might be necessary, however, for other species.

3.4.3.3 Avermectin-B1

Avermectin-B1 is a widely used pesticide that can be leached into nearby bodies of water (Halley et al., 1993; Shen et al., 2005). In fish, avermectin-B1 shows minimal bioconcentration (Halley et al., 1993; Van den Heuvel et al., 1996) and is not readily biotransformed (Shen et al., 2005). Therefore, it is unlikely the absence of biotransformation in the model would contribute to the over-predictions. Instead, it is suggested the large molecular size of avermectin-B1, which is not represented in the model, inhibits membrane permeability, and subsequently, bioaccumulation (Van den Heuvel et al., 1996). Additionally, it has been shown that interspecies differences in kinetics exist for avermectin-B1 (Shen et al., 2005). Therefore, it is possible that differences between Chinese and white sturgeon also contributed to the inaccuracies in model predictions.

3.4.3.4 Sulfamethazine

Sulfamethazine is a multi-purpose agricultural product used as a growth promoter and prophylactic treatment in production animals that can be excreted and contaminate the surrounding water bodies (Hou et al.,2003; Guo et al., 2018). In fish, the compound has been shown to have acute toxicity, reproductive effects, and alter biochemical, hematological, and antioxidant responses (Ji et al., 2012; Ramesh et al., 2018). Sulfamethazine is an ionizable chemical that is primarily biotransformed into N^4-acetyl-sulfamethazine (Hou et al., 2003). The absence of biotransformation in the model might be a contributing factor to the observed over-predictions. Additionally, bioaccumulation of ionizable compounds is shown to be difficult to predict as the ambient pH will affect the extent of uptake (McKim et al., 1991; Hou et al., 2003; Brinkmann et al., 2016).

3.4.4 Conclusions and further directions

The present study parameterized and validated a one-compartment embryo-larval model and a sub-adult PBTK model for the uptake and biotransformation of organic chemicals in white sturgeon. Both models were shown to be accurate, with 81% to 90% of predictions within 10-fold of measured values. However, the parameterization of biotransformation remains a limitation to the current models. For the embryo-larval model, further research should pertain to developing techniques to measure chemical-specific biotransformation rates (Nichols et al., 2013; Chen et al., 2016; Fay et al., 2017). In the sub-adult stages, the data sets regarding chemical-specific biotransformation in white sturgeon should continue to be expanded.

As white sturgeon are presently an endangered species in northwestern Canadian and U.S. rivers, TK models are particularly advantageous as they can be used to simulate exposure scenarios when *in vivo* assessment is unethical or impractical. Using TK models in this context can support risk assessment in this species by allowing for a better understanding of chemical bioaccumulation and the concentrations that reach the target tissues. Furthermore, the power of TK models for white sturgeon could be further improved if combined with toxicodynamic (TD) models to create a TK-TD model framework, allowing for predictions of both chemical bioaccumulation and associated effects. The models presented in this research must continue to be tested against more chemicals and exposure scenarios in order to broaden the understanding of the kinetics of contaminants in white sturgeon, and the influence bioaccumulation of such chemicals might have on their health and survival.

3.5 Acknowledgements

CHAPTER 4: GENERAL DISCUSSION

4.1 Thesis objectives and overview

The main objective of this thesis, in its entirety, was to develop life stage-specific toxicokinetic (TK) models for two species of fish with distinctly different physiology, the fathead minnow and white sturgeon. These models were then used to characterize the uptake and biotransformation of the rapidly biotransformed model chemical benzo[*a*]pyrene (B[*a*]P). As described in Chapter 1, TK models for aquatic species are presently developed and validated for neutral organic chemicals (Nichols et al., 1990; Arnot & Gobas, 2004; Stadnicka et al., 2012; Brinkmann et al., 2016). These models, however, often lack specificity for chemicals that are actively biotransformed, and few have been developed specifically for early life stages (ELS). Many environmental pollutants of concern are subject to biotransformation that results in either their detoxification or activation. The effect of metabolism is further complicated in ELS that are often considered more sensitive and are shown to have different metabolic capacities compared to the adult life stage (Knöbel et al., 2012; Le Fol et al., 2017). Therefore, life stage-specific TK models developed for actively biotransformed chemicals would contribute to increasing the applications that TK models have in research and ecological risk assessment (ERA). The TK models developed and described in this thesis can also be used to extrapolate between life stages and better understand life stage differences in biotransformation. Life stage extrapolation is a useful application as ELS are increasingly being used as alternatives to replace or refine *in vivo* exposure experiments with adult organisms. Understanding life stage differences is essential for being able to draw accurate conclusions on the toxicity in adult organisms from data gathered in the ELS.

The objective of the research conducted in Chapter 2 was to characterize the biotransformation of B[*a*]P in the embryo-larval and adult life stages of fathead minnow, extrapolate biotransformation from *in vitro* to *in vivo* and across life stages, and to parameterize and validate life stage-specific TK models. To meet this objective, *in vivo* exposures to aqueous B[*a*]P were conducted with embryo-larval and adult fathead minnows in which measurements of phase I and II biotransformation, major B[*a*]P metabolites, and physiological parameters, such as lipid fractions and cardiac output, were obtained. The first major finding of Chapter 2 was that at low exposure concentrations (<5 μg B[*a*]P/L), there was no induction in either phase I or II biotransformation in either life stage of fathead minnows. This observation indicates that our exposures likely occurred in the first-order portion of the Michaelis-Menten curve and did not approach enzyme saturation conditions. First-order kinetics are preferred for integrating biotransformation into TK models, as they indicate that biotransformation will increase

proportionally with substrate concentration and, therefore, saturation does not need to be accounted for. The conclusion of first-order kinetics was complementary to the second major finding of Chapter 2, which was that in both life stages, the abundances of B[*a*]P metabolites increased in a proportional manner with increasing aqueous B[*a*]P concentrations. As a result of the above findings, a single value of B[*a*]P biotransformation was determined from measurements in the livers of adult fathead minnows. This value was extrapolated to *in vivo* in the adult life stage, and allometrically scaled to whole-body metabolism in the embryo-larval life stage using measurements of embryo-larval cardiac output. The respective life stage-specific biotransformation values were integrated into life stage TK models, which were used to make predictions of the abundances of B[*a*]P metabolites. Both the embryo-larval and adult model generated accurate predictions of B[*a*]P metabolites within one order of magnitude. The findings of Chapter 2 demonstrate that biotransformation of B[*a*]P can be successfully integrated into life stage-specific models for the fathead minnow.

For Chapter 3, the objectives were to develop life stage-specific TK models for the accumulation of organic contaminants in embryo-larval and sub-adult white sturgeon. In this chapter, only the embryo-larval study and associated model focused on biotransformation of B[*a*]P, as an aqueous exposure to B[*a*]P in the sub-adult life stage was not logistically possible. Instead of conducting an exposure to B[*a*]P in the sub-adult life stage, experimental data sets of aqueous exposures to organic contaminants were compiled from the literature and used for model validation. Biotransformation of B[*a*]P, however, was measured in sub-adult white sturgeon. Therefore, the model can be used to make predictions of B[*a*]P metabolites in the tissues, but the model predictions cannot be validated. This concept was used to make comparisons between life stages in Section 4.2 and between species in Section 4.3. The first and second main findings of Chapter 3 were that, similar to fathead minnows, there was no observed induction of either phase I or phase II activity with B[*a*]P exposure in the embryo-larval stage, and abundance of B[*a*]P metabolites increased with increasing B[*a*]P exposure concentrations. However, compared to the fathead minnow, embryo-larval sturgeon showed significantly lesser abundance (1,000-fold less) of B[*a*]P metabolites, despite higher exposure concentrations. This observation led to the conclusion that embryo-larval white sturgeon might have significantly lesser metabolic capacity compared to other species of fishes. Measurements of biotransformation in the embryo-larval and sub-adult white sturgeon supported this conclusion, as the biotransformation rates were shown to be approximately 832-fold and 3.5-fold less than what was measured in fathead minnows, respectively. The final finding of Chapter 3 was that the embryo-larval one-compartment model could accurately predict the uptake and biotransformation of B[*a*]P and the sub-adult multi-

compartment models could accurately predict the internal concentrations of organic chemicals within one order of magnitude of equality. Findings from Chapter 3 demonstrated that the one-compartment embryo-larval and adult multi-compartment TK models can be used for inter-species extrapolation; however, more research regarding life stage and species-specific biotransformation is required to improve model accuracy.

4.2 Cross life stage differences in the uptake and biotransformation of B[*a*]P

Understanding life stage differences in uptake and biotransformation of chemicals is essential for better understanding differences in species sensitivity. In both fathead minnows and white sturgeon, differences in the uptake and biotransformation of B[*a*]P between the embryo-larval and adult life stages were observed. However, these life stage-specific differences were difficult to quantify as the individual life stage/species exposures were conducted at different exposure concentrations and durations, biotransformation capacity and metabolite concentrations were measured in non-comparable tissues, and in the case of white sturgeon, a B[*a*]P exposure with sub-adult white sturgeon was not logistically possible. Therefore, to better quantify life stage differences in uptake and biotransformation of B[*a*]P, the TK models, developed and described in this thesis (Appendix I and J), were run for 30 days using the same exposure concentration (2.0 μg B[*a*]P/L) for each species and life stage and used to make predictions of whole-body internal concentrations of parent B[*a*]P and B[*a*]P metabolites (represented as B[*a*]P equivalents). The sub-adult white sturgeon model was parameterized using a measured value for intrinsic clearance, and the bile volume was assumed to be 20% of the liver volume, based off information from the fathead minnow measurements and previous studies (Talbot & Higgins, 1982), as this parameter was not measured. The respective concentrations were plotted against exposure time and a four-parameter variable slope non-linear regression model was fitted to the data using GraphPad Prism 8® (GraphPad Software, Inc., San Diego, CA, USA) (Figure 4.1).

In the fathead minnow, the adult life stage had lesser uptake of parent B[*a*]P and lesser abundances of B[*a*]P metabolites compared to the embryo-larval life stage (Figure 4.1 A,B). However, in the embryo-larval life stage uptake of B[*a*]P was more rapid compared to the adults and reached steady-state essentially at the onset of exposure. This observation was likely a result of a higher rate of biotransformation and the high intrinsic clearance of B[*a*]P by the liver, the major organ of biotransformation, of adult fishes. High intrinsic clearance means, in this case, that the adult liver had the capacity to almost quantitatively clear the inflow fraction of unbound chemical from the systemic circulation. Therefore, the adult life stage was able to completely biotransform and clear the unbound parent compound from the liver throughout the entire exposure

period and maintain a steady-state. While the embryo-larval fathead minnows showed greater concentrations of B[*a*]P and B[*a*]P metabolites relative to adult fish, the comparative uptake and accumulation was slower and did not reach steady-state. This observation suggests that embryo-larval fathead minnows had a slower rate of biotransformation of B[*a*]P and had a lesser capacity to clear B[*a*]P from the systemic circulation.

In white sturgeon, the two life-stages showed similar uptake of parent B[*a*]P, but the sub-adult life stage showed a slightly higher accumulation of B[*a*]P metabolites. For parent B[*a*]P, the embryo-larval uptake was linear while the sub-adult uptake appeared to be approaching steady-state (Figure 4.1C). This observation was partly a result of a greater biotransformation rate and capacity of B[*a*]P in the sub-adult stage, which was supported by the observation of greater B[*a*]P metabolites predicted in the sub-adult life stage (Figure 4.1D) but might also be a result of embryo-larval growth. An increase in biomass with embryo-larval growth and development allows for a greater uptake of parent B[*a*]P. Because embryo-larval white sturgeon do not have the capacity to fully clear parent B[*a*]P from the systemic circulation, the internal parent B[*a*]P concentration continues to increase, and a steady-state will not occur. The differences between life stages of white sturgeon, in contrast with what was observed between life stages in the fathead minnow, however, was small. The comparatively less drastic response between life stages of white sturgeon was likely because of the substantially slower rate of biotransformation observed in fathead minnows compared to white sturgeon. As a result, the onset of steady-state in the sub-adult white sturgeon was later in exposure compared to fathead minnows, which allows the accumulation of B[*a*]P and B[*a*]P metabolites in embryo-larval white sturgeon to approach similar concentrations as in the sub-adults.

The slower uptake and accumulation of B[*a*]P and B[*a*]P metabolites in the embryo-larval life stage are a result of slower biotransformation compared to the adult life stage. Likely, embryo-larval livers are limited in their ability to produce a metabolic response, and therefore, the phase I and II enzymes required for biotransformation of B[*a*]P might not be fully expressed. This conclusion was supported by a complementary study to the fathead minnow described in Chapter 2, which used samples from the Chapter 2 exposures to examine the expression of the *cyp1a1* gene in embryo-larval and adult fathead minnows after four and 21 days of exposure (DeBofsky et al., 2020; Appendix H). The results showed that initially, the embryo-larval and adult stages had comparable expression of *cyp1a1*. After 21 days of exposure, however, the embryo-larval life stage showed a lesser expression of *cyp1a1*, despite having been exposed to a higher B[*a*]P concentration than adult fish. These results suggest that the ability to generate the phase I biotransformation enzyme, CYP1A, might had been limited in the embryo-larval life stage compared to the adult life

stage. Similar results have been shown in studies conducted with embryo-larval zebrafish in which *cyp1a1* induction was shown to be relatively unchanged over the initial phases of development (Bräunig et al., 2015; Meyer-Alert et al., 2018; Meyer-Alert et al., 2019). However, definite conclusions on the extent of these differences cannot be made as gene expression was measured in the whole body of the embryo-larval fishes and liver of the adult fishes, and therefore, *cyp1a1* expression in the embryo-larval fish was likely subject to dilution.

The observed life stage differences in the uptake and biotransformation will likely result in differential effects of B[*a*]P at different life stages. Greater rates of biotransformation in the adult life stage would suggest greater susceptibility to the genotoxic effects of B[*a*]P exposure. The greater risk of genotoxicity is because the enzyme, CYP1A, responsible for detoxification of B[*a*]P, is also responsible for producing the highly genotoxic epoxide benzo[*a*]pyrene diol epoxide (BPDE) by reacting with a primary metabolite through the epoxide pathway (described in Section 1.4.2). Higher rates of biotransformation suggest that the epoxide pathway will occur more often, and a greater abundance of BPDE will be generated. Once BPDE is generated, the epoxide can form DNA adducts and result in carcinogenesis, neoplasms, carcinomas, and adenomas (Wessel et al., 2010; Corrales et al., 2014; Lerebours et al., 2014, Yuan et al., 2017). These genotoxic effects might contribute to further effects such as reduced growth and reproduction, and increased mortality. As a result of the slower rates of biotransformation and greater uptake of parent B[*a*]P in the embryo-larval life stage, genotoxicity was not hypothesized to represent the main effect associated with embryo-larval exposure to B[*a*]P. It should be noted, however, that some extent of genotoxicity might still occur in the embryo-larval stage and might act as precursor to the carcinogenic effects of B[*a*]P expected in the adult life stage. Instead, other effects associated with increased binding to the aryl hydrocarbon receptor (AhR) are of concern for the embryo-larval life stage. These effects include teratogenicity, embryotoxicity, pericardial and yolk-sac edema, immunosuppression, and oxidative stress signaling (Carlson, Li & Zelikoff, 2004; Kim & Lee, 2000; Chikae et al., 2004; Doering et al., 2014; Schiwy et al., 2015). A study conducted by Pannetier et al. (2019) provides an example of such differential toxicity of B[*a*]P across life stages. In this study, the differences in biometrics, malformations, DNA damage, ethoxyresorufin-O-deethylase (EROD) activity, and swim speed among the embryonic, larval and juvenile stages of Japanese medaka when exposed aqueously to B[*a*]P were investigated. The results of the study showed that the embryonic and larval life stages had a comparatively higher incidence of lethality, malformations, and DNA breaks than the adult life stage. It was concluded that, as a result of the differences, the embryonic life stage was accordingly more sensitive.
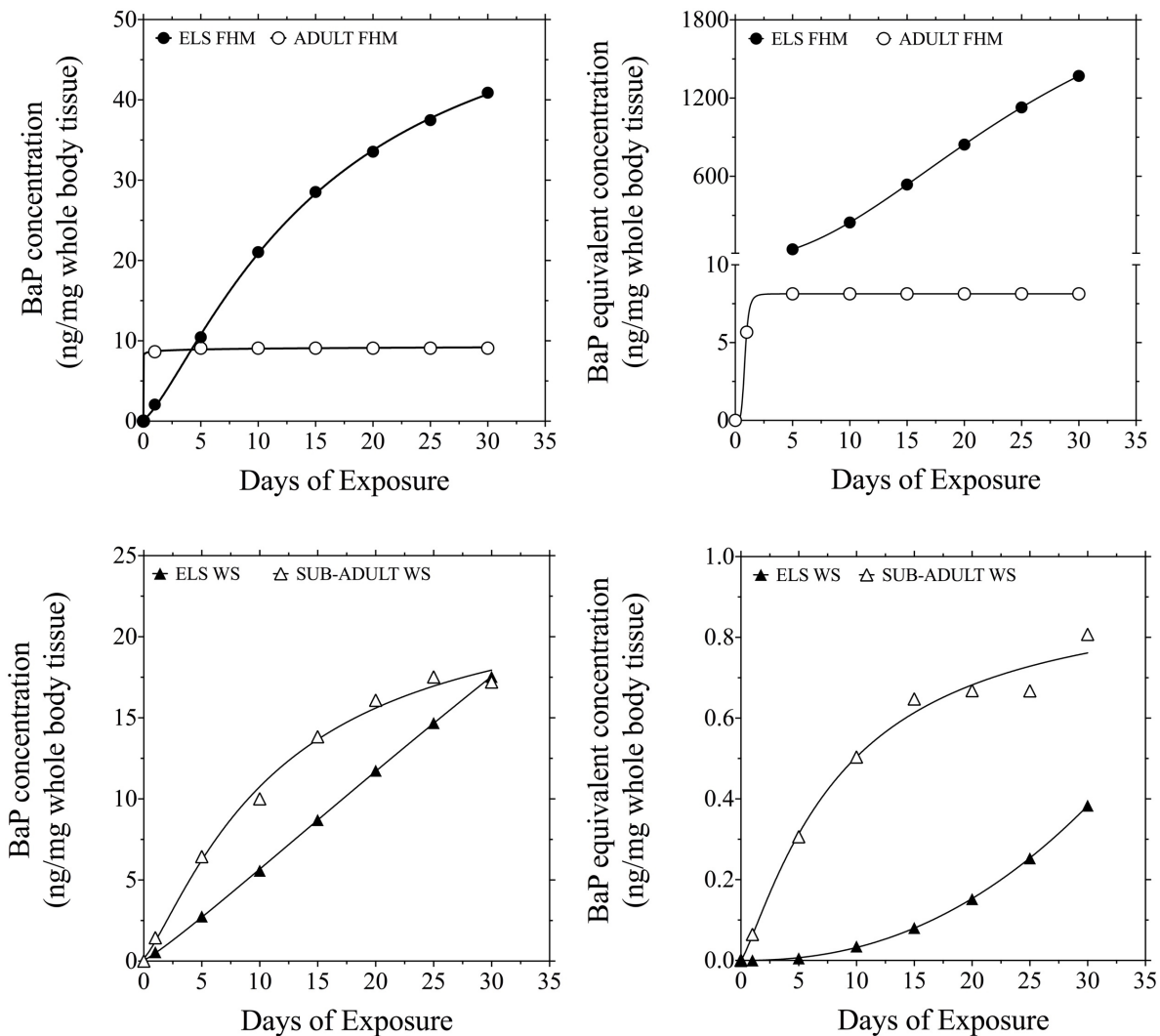
Figure 4.1. Comparison of the uptake and biotransformation of B[*a*]P between life stages within species when a 2.0 µg B[*a*]P/L aqueous exposure was simulated for 30 days. Figure A (fathead minnow; FHM) and C (white sturgeon; WS) show the differences in predicted internal parent B[*a*]P concentrations (ng/mg whole body tissue) between the embryo-larval (ELS) and adult stages within the respective species. Figure B (FHM) and D (WS) show the differences in predicted internal B[*a*]P metabolites (ng/mg whole body tissue), represented as B[*a*]P equivalents, between the embryo-larval and adult life stages within the respective species. All concentration values were generated as predictions using the one-compartment embryo-larval model and multi-compartment adult model described in Appendices I and J, respectively. A four-parameter variable slope non-linear regression model was used to generate the trend line.

4.3 Inter-species differences in the uptake and biotransformation of B[*a*]P

Species differences in uptake and biotransformation of chemicals are known to exist. In this section, the inter-species differences in the uptake and biotransformation of B[*a*]P between fathead minnows and white sturgeon will be examined. Expanding on the analysis of uptake and biotransformation of B[*a*]P as a function of life stage that was conducted in Section 4.2, the prediction data from the TK models was rearranged to compare toxicokinetic properties between the two species of fish for each life stage (Figure 4.2). The results show that, for the embryo-larval life stage, white sturgeon had significantly slower uptake and lesser biotransformation of B[*a*]P compared to fathead minnows. This result was expected, as embryo-larval white sturgeon showed a substantially lower abundance of B[*a*]P metabolites compared to fathead minnows (Figure 2.2, Figure 3.1), despite white sturgeon having been exposed to higher concentrations of B[*a*]P. For the adult life stage, the results show that white sturgeon had a greater uptake of parent B[*a*]P compared to the fathead minnow; however, white sturgeon showed a lesser abundance of metabolites. The differences in the adult life stage were likely an outcome of the slower rate of intrinsic clearance measured in sub-adult white sturgeon compared to fathead minnows (3.5-fold less).

These observed differences in uptake and biotransformation of B[*a*]P can be attributed to the distinctly different physiology between fathead minnows and white sturgeon. Fathead minnows are a small, warm water fish, with rapid development, while white sturgeon are a large, cold water, slow-growing fish species. As discussed in Section 1.1.1, the water temperature can have a vast influence on the extent of adsorption at the gill. Higher temperatures result in increases in respiration and ventilation rate, which suggests a greater flux of water to and from the gill. As a result of increased flux, the gills are exposed to a greater amount of a water-borne chemical that can be absorbed. Because the natural environment of fathead minnows is approximately 10°C warmer than the environment of white sturgeon, fathead minnows are comparatively subject to greater and quicker absorption rates. Correspondingly, the rapid development of fathead minnows might also contribute to a greater uptake of B[*a*]P in the embryo-larval fathead minnow by showing increased ventilation rates sooner than embryo-larval white sturgeon. This is because fathead minnow larvae absorb their yolk sacs and transition to the free-feeding stage approximately 5-7 dpf, while white sturgeon do not make the transition to the free-feeding stage until approximately 15-20 dpf. Earlier transition to the free-feeding stage means that fathead minnows are more active, which might result in increased respiration and consequently increased uptake of B[*a*]P from the water. Studies conducted with Senegal sole (*Solea senegalensis*) and sparid gilthead (*Sparus aurata*) larvae showed an allometric relationship between biomass and oxygen consumption,

indicating increases in respiration with development (Parra et al., 2001), and a significant correlation was observed between oxygen uptake and chemical absorption in multiple fish species when exposed to different toxicants (Yang et al., 2000). Additionally, although not a direct species comparison, similar results and conclusions had been made in previous research by Vardy et al. (2013), who attributed greater copper sensitivity in post-yolk sac white sturgeon compared to yolk-sac stage white sturgeon to increased uptake from increased respiration.

Another primary factor, discussed in Section 1.1.1., influencing chemical uptake was tissue lipid content and chemical lipophilicity. B[*a*]P is a lipophilic contaminant that will bioaccumulate in lipid-rich tissues. White sturgeon have a unique aspect in physiology as they generally have higher lipid content compared to other fish species. This higher lipid content was apparent when comparing the sub-adult white sturgeon and adult fathead minnow lipid values (Table 3.2, Table I.2). For example, sub-adult white sturgeon had a liver lipid content of 30%, while fathead minnows only had a liver lipid content of only 7.4%. The higher lipid content likely contributes to the greater uptake of parent B[*a*]P observed in white sturgeon. In contrast, the embryo-larval white sturgeon showed lesser whole-body lipid content compared to the fathead minnow (Table 2.1, Table 3.1), which likely contributes to the lesser uptake of parent B[*a*]P observed in the embryo-larval white sturgeon compared to the embryo-larval fathead minnow. The conclusion of species differences in lipid content contributing to species differences in bioaccumulation is supported by previous studies. An example is provided by Pastor et al. (1996), who observed higher concentrations of organochlorines in red mullet (*Mullus barbatus*) compared to sea mullet (*Mugil cephalus*) and sea bass (*Dicentrarchus labrax*), which had comparatively lower lipid contents.

The differences in biotransformation of B[*a*]P between species can be largely attributed to differences in enzyme abundance and catalytic activities. In the adult life stage, the greater intrinsic clearance rate observed in the adult fathead minnow compared to the sub-adult white sturgeon was indicative of higher enzyme abundance and activity. The conclusion of higher enzyme activity was supported by adult fathead minnows having a larger measured rate of *in vitro* intrinsic clearance (0.742 ± 0.061 mL/h/mg protein) compared to white sturgeon (0.219 ± 0.070 mL/h/mg/protein) and is suggestive of fathead minnows having comparatively larger enzyme abundances, higher enzyme activity, and a higher enzyme affinity for B[*a*]P than white sturgeon. However, measurements of gene expression, such as *cyp1a1*, might better support this conclusion. Phase I and II activity measurements were only assessed in the adult fathead minnow. Therefore, it is not presently possible to directly compare catalytic activity between species for the adult life stage; however, as mentioned above, an assumption of higher catalytic activity in the fathead minnows was made based on the faster measured rate of clearance.

In the embryo-larval stage, while the differences in accumulation of parent B[*a*]P between species was small (1 to 3-fold), large differences (2400-fold) in B[*a*]P metabolite abundances were observed between species (Figure 4.2B). The results suggest that fathead minnows clear much larger amounts of B[*a*]P through their system than white sturgeon. This could result in differences in effects such as genotoxicity. It is likely that, similar to the adult life stage, fathead minnow larvae had larger enzyme abundances, higher enzyme activity, and a higher enzyme affinity for B[*a*]P compared to embryo-larval white sturgeon, possibly due to their more rapid development. While both species showed relatively similar phase I and II activity (Figure 2.2, Figure E.1, Figure F.1), these measurements were only indicative of the potential maximum rate of activity under saturation conditions and do not reflect the actual rates of biotransformation. The direct measurements of whole-body biotransformation showed that embryo-larval fathead minnows had higher rates of biotransformation compared to embryo-larval white sturgeon, which suggests greater comparative enzyme abundance and activity in the embryo-larval fathead minnow. This factor, in combination with greater comparative uptake, was likely the major contributing factor for the differences in B[*a*]P metabolite abundances between species in both life stages. Similar conclusions were made by Liu et al. (2012), who attributed differences in the biotransformation of 6-methoxylated-brominated diphenyl ether-47 (6-MeO-BDE-47) between rainbow trout, goldfish (*Carassius auratus*), and white sturgeon to differences in the abundances and catalytic activity of CYP enzymes.

These species differences in uptake and biotransformation of B[*a*]P are likely to contribute to differences in species sensitivity to B[*a*]P exposure. Based strictly on exposure metrics, as a result of white sturgeon showing a lesser extent of uptake and biotransformation compared to the fathead minnow, white sturgeon are comparatively less likely to be subject to the toxic effects of B[*a*]P. Specifically, these toxic effects include the genotoxicity associated with B[*a*]P biotransformation, and the teratogenic, embryotoxic, and physiological effects of increased AhR ligand binding (discussed above in Section 4.2, and in greater detail in Sections 1.4.2 and 1.4.3). However, mature adult white sturgeon are known to have a greater lipid content compared to other species, and therefore, because of the lipophilic nature of B[*a*]P, white sturgeon might be subject to chronic effects of B[*a*]P exposure, such as carcinogenicity. In contrast, fathead minnows might show increased sensitivity to B[*a*]P exposure relative to white sturgeon due to their larger comparative uptake and biotransformation of B[*a*]P. Compared to other species, however, cyprinids generally show reduced levels of CYP1A activity and do not commonly show genotoxic and carcinogenic effects, even when exposed to a potent carcinogen, such as B[*a*]P (Hawkins et al., 1991, van den Hurk et al., 2017).

Toxicodynamic differences, such as differences in AhR dynamics and transactivation, should also be accounted for when assessing species differences in toxicity. The contributing role of species differences in AhR dynamics to species differences in dioxin-like compound sensitivity was discussed by Doering et al. (2013). It was concluded that differences in species sensitivity are partly a result of species affinity differences to different AhR isoforms. Species differences in transactivation as a result of B[*a*]P exposure have also been reported previously. Lee et al. (2015) observed that the common carp showed the highest CYP1A mRNA induction compared to the Japanese rice fish (*Oryzias latipes*), pale chub (*Zacco platypus*), and zebrafish. In that study, it was concluded that CYP1A mRNA expression correlated with species sensitivity, and therefore, the common carp was determined to be the most sensitive species.
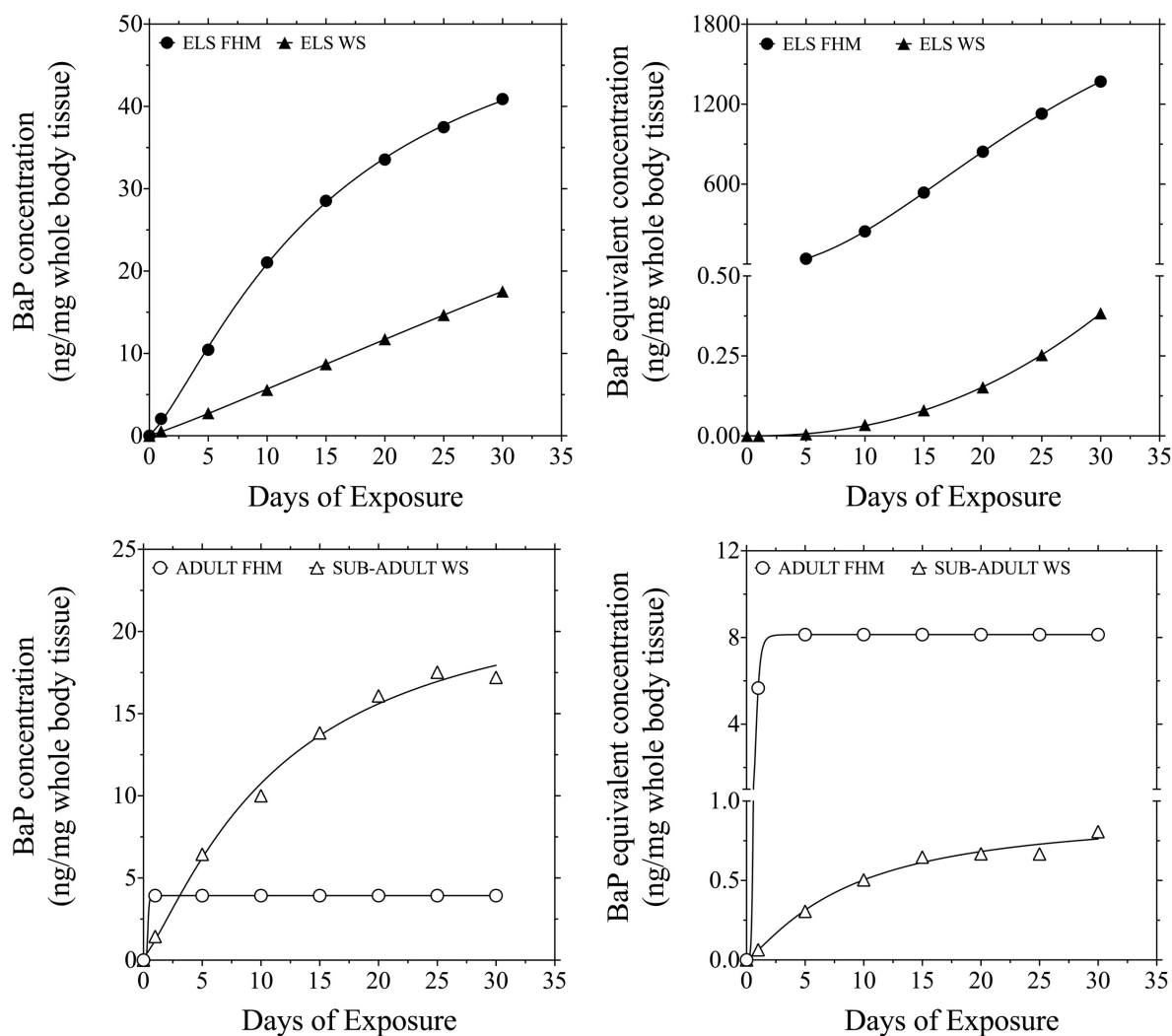
Figure 4.2. Comparison of the uptake and biotransformation of B[*a*]P between the fathead minnow (FHM) and white sturgeon (WS) within life stages when a 2.0 µg B[*a*]P/L aqueous exposure was simulated for 30 days. Figure A (embryo-larval life stage; ELS) and C (adult) show the differences in predicted internal parent B[*a*]P concentrations (ng/mg whole body tissue) between the FHM and WS within the respective life stages. Figure B (ELS) and D (adult) show the differences in predicted internal B[*a*]P metabolites, represented as B[*a*]P equivalents (ng/mg whole body tissue), between the FHM and WS within the respective life stages. All concentration values were generated as predictions using the one-compartment embryo-larval model and multi-compartment adult model described in Appendix I and Appendix J, respectively. A four-parameter variable slope non-linear regression model was used to generate the trend line.

4.4 Advantages of toxicokinetic models in ecological risk assessment

ERA evaluates the relationship between a hazard, i.e., toxicity, and the environmental fate of a chemical, i.e., exposure. A challenge for this type of assessment, however, is the substantial number of chemicals that are released into the environment, and the vast number of species that might be affected. Additionally, exposure patterns of environmental pollutants are often inconsistent, and contaminants typically occur in complex mixtures of several chemicals in the environment (Ashauer & Escher, 2010). TK models might be of advantage and provide useful tools to address some of these challenges. These advantages can be furthered in combination with other assessment tools such as toxicodynamic (TD) modelling, omics, quantitative structure-activity relationships (QSARs), and adverse outcome pathway (AOP) modeling. In the case of omics and AOPs, TK models are useful in relating the internal concentration of a chemical at the target site to molecular initiating events, and key events that result in adverse outcomes. This allows for a framework that can better characterize the specific mechanism of chemical toxicity from exposure to toxic effect.

As described in section 1.2, TK models are predictive *in silico* tools that can estimate the internal chemical concentration in target tissues over the time course of exposure and are parameterized explicitly for the species and chemical of interest. Because of species-specific parameterization, the same TK model structure can be used for cross-species extrapolation. In this thesis, such species extrapolation was conducted between fathead minnow and white sturgeon to make predictions of the internal B[*a*]P metabolite concentrations. Additional examples include previous work conducted by Stadnicka et al. (2012), who used three types of TK models to make predictions of the internal tissue concentrations of 24 organic chemicals in fathead minnow and rainbow trout. Brinkmann et al. (2016) used a multi-species PBTK model to make predictions of the internal tissue concentrations of four to 24 organic chemicals in the fathead minnow, lake trout, rainbow trout, roach, and zebrafish. The ability to extrapolate across-species is important for ERA as often, assessment of a large number of species is required. TK models can make predictions of internal concentrations for species with which *in vivo* exposures have not been conducted or are not ethical and/or practical. When combined with TD models, a TK-TD model framework can provide a better understanding of the species-specific traits that contribute to differences in species sensitivity (Ashauer & Escher, 2010). Examples of such TK-TD models include the model developed by Li et al. (2011), which examined the impact of estrogen and androgen exposure on concentrations of exogenous and endogenous hormones and vitellogenin in fathead minnows and a model developed by Liu et al. (2014), which evaluated the effect of bioaccumulation of B[*a*]P in

the digestive gland of scallops to biomarkers of toxicity, such as hydrocarbon hydroxylase activity and lipid peroxidation.

A challenge to having a large number of chemicals to evaluate, however, is that not all of the chemicals can be used in *in vivo* testing. This lack of ability is because of the ethical, time, and economic limitations associated with *in vivo* testing. In these instances, TK models are particularly useful, as exposure simulations can be conducted to predict the accumulation of the chemical in the target tissues (Ashauer & Escher, 2010). This type of evaluation can be combined with TD models, omics and AOPs, to help explain differences in toxicity between chemicals. TK models, in combination with QSARs, are also useful to evaluate untested chemicals that are actively biotransformed. QSARs relate chemical structure to chemical activity, and therefore, can use information from chemicals with a similar structure to estimate the biotransformation activity of an untested chemical (Ashauer & Escher, 2010; Escher et al., 2011; Grech et al., 2017). This parameter can then be used in TK models to predict accumulation and further evaluated with TD models, omics, or AOPs to make predictions of toxicity. Using this type of evaluation, environmental pollutants that show potential for elevated toxicity can be prioritized for further *in vivo* testing.

Last, in addition to species extrapolations, TK models can be used for *in vitro-in vivo* extrapolation (IVIVE). As demonstrated in this thesis, and in previous research conducted by Nichols et al. (2007), IVIVE can be used to determine TK model parameters, such as biotransformation. IVIVE can also be used in combination with TK models to extrapolate toxicity data. Such extrapolations were conducted by Brinkmann et al. (2014) and Stadnicka-Michalak et al. (2014). TK models used in this capacity are especially useful in ERA as they work to reduce the use of animals, in addition to the cost and time associated with chemical testing.

4.5 Limitations of current work and recommendations for future research

The results of this research increase the scope of applications in which TK models can be used in ERA and for research. However, there are some limitations to the methods used in this thesis, which further research could improve. The limitations and recommendations are as follows:

Parameterization of biotransformation in the embryo-larval life stage:
Accurately parameterizing biotransformation in the embryo-larval stage of both the fathead minnow and white sturgeon was a limitation to achieving accurate predictions from the one-compartment embryo-larval model. In chapter 2, it was observed that biotransformation of B[*a*]P was slightly underestimated in the embryo-larval life stage of fathead minnow, while in chapter 3, biotransformation of B[*a*]P was significantly overestimated in white sturgeon when scaled from

measurements of sub-adult intrinsic clearance. Presently, accurately parameterizing biotransformation in the embryo-larval life stage is difficult as, to our knowledge, measuring the intrinsic clearance in the embryo-larval life stage using the substrate depletion assay is not possible. Attempts to measure intrinsic clearance using whole-body larvae were made in this research study; however, the attempts were unsuccessful. This was likely a result of enzyme dilution while generating the S9 fraction used in the assay from whole-body organisms. The substrate depletion assay requires the S9 to contain a protein concentration of at least 10 mg/mL. While it is possible to achieve this protein concentration in the S9 generated from the whole-body embryo-larval organisms, it is uncertain how much of the protein is the phase I and II enzymes required for biotransformation of B[a]P, and if other proteins and small molecules will inhibit or restrict the enzyme reactions.

Whole-body embryo-larval biotransformation was allometrically scaled from biotransformation measured in adult livers to adapt to this limitation. This method, however, was based on assumptions that parameters such as fractional liver weight, fractional liver blood flow, and intrinsic clearance would be similar between the embryo-larval and adult life stages. It would be beneficial to obtain direct measurements of such parameters in the embryo-larval life stage to improve the estimates of whole-body biotransformation through scaling. Due to the small size of larval fish, direct sampling of the liver through dissection is often impractical. In this case, using methods such as microscopy and histology might be more appropriate to measure liver volume and blood flow. Histology has been used to estimate embryo-larval liver volume in Atlantic cod (*Gadus morhua*) (Wold et al., 2009) and common carp (Fontagné et al., 1998), and microscopy has been used to detect blood flow in the livers of embryo-larval zebrafish (Korzh et al., 2008). To our knowledge, however, no studies have directly measured the rate of blood flow to embryo-larval livers.

Estimates of intrinsic clearance might be improved if livers from pre-maturation free-feeding larvae, large enough for dissection, can be obtained for use in the substrate depletion assays. A limitation to this method, however, would be the number of specimens required to obtain enough liver tissue to generate quality S9 for the assay. Concerning direct measurements of biotransformation from whole-body larvae, generating microsomes from whole-body S9 for use in the substrate depletion assay might be a better choice as microsomes isolate the main enzymes responsible for biotransformation of B[a]P (CYPs and UDPGT) (Guengerich, 1989). However, while microsomes might better concentrate the target enzymes responsible for biotransformation of B[a]P, similar to using S9, the potential of interference from other proteins might still pose a limitation to this method.

Parameterization of bile volume and flow:

A limitation to accurate predictions using the multi-compartment adult model in both the fathead minnow and white sturgeon was the inability to accurately parameterize bile volume and flow. In the fathead minnow, bile volume estimates were based on gall bladder weight in which 1 mg equaled 1 μL. For white sturgeon, bile volume was assumed to be 20% of the liver weight, based on the fathead minnow measurements and previous studies with Atlantic salmon (*Salmo salar*) (Talbot & Higgins, 1982), since direct gall bladder measurements were not obtained. In both species, daily bile flow was estimated to be 50% of the bile volume. The value for bile flow was based on our best judgment as measurement techniques for this parameter were not available.

As shown by the sensitivity analysis conducted in Appendix K.1, changes in bile dynamics will result in sizable changes in model outputs. Therefore, for the best predictive power of the models, these parameter values must be as accurate as possible. Improvements to bile volume measurements could be made by directly aspirating and measuring the bile liquid from the gall bladder (Brumley et al., 1998). No information regarding measurements of bile flow in fish could be obtained from the literature, which emphasizes the requirement for further research in this area. A potential method for measuring bile flow would be by obtaining a series of bile volume measurements over a designated time period, e.g., samples taken every hour for six hours. Because the gall bladder typically purges with feeding, the sampling period would need to begin directly after a feeding event. This method has been used to measure bile flow in rats (Levy et al., 1995). A limitation to this method, however, is that unlike in rats that can be anesthetized and cannulated, measurements could not be taken from the same fish, as the fish would need to be euthanized to obtain the bile measurement. Therefore, it would be difficult to normalize an equal bile volume among fish at the start of the measurement period. Another potential method to note is the use of ultrasound imaging. However, this method has not been well described in the literature for measurements of bile flow.

Number of B[*a*]P metabolites measured:

In this thesis, only two metabolites generated from the biotransformation of B[*a*]P were measured, OH-B[*a*]P and Gluc-B[*a*]P. However, there are several other metabolites that can be generated from biotransformation of B[*a*]P (discussed in Section 1.4.2). In chapter 2 (Section 2.5.2), accurately determining what fraction of total metabolites the OH-B[*a*]P and the associated glucuronide would account for was discussed as a limitation to accurate model predictions. It was determined that 60% of the metabolites produced would be the OH-B[*a*]P and the associated glucuronide in the adult life stage based on previous studies with mummichog (Zhu et al., 2008). It is likely, however, that this fraction will differ among species. Therefore, improvements to the

models developed in this thesis could be improved by directly measuring a larger number of B[*a*]P metabolites in the fathead minnow and white sturgeon to determine species-specific metabolite fractions.

4.5 Concluding statement

The research described in this thesis contributes to the increasing scope of applications of TK models. The data generated showed that biotransformation could be successfully integrated into life stage-specific models and that the models could be successfully used for inter-species extrapolations. Major research gaps regarding embryo-larval biotransformation were identified in regard to measurement techniques and evaluation of life stage- and species-specific differences. Additionally, to further improve the multi-compartment adult model, methods that improve the parametrization of biotransformation in the adult life stage should be further investigated. In conclusion, the TK models developed in this thesis work to support ERA by providing a method to characterize, manage, and prioritize environmental pollutants.

LIST OF REFERENCES

Abbas, R., & Hayton, W. L. (1997). A physiologically based pharmacokinetic and pharmacodynamic model for paraoxon in rainbow trout. *Toxicology and Applied Pharmacology*, 145(1), 192-201.

Abdel-Shafy, H. I., & Mansour, M. S. (2016). A review on polycyclic aromatic hydrocarbons: source, environmental impact, effect on human health and remediation. *Egyptian Journal of Petroleum*, *25*(1), 107-123.

Andelman, J. B., & Suess, M. J. (1970). Polynuclear aromatic hydrocarbons in the water environment. *Bulletin of the World Health Organization*, *43*(3), 479.

Andersson, T., & Förlin, L. (1992). Regulation of the cytochrome P450 enzyme system in fish. *Aquatic Toxicology*, *24*(1-2), 1-19.

Ankley, G. T., & Villeneuve, D. L. (2006). The fathead minnow in aquatic toxicology: Past, present and future. *Aquatic Toxicology*, 78(1), 91–102.

Arnot, J. A., & Gobas, F. A. (2004). A food web bioaccumulation model for organic chemicals in aquatic ecosystems. *Environmental Toxicology and Chemistry: An International Journal*, *23*(10), 2343-2355.

Ashauer, R., & Escher, B. I. (2010). Advantages of toxicokinetic and toxicodynamic modelling in aquatic ecotoxicology and risk assessment. *Journal of Environmental Monitoring*, 12(11), 2056–2061.

Agency for Toxic Substances and Disease Registry (ATSDR). (1995). Toxicological profile for polycyclic aromatic hydrocarbons [ATSDR Tox Profile]. Washington, DC: U.S. Department of Health and Human Services. http://www.atsdr.cdc.gov/toxprofiles/tp69.pdf

Basu, D. K., & Saxena, J. (1978). Polynuclear aromatic hydrocarbons in selected US drinking waters and their raw water sources. *Environmental Science and Technology*, *12*(7), 795-798.

Basu, N., Crump, D., Head, J., Hickey, G., Hogan, N., Maguire, S., ... & Hecker, M. (2019). EcoToxChip: A next-generation toxicogenomics tool for chemical prioritization and environmental management. *Environmental Toxicology and Chemistry*, *38*(2), 279.

Barron, M. G., Tarr, B. D., & Hayton, W. L. (1987). Temperature-dependence of cardiac output and regional blood flow in rainbow trout, *Salmo gairdneri* Richardson. *Journal of Fish Biology*, *31*(6), 735-744.

Baumann, P. C. (1998). Epizootics of cancer in fish associated with genotoxins in sediment and water. *Mutation Research/Reviews in Mutation Research*, 411(3), 227-233.

Beach, J. B., Pellizzari, E., Keever, J. T., & Ellis, L. (2000). Determination of benzo[*a*]pyrene and other polycyclic aromatic hydrocarbons (PAHs) at trace levels in human tissues. *Journal of Analytical Toxicology*, *24*(8), 670-677.

Bennett, R. H., Ellender, B. R., Mäkinen, T., Miya, T., Pattrick, P., Wasserman, R. J., ... & Weyl, O. L. (2016). Ethical considerations for field research on fishes. *Koedoe*, 58(1), 1-15.

Bennett, W. R., & Farrell, A. P. (1993). Acute toxicity testing with juvenile white sturgeon (*Acipenser transmontanus*). *Water Quality Research Journal*, *33* (1), 95-110.

Bertelsen, S. L., Hoffman, A. D., Gallinat, C. A., Elonen, C. M., & Nichols, J. W. (1998). Evaluation of log Kow and tissue lipid content as predictors of chemical partitioning to fish tissues. *Environmental Toxicology and Chemistry: An International Journal*, *17*(8), 1447-1455.

Birstein, V. (1993). Sturgeons and Paddlefishes: Threatened Fishes in Need of Conservation. *Conservation Biology*,7(4), 773-787.

Blumer, M. (1976). Polycyclic aromatic compounds in nature. *Scientific American*, *234*(3), 34-45.

Booc, F., Thornton, C., Lister, A., MacLatchy, D., & Willett, K. L. (2014). Benzo [a] pyrene effects on reproductive endpoints in *Fundulus heteroclitus*. *Toxicological Sciences*, *140*(1), 73-82.

Bräunig, J., Schiwy, S., Broedel, O., Müller, Y., Frohme, M., Hollert, H., & Keiter, S. H. (2015). Time-dependent expression and activity of cytochrome P450 1s in early life-stages of the zebrafish (*Danio rerio*). *Environmental Science and Pollution Research*, 22(21), 16319-16328.

Breen, M., Villeneuve, D. L., Ankley, G. T., Bencic, D., Breen, M. S., Watanabe, K. H., … Conolly, R. B. (2016). Computational model of the fathead minnow hypothalamicpituitary-gonadal axis: Incorporating protein synthesis in improving predictability of responses to endocrine active chemicals. *Comparative Biochemistry and Physiology Part - C: Toxicology and Pharmacology*, 183–184, 36–45.

Brinkmann, M., Eichbaum, K., Kammann, U., Hudjetz, S., Cofalla, C., Buchinger, S., ... & Hollert, H. (2014). Physiologically-based TK models help identifying the key factors affecting contaminant uptake during flood events. *Aquatic Toxicology*, *152*, 38-46.

Brinkmann, M., Freese, M., Pohlmann, J. D., Kammann, U., Preuss, T. G., Buchinger, S., ... & Hollert, H. (2015). A physiologically based toxicokinetic (PBTK) model for moderately hydrophobic organic chemicals in the European eel (*Anguilla anguilla*). *Science of the Total Environment*, 536, 279-287.

Brinkmann, M., Schlechtriem, C., Reininghaus, M., Eichbaum, K., Buchinger, S., Reifferscheid, G., ... & Preuss, T. G. (2016). Cross-species extrapolation of uptake and disposition of neutral organic chemicals in fish using a multispecies physiologically-based toxicokinetic model framework. *Environmental Science and Technology*, 50(4), 1914-1923.

Broman, D., Naef, C., Rolff, C., & Zebuehr, Y. (1991). Occurrence and dynamics of polychlorinated dibenzo-p-dioxins and dibenzofurans and polycyclic aromatic hydrocarbons in the mixed surface layer of remote coastal and offshore waters of the Baltic. *Environmental Science and Technology*, *25*(11), 1850-1864.

Brumley, C. M., Haritos, V. S., Ahokas, J. T., & Holdway, D. A. (1998). The effects of exposure duration and feeding status on fish bile metabolites: implications for biomonitoring. *Ecotoxicology and Environmental Safety*, *39*(2), 147-153.

Buhler, D. R., & Williams, D. E. (1988). The role of biotransformation in the toxicity of chemicals. *Aquatic Toxicology*, *11*(1-2), 19-28.

Bungay, P., Dedrick, M., & Guarino, R. (1976). Pharmacokinetic modeling of the dogfish shark (*Squalus acanthias*): Distribution and urinary and biliary excretion of phenol red and its glucuronide. *Journal of Pharmacokinetics and Biopharmaceutics*, 4(5), 377-388.

Carlson, E. A., Li, Y., & Zelikoff, J. T. (2002). The Japanese medaka (*Oryzias latipes*) model: applicability for investigating the immunosuppressive effects of the aquatic pollutant benzo[*a*]pyrene (BaP). *Marine Environmental Research*, *54*(3-5), 565-568.

Carlson, E. A., Li, Y., & Zelikoff, J. T. (2004). Suppressive effects of benzo[*a*]pyrene upon fish immune function: evolutionarily conserved cellular mechanisms of immunotoxicity. *Marine Environmental Research*, *58*(2-5), 731-734.

Carrasco-Navarro, V., Jæger, I., Honkanen, J. O., Kukkonen, J. V. K., Carroll, J., & Camus, L. (2015). Bioconcentration, biotransformation and elimination of pyrene in the arctic crustacean *Gammarus setosus* (*Amphipoda*) at two temperatures. *Marine Environmental Research*, *110*, 101-109.

CCME (Canadian Council of Ministers of the Environment). (1999). Canadian water quality guidelines for the protection of aquatic life - Polycylic aromatic hydrocarbons. Canadian Environmental Quality Guidelines, 1–13.

Chambers, J. E., & Yarbrough, J. D. (1976). Xenobiotic biotransformation systems in fishes. *Comparative Biochemistry and Physiology Part C: Comparative Pharmacology*, *55*(2), 77-84.

Chen, Y., Hermens, J. L., Jonker, M. T., Arnot, J. A., Armitage, J. M., Brown, T., ... & Droge, S. T. (2016). Which molecular features affect the intrinsic hepatic clearance rate of ionizable organic chemicals in fish?. *Environmental Science and Technology*, *50*(23), 12722-12731.

Chhabra, R. S. (1979). Intestinal absorption and metabolism of xenobiotics. *Environmental Health Perspectives*, *33*, 61-69.

Chikae, M., Hatano, Y., Ikeda, R., Morita, Y., Hasan, Q., & Tamiya, E. (2004). Effects of bis (2-ethylhexyl) phthalate and benzo [a] pyrene on the embryos of Japanese medaka (*Oryzias latipes*). *Environmental Toxicology and Pharmacology*, 16(3), 141-145.

Chiu, W., Barton, H., DeWoskin, R., Schlosser, P., Thompson, C., Sonawane, B., . . . Krishnan, K. (2007). Evaluation of physiologically based pharmacokinetic models for use in risk assessment. *Journal of Applied Toxicology*, 27(3), 218-237.

Cochran, R. C., Formoli, T. A., Pfeifer, K. F., & Aldous, C. N. (1997). Characterization of risks associated with the use of molinate. *Regulatory Toxicology and Pharmacology*, *25*(2), 146-157.

Coecke, S., Pelkonen, O., Leite, S. B., Bernauer, U., Bessems, J. G. M., Bois, F. Y., … Zald.var, J. M. (2013). Toxicokinetics as a key to the integrated toxicity risk assessment based primarily on non-animal approaches. *Toxicology In Vitro*, 27(5), 1570–1577.

Cok, I., Wang-Buhler, J. L., Kedzierski, M. M., Miranda, C. L., Yang, Y. H., & Buhler, D. R. (1998). Expression of CYP2M1, CYP2K1, and CYP3A27 in brain, blood, small intestine, and other tissues of rainbow trout. *Biochemical and Biophysical Research Communications*, *244*(3), 790-795.

Cook, P. M., Robbins, J. A., Endicott, D. D., Lodge, K. B., Guiney, P. D., Walker, M. K., ... & Peterson, R. E. (2003). Effects of aryl hydrocarbon receptor-mediated early life stage toxicity on lake trout populations in Lake Ontario during the 20th century. *Environmental Science and Technology*, 37(17), 3864-3877

Corrales, J., Thornton, C., White, M., & Willett, K. L. (2014). Multigenerational effects of benzo[*a*]pyrene exposure on survival and developmental deformities in zebrafish larvae. *Aquatic Toxicology*, 148, 16-26.

Committee on the Status of Endangered Wildlife in Canada (COSEWIC). (2012). COSEWIC assessment and status report on the White Sturgeon *Acipenser transmontanus* in Canada. Committee on the Status of Endangered Wildlife in Canada Ottawa. xxvii + 75 pp.

Costa, J., Ferreira, M., Rey-Salgueiro, L., & Reis-Henriques, M. A. (2011). Comparison of the waterborne and dietary routes of exposure on the effects of benzo[*a*]pyrene on biotransformation pathways in Nile tilapia (*Oreochromis niloticus*). *Chemosphere*, *84*(10), 1452-1460.

Costa, J., Reis-Henriques, M. A., Castro, L. F. C., & Ferreira, M. (2012). Gene expression analysis of ABC efflux transporters, CYP1A and GSTα in Nile tilapia after exposure to benzo[*a*]pyrene. *Comparative Biochemistry and Physiology Part C: Toxicology and Pharmacology*, *155*(3), 469-482.

Costa, J., Reis-Henriques, M. A., Wilson, J. M., & Ferreira, M. (2013). P-glycoprotein and CYP1A protein expression patterns in Nile tilapia (*Oreochromis niloticus*) tissues after waterborne exposure to benzo[*a*]pyrene (BaP). *Environmental Toxicology and Pharmacology*, *36*(2), 611-625.

Crowell, S. R., Amin, S. G., Anderson, K. A., Krishnegowda, G., Sharma, A. K., Soelberg, J. J., Corley, R. A. (2011). Preliminary physiologically based pharmacokinetic models for benzo[*a*]pyrene and dibenzo[def,p]chrysene in rodents. *Toxicology and Applied Pharmacology*, 257(3), 365–376.

Davila, D. R., Davis, D. P., Campbell, K., Cambier, J. C., Zigmond, L. A., & Burchiel, S. W. (1995). Role of alterations in ca2+-associated signaling pathways in the immunotoxicity of polycyclic aromatic hydrocarbons. *Journal of Toxicology and Environmental Health, Part A Current Issues*, *45*(2), 101-126.

DeBofsky, A., Xie, Y., Grimard, C., Alcaraz, A. J., Brinkmann, M., Hecker, M., & Giesy, J. P. (2020). Differential responses of gut microbiota of male and female fathead minnow (*Pimephales promelas*) to a short-term environmentally-relevant, aqueous exposure to benzo[*a*]pyrene. *Chemosphere*, 126461.

DiGiovanni, J.; Gill, R.D.; Nettikumara, A.N.; Colby, A.B.; Reiners, J.J.; Jr. (1989).cEffect of Extracellular Calcium Concentration on the Metabolism of Polycyclic Aromatic Hydrocarbons by Cultured Mouse Keratinocytes. *Cancer Research*, 49, 5567–5574.

Doering, J. A., Wiseman, S., Beitel, S. C., Giesy, J. P., & Hecker, M. (2014). Identification and expression of aryl hydrocarbon receptors (AhR1 and AhR2) provide insight in an evolutionary context regarding sensitivity of white sturgeon (*Acipenser transmontanus*) to dioxin-like compounds. *Aquatic Toxicology*, *150*, 27-35.

Doering, J. A., Beitel, S. C., Eisner, B. K., Heide, T., Hollert, H., Giesy, J. P., ... & Wiseman, S. B. (2015). Identification and response to metals of metallothionein in two ancient fishes: White sturgeon (*Acipenser transmontanus*) and lake sturgeon (*Acipenser fulvescens*). *Comparative Biochemistry and Physiology Part C: Toxicology and Pharmacology*, *171*, 41-48.

Doering, J., Wiseman, S., Giesy, J., & Hecker, M. (2018). A Cross-species Quantitative Adverse Outcome Pathway for Activation of the Aryl Hydrocarbon Receptor Leading to Early Life Stage Mortality in Birds and Fishes. *Environmental Science and Technology*, 52(13), 7524-7533.

Duke, S. D., P. Anders, G. Ennis, R. Hallock, J. Hammond, S. Ireland, J. Laufle, R. Lauzier, L. Lockhard, B. Marotz, V. L. Paragamian, and R. Westerhof. (1999). Recovery plan for Kootenai River white sturgeon (*Acipenser transmontanus*). *Journal of Applied Ichthyology* 15:157-163.

Eadie, B. J., Faust, W., Gardner, W. S., & Nalepa, T. (1982). Polycyclic aromatic hydrocarbons in sediments and associated benthos in Lake Erie. *Chemosphere*, 11(2), 185-191.

Embry, M. R., Belanger, S. E., Braunbeck, T. A., Galay-Burgos, M., Halder, M., Hinton, D. E., ... & Whale, G. (2010). The fish embryo toxicity test as an animal alternative method in hazard and risk assessment and scientific research. *Aquatic Toxicology*, *97*(2), 79-87.

Erickson, R. J., & McKim, J. M. (1990). A simple flow-limited model for exchange of organic chemicals at fish gills. *Environmental Toxicology and Chemistry: An International Journal*, *9*(2), 159-165.

Erickson, R., McKim, J., Lien, G., Hoffman, A., & Batterman, S. (2006). Uptake and elimination of ionizable organic chemicals at fish gills: II. Observed and predicted effects of pH, alkalinity, and chemical properties. *Environmental Toxicology and Chemistry*, 25(6), 1522-1532.

Escher, B. I., Cowan-Ellsberry, C. E., Dyer, S., Embry, M. R., Erhardt, S., Halder, M., ... & Segner, H. (2011). Protein and lipid binding parameters in rainbow trout (*Oncorhynchus mykiss*) blood and liver fractions to extrapolate from an *in vitro* metabolic degradation assay to *in vivo* bioaccumulation potential of hydrophobic organic chemicals. *Chemical Research in Toxicology*, *24*(7), 1134-1143.

European Commission. (2018). European Union Reference Laboratory for Alternatives to Animal Testing (EURL ECVAM) Fish *In vitro* Intrinsic Clearance Database. Retrieved from https://ec.europa.eu/knowledge4policy/node/30101_fr. Date accessed July 14, 2020.

European Food Safety Authority (EFSA). (2005). Opinion of the Scientific Panel on Animal Health and Welfare (AHAW) on a request from the Commission related to the aspects of the biology and welfare of animals used for experimental and other scientific purposes. *EFSA Journal, 3*(12), N/a.

European Food Safety Authority (EFSA). (2015). Scientific Colloquium 21 Harmonisation of human andecological risk assessment of combined exposure to multiple chemicals 11-12 September2014 Edinburgh, UK European Food Safety Authority.

Evans, D. H. (1987). The fish gill: site of action and model for toxic effects of environmental pollutants. *Environmental Health Perspectives*, *71*, 47-58.

Fay, K. A., Fitzsimmons, P. N., Hoffman, A. D., & Nichols, J. W. (2017). Comparison of trout hepatocytes and liver S9 fractions as *in vitro* models for predicting hepatic clearance in fish. *Environmental Toxicology and Chemistry*, *36*(2), 463-471.

Feist, G. W., Webb, M. A., Gundersen, D. T., Foster, E. P., Schreck, C. B., Maule, A. G., & Fitzpatrick, M. S. (2005). Evidence of detrimental effects of environmental contaminants on growth and reproductive physiology of white sturgeon in impounded areas of the Columbia River. *Environmental Health Perspectives*, *113*(12), 1675-1682.

Feldman, G., Remsen, J., Shinohara, K., & Cerutti, P. (1978). Excisability and persistence of benzo[*a*]pyrene DNA adducts in epithelioid human lung cells. *Nature*, *274*(5673), 796.

Fernandes, M. B., Sicre, M. A., Boireau, A., & Tronczynski, J. (1997). Polyaromatic hydrocarbon (PAH) distributions in the Seine River and its estuary. *Marine Pollution Bulletin*, *34*(11), 857-867.

Freidig, A. P., Ploeger, B. A., & Hermens, J. L. (2000). A preliminary physiologically based pharmacokinetic and pharmacodynamic model for ethyl acrylate in the rainbow trout. *Models for Risk Assessment of Reactive Chemicals in Aquatic Toxicology*, 87.

Feist, G. W., Webb, M. A. H., Gundersen, D. T., Foster, E. P., Schreck, C. B., Maule, A. G., & Fitzpatrick, M. S. (2005). Evidence of detrimental effects of environmental contaminants on growth and reproductive physiology of white sturgeon in impounded areas of the Columbia River. *Environmental Health Perspectives*, 113(12), 1675–1682.

Fisheries and Oceans Canada. (2014). Recovery strategy for White Sturgeon (Acipenser transmontanus) in Canada [Final]. In Species at Risk Act Recovery Strategy Series. Ottawa: Fisheries and Oceans Canada. 252 pp.

Fitzsimmons, P.N., Fernandez, J.D., Hoffman, A.D., Butterworth, B.C., Nichols, J.W., 2001. Branchial elimination of superhydrophobic organic compounds by rainbow trout (*Oncorhynchus mykiss*). *Aquatic Toxicology*, 55, 23–34.

Foekema, E. M., Fischer, A., Parron, M. L., Kwadijk, C., de Vries, P., & Murk, A. J. (2012). Toxic concentrations in fish early life stages peak at a critical moment. *Environmental Toxicology and Chemistry*, 31(6), 1381–1390.

Fontagne, S., Geurden, I., Escaffre, A. M., & Bergot, P. (1998). Histological changes induced by dietary phospholipids in intestine and liver of common carp (*Cyprinus carpio* L.) larvae. *Aquaculture*, *161*(1-4), 213-223.

Franco, M. E., & Lavado, R. (2019). Applicability of *in vitro* methods in evaluating the biotransformation of polycyclic aromatic hydrocarbons (PAHs) in fish: Advances and challenges. *Science of The Total Environment*, *671*, 685-695.

Fricker, G., Wössner, R., Drewe, J., Fricker, R., & Boyer, J. L. (1997). Enterohepatic circulation of scymnol sulfate in an elasmobranch, the little skate (*Raja erinacea*). *American Journal of Physiology-Gastrointestinal and Liver Physiology*, *273*(5), G1023-G1030.

Froese, R., & Pauly, D. (2019). FishBase. *World Wide Web electronic publication*, (version (12/2019).), www.fishbase.org.

Fukami, J., Shishido, T., Fukunaga, K., & Casida, J. E. (1969). Oxidative metabolism of rotenone in mammals, fish, and insects and its relation to selective toxicity. *Journal of Agricultural and Food Chemistry*, *17*(6), 1217-1226.

Gao, D., Lin, J., Ou, K., Chen, Y., Li, H., Dai, Q., ... & Wang, C. (2018). Embryonic exposure to benzo[*a*]pyrene inhibits reproductive capability in adult female zebrafish and correlation with DNA methylation. *Environnemental Pollution*, *240*, 403-411.

Garnier-Laplace, J., Adam, C., Lathuilli.re, T., Baudin, J. P., & Clabaut, M. (2000). A simple fish physiological model for radioecologists exemplified for 54Mn direct transfer and rainbow trout (*Oncorhynchus mykiss*). *Journal of Environmental Radioactivity*, 49(1), 35-53.

Gelboin, H. V. (1980). Benzo[*a*]pyrene metabolism, activation, and carcinogenesis: Role and regulation of mixed-function oxidases and related enzymes. *Physiological Reviews*, 60(4), 1107–1166.

George, S. G. (1994). Enzymology and molecular biology of phase II xenobiotic-conjugating enzymes in fish. *Aquatic Toxicology: Molecular, Biochemical and Cellular Perspectives*, 37-85.

Gerger, C. J., & Weber, L. P. (2015). Comparison of the acute effects of benzo-a-pyrene on adult zebrafish (*Danio rerio*) cardiorespiratory function following intraperitoneal injection versus aqueous exposure. *Aquatic Toxicology*, *165*, 19-30.

GLC (Great Lakes Commission). (2007). Assessment of benzo(a)pyrene air emissions in the Great Lakes region: A report of the Great Lakes Regional Toxic Air Emissions Inventory Steering Committee. Ann Arbor, MI.

Gluth, G., Freitag, D., Hanke, W., & Korte, F. (1985). Accumulation of pollutants in fish. *Comparative Biochemistry and Physiology. C, Comparative Pharmacology and Toxicology*, *81*(2), 273-277.

Goksøyr, A., & Förlin, L. (1992). The cytochrome P-450 system in fish, aquatic toxicology and environmental monitoring. *Aquatic Toxicology*, *22*(4), 287-311.

Government of Canada. (2016.) Chemicals management plan. Retrieved from Government of Canada https://www.canada.ca/en/health-canada/services/chemicalsubstances/chemicalsmanagement-plan.html

Gravato, C., & Guilhermino, L. (2009). Effects of benzo (a) pyrene on seabass (*Dicentrarchus labrax L.*): biomarkers, growth and behavior. *Human and Ecological Risk Assessment*, *15*(1), 121-137.

Grech, A., Brochot, C., Dorne, J. Lou, Quignot, N., Bois, F. Y., & Beaudouin, R. (2017). Toxicokinetic models and related tools in ecological risk assessment of chemicals. *Science of the Total Environment*, 578, 1–15.

Grech, A., Tebby, C., Brochot, C., Bois, F. Y., Bado-Nilles, A., Dorne, J. L., ... & Beaudouin, R. (2019). Generic physiologically-based toxicokinetic modelling for fish: Integration of environmental factors and species variability. *Science of the Total Environment*, *651*, 516-531.

Greenfield, B. K., Davis, J. A., Fairey, R., Roberts, C., Crane, D., & Ichikawa, G. (2005). Seasonal, interannual, and long-term variation in sport fish contamination, San Francisco Bay. *Science of the Total Environment*, *336*(1-3), 25-43.

Grimard, C., Mangold-Döring, A., Schmitz, M., Alharbi, H., Jones, P. D., Giesy, J. P., ... & Brinkmann, M. (2020). *In vitro-in vivo* and cross-life stage extrapolation of uptake and biotransformation of benzo [a] pyrene in the fathead minnow (Pimephales promelas). *Aquatic Toxicology*, *228*, 105616.

Gross, M. R., Repka, J., Robertson, C. T., Secor, D. H., & Van Winkle, W. (2002). Sturgeon conservation: insights from elasticity analysis. In *American Fisheries Society Symposium* (Vol. 28, pp. 13-30).

Guengerich F.P. Analysis and Characterization of Enzymes. In: Hayes A.W., editor. Principles and Methods of Toxicology. New York: Raven Press; 1989. pp. 777–813.

Gueorguieva, I., Nestorov, I. A., & Rowland, M. (2006). Reducing whole body physiologically based pharmacokinetic models using global sensitivity analysis: diazepam case study. *Journal of Pharmacokinetics and Pharmacodynamics*, *33*(1), 1-27.

Gundersen, D. T., Webb, M. A. H., Fink, A. K., Kushner, L. R., Feist, G. W., Fitzpatrick, M. S., ... & Schreck, C. B. (2008). Using blood plasma for monitoring organochlorine contaminants in juvenile white sturgeon, *Acipenser transmontanus*, from the lower Columbia River. *Bulletin of Environmental Contamination and Toxicology*, *81*(3), 225-229.

Gundersen, D. T., Zeug, S. C., Bringolf, R. B., Merz, J., Jackson, Z., & Webb, M. A. H. (2017). Tissue Contaminant Burdens in San Francisco Estuary White Sturgeon (*Acipenser transmontanus):* Implications for Population Recovery. *Archives of Environmental Contamination and Toxicology,* 73(2), 334–347.

Gülden, M., Mörchel, S., Tahan, S., & Seibert, H. (2002). Impact of protein binding on the availability and cytotoxic potency of organochlorine pesticides and chlorophenols *in vitro*. *Toxicology*, *175*(1-3), 201-213.

Gülden, M., & Seibert, H. (2007). The improvement of *in vitro* cytotoxicity testing for the assessment of acute toxicity in fish. *Alternatives to Laboratory Animals*, *35*(1), 39-46.

Guo, X., Peng, Z., Huang, D., Xu, P., Zeng, G., Zhou, S., ... & Luo, H. (2018). Biotransformation of cadmium-sulfamethazine combined pollutant in aqueous environments: *Phanerochaete chrysosporium* bring cautious optimism. *Chemical Engineering Journal*, *347*, 74-83.

Guyda, H. J., Mathieu, Louis., Lai, W., Manchester, David., Wang, S. L., Ogilvie, Susan, & Shiverick, K. T. (1990). Benzo[*a*]pyrene inhibits epidermal growth factor binding and receptor autophosphorylation in human placental cell cultures. *Molecular Pharmacology*, *37*(2), 137-143.

Haarmann-Stemmann, T., Bothe, H., & Abel, J. (2009). Growth factors, cytokines and their receptors as downstream targets of aryl hydrocarbon receptor (AhR) signaling pathways. *Biochemical Pharmacology*, *77*(4), 508-520.

Haber LT, Maier A, Gentry PR, Clewell HJ, Dourson ML. 2002. Genetic polymorphisms in assessing interindividual variability in delivered dose. *Regulatory Toxicology and Pharmacology*, 35: 177–197.

Habig, W. H., Pabst, M. J., & Jakoby, W. B. (1974). Glutathione S-transferases the first enzymatic step in mercapturic acid formation. *Journal of Biological Chemistry*, *249*(22), 7130-7139.

Haddad, S., Gad, S. C., Tardif, R., & Krishnan, K. (1995). Statistical approaches for the validation of physiologically-based pharmacokinetic (PBPK) model. *Toxicologist,* 15,48.

Halley, B. A., VandenHeuvel, W. J., & Wislocki, P. G. (1993). Environmental effects of the usage of avermectins in livestock. *Veterinary Parasitology*, *48*(1-4), 109-125.

Han, X., Nabb, D. L., Yang, C. H., Snajdr, S. I., & Mingoia, R. T. (2009). Liver microsomes and S9 from rainbow trout (*Oncorhynchus mykiss*): Comparison of basal-level enzyme activities with rat and determination of xenobiotic intrinsic clearance in support of bioaccumulation assessment. *Environmental Toxicology and Chemistry: An International Journal*, *28*(3), 481-488.

Hattemer-Frey, H. A., & Travis, C. C. (1991). Benzo[*a*]pyrene: environmental partitioning and human exposure. *Toxicology and Industrial Health*, *7*(3), 141-157.

Hawkins, W. E., Walker, W. W., Overstreet, R. M., Lytle, T. F., & Lytle, J. S. (1988). Dose related carcinogenic effects of water-borne benzo[a]pyrene on livers of two small fish species. *Ecotoxicology and Environmental Safety,* 16(3), 219-231

Hawkins, W. E., Walker, W. W., Overstreet, R. M., Lytle, J. S., & Lytle, T. F. (1990). Carcinogenic effects of some polycyclic aromatic hydrocarbons on the Japanese medaka and guppy in waterborne exposures. *Science of the Total Environment*, 94(1-2), 155-167.

Hawkins, W. E., Walker, W. W., Lytle, T. F., Lytle, J. S., & Overstreet, R. M. (1991). Studies on the carcinogenic effects of benzo[a]pyrene and 7, 12-dimethylbenz[a]anthracene on the sheepshead minnow (*Cyprinodon variegatus*). In *Aquatic Toxicology and Risk Assessment: Fourteenth Volume*. ASTM International.

Health Canada. (2015). Benzo[a]pyrene in drinking water. Retrieved from Health Canada, https://www.canada.ca/en/health-canada/services/environmental-workplacehealth/consultations/benzo-pyrene-drinking-water-health-canada-2015/consultationdocument.html

Henderson, J. R., & Daniel, P. M. (1978). Portal circulations and their relation to countercurrent systems. *Quarterly Journal of Experimental Physiology and Cognate Medical Sciences: Translation and Integration*, *63*(4), 355-369.

Hendriks, A. J., & Heikens, A. (2001). The power of size. 2. Rate constants and equilibrium ratios for accumulation of inorganic substances related to species weight. *Environmental Toxicology and Chemistry: An International Journal*, *20*(7), 1421-1437.

Heredia-ortiz, R., Bouchard, M., Marie-desvergne, C., Viau, C., & Ma.tre, A. (2011). Modeling of the internal kinetics of benzo[a]pyrene and 3-hydroxybenzo[a]pyrene biomarker from rat data. *Toxicological Sciences*, 122(2), 275–287.

Heringa, M. B., Schreurs, R. H., Busser, F., Van Der Saag, P. T., Van Der Burg, B., & Hermens, J. L. (2004). Toward more useful *in vitro* toxicity data with measured free concentrations. *Environmental Science and Technology*, *38*(23), 6263-6270.

Herwig, B. R., & Zimmer, K. D. (2007). Population ecology and prey consumption by fathead minnows in prairie wetlands: importance of detritus and larval fish. *Ecology of Freshwater Fish*, *16*(3), 282-294.

Hoffman, A. D., Bertelsen, S. L., & Gargas, M. L. (1992). An *in vitro* gas equilibration method for determination of chemical partition coefficients in fish. *Comparative Biochemistry and Physiology. A, Comparative Physiology*, *101*(1), 47-51.

Hoffmann, J. L., & Oris, J. T. (2006). Altered gene expression: A mechanism for reproductive toxicity in zebrafish exposed to benzo[a]pyrene. *Aquatic Toxicology*, *78*(4), 332-340.

Hose, J. E., Hannah, J. B., DiJulio, D., Landolt, M. L., Miller, B. S., Iwaoka, W. T., & Felton, S. P. (1982). Effects of benzo[a]pyrene on early development of flatfish. *Archives of Environmental Contamination and Toxicology*, *11*(2), 167-171.

Hose, J. E., Hannaht, J. B., Puffer, H. W., & Landolt, M. L. (1984). Histologic and skeletal abnormalities in benzo[a]pyrene-treated rainbow trout alevins. *Archives of Environmental Contamination and Toxicology*, *13*(6), 675-684.

Hou, X., Shen, J., Zhang, S., Jiang, H., & Coats, J. R. (2003). Bioconcentration and elimination of sulfamethazine and its main metabolite in sturgeon (*Acipenser schrenkii*). *Journal of Agriculture and Food Chemistry*, *51*(26), 7725-7729.

Howe, G. E., Marking, L. L., Bills, T. D., Rach, J. J., & Mayer Jr, F. L. (1994). Effects of water temperature and pH on toxicity of terbufos, trichlorfon, 4-nitrophenol and 2, 4-dinitrophenol to the amphipod *Gammarus pseudolimnaeus* and rainbow trout (*Oncorhynchus mykiss*). *Environmental Toxicology and Chemistry: An International Journal*, *13*(1), 51-66.

Hughes, G. M. (1984). 1 General anatomy of the gills. In *Fish physiology* (Vol. 10, pp. 1-72). Academic Press.

Hunn, J. B., & Allen, J. L. (1974). Movement of drugs across the gills of fishes. *Annual Review of Pharmacology*, *14*(1), 47-54.

IARC. (2010). BENZO[*a*]PYRENE. IARC Monographs Vol 100F, 2005, 111–144.

Ji, K., Kim, S., Han, S., Seo, J., Lee, S., Park, Y., ... & Choi, K. (2012). Risk assessment of chlortetracycline, oxytetracycline, sulfamethazine, sulfathiazole, and erythromycin in aquatic environment: are the current environmental concentrations safe?. *Ecotoxicology*, *21*(7), 2031-2050.

Jongeneelen, F., & Ten Berge, W. (2012). Simulation of urinary excretion of 1-hydroxypyrene in various scenarios of exposure to polycyclic aromatic hydrocarbons with a generic, crosschemical predictive PBTK-model. *International Archives of Occupational and Environmental Health*, 85(6), 689–702.

Jonsson, F., & Johanson, G. (2001). Bayesian estimation of variability in adipose tissue blood flow in man by physiologically based pharmacokinetic modeling of inhalation exposure to toluene. *Toxicology*, *157*(3), 177-193.

Jönsson, M. E., Brunström, B., Ingebrigtsen, K., & Brandt, I. (2004). Cell-specific CYP1A expression and benzo [a] pyrene adduct formation in gills of rainbow trout (*Oncorhynchus mykiss*) following CYP1A induction in the laboratory and in the field. *Environmental Toxicology and Chemistry: An International Journal*, *23*(4), 874-882.

Jönsson, E. M., Abrahamson, A., Brunström, B., & Brandt, I. (2006). Cytochrome P4501A induction in rainbow trout gills and liver following exposure to waterborne indigo, benzo[*a*]pyrene and 3, 3′, 4, 4′, 5-pentachlorobiphenyl. *Aquatic Toxicology*, *79*(3), 226-232.

Jönsson, M. E., Jenny, M. J., Woodin, B. R., Hahn, M. E., & Stegeman, J. J. (2007). Role of AHR2 in the expression of novel cytochrome P450 1 family genes, cell cycle genes, and morphological defects in developing zebra fish exposed to 3, 3′, 4, 4′, 5-pentachlorobiphenyl or 2, 3, 7, 8-tetrachlorodibenzo-p-dioxin. *Toxicological Sciences*, *100*(1), 180-193.

Kais, B., Schiwy, S., Hollert, H., Keiter, S. H., & Braunbeck, T. (2017). *In vivo* EROD assays with the zebrafish (*Danio rerio*) as rapid screening tools for the detection of dioxin-like activity. *Science of the Total Environment*, *590*, 269-280.

Kammann, U. (2007). PAH metabolites in bile fluids of dab (*Limanda limanda*) and flounder (*Platichthys flesus*): spatial distribution and seasonal changes (7 pp). *Environmental Science and Pollution Research-International*, *14*(2), 102-108.

Kasokat, T., Nagel, R., & Urich, K. (1987). The metabolism of phenol and substituted phenols in zebra fish. *Xenobiotica*, *17*(10), 1215-1221.

Kennedy, S. W., & Jones, S. P. (1994). Simultaneous measurement of cytochrome P4501A catalytic activity and total protein concentration with a fluorescence plate reader. *Analytical Biochemistry*, *222*(1), 217-223.

Kennedy, C. J., & Tierney, K. B. (2008). Energy intake affects the biotransformation rate, scope for induction, and metabolite profile of benzo[*a*]pyrene in rainbow trout. *Aquatic Toxicology*, *90*(3), 172-181.

Kim, K. B., & Lee, B. M. (1997). Oxidative stress to DNA, protein, and antioxidant enzymes (superoxide dismutase and catalase) in rats treated with benzo[*a*]pyrene. *Cancer Letters*, *113*(1-2), 205-212.

Kim, H. S., Kwack, S. J., & Lee, B. M. (2000). Lipid peroxidation, antioxidant enzymes, and benzo [a] pyrene-quinones in the blood of rats treated with benzo[*a*]pyrene. *Chemico-biological Interactions*, *127*(2), 139-150.

Kim, J. H., Stansbury, K. H., Walker, N. J., Trush, M. A., Strickland, P. T., & Sutter, T. R. (1998). Metabolism of benzo[*a*]pyrene and benzo [a] pyrene-7, 8-diol by human cytochrome P450 1B1. *Carcinogenesis*, *19*(10), 1847-1853.

Kishino, T., & Kobayashi, K. (1995). Relation between toxicity and accumulation of chlorophenols at various pH, and their absorption mechanism in fish. *Water Research*, *29*(2), 431-442.

Klaassen, C., Watkins, John B., ed, McGraw-Hill Companies, & Casarett, Louis J. (2010). Casarett and Doull's essentials of toxicology (2nd ed., McGraw-Hill's AccessPharmacy). New York: McGraw-Hill Medical.

Knöbel, M., Busser, F. J., Rico-Rico, A., Kramer, N. I., Hermens, J. L., Hafner, C., ... & Scholz, S. (2012). Predicting adult fish acute lethality with the zebrafish embryo: relevance of test duration, endpoints, compound properties, and exposure concentration analysis. *Environmental Science and Technology*, *46*(17), 9690-9700.

Kock, T. J., Congleton, J. L., & Anders, P. J. (2006). Effects of sediment cover on survival and development of white sturgeon embryos. *North American Journal of Fisheries Management*, *26*(1), 134-141.

Kooijman, S. A. L. M., Sousa, T., Pecquerie, L., Van Der Meer, J., & Jager, T. (2008). From food-dependent statistics to metabolic parameters, a practical guide to the use of dynamic energy budget theory. *Biological Reviews*, 83(4), 533–552.

Korzh, S., Pan, X., Garcia-Lecea, M., Winata, C. L., Pan, X., Wohland, T., ... & Gong, Z. (2008). Requirement of vasculogenesis and blood circulation in late stages of liver growth in zebrafish. *BMC Developmental Biology*, *8*(1), 84.

Krishnan, K., & Peyret, T. (2009). Physiologically based toxicokinetic (PBTK) modeling in ecotoxicology. In *Ecotoxicology Modeling* (pp. 145-175). Springer, Boston, MA.

Kurelec, B., Krča, S., Garg, A., & Gupta, R. C. (1991). The potential of carp to bioactivate benzo[*a*]pyrene to metabolites that bind to DNA. *Cancer letters*, *57*(3), 255-260.

Lam, S. H., Ung, C. Y., Hlaing, M. M., Hu, J., Li, Z. H., Mathavan, S., & Gong, Z. (2013). Molecular insights into 4-nitrophenol-induced hepatotoxicity in zebrafish: Transcriptomic, histological and targeted gene expression analyses. *BBA-Gen. Subjects*, *1830*(10), 4778-4789.

Lammer, E., Carr, G. J., Wendler, K., Rawlings, J. M., Belanger, S. E., & Braunbeck, T. (2009). Is the fish embryo toxicity test (FET) with the zebrafish (*Danio rerio*) a potential alternative for the fish acute toxicity test?. *Comparative Biochemistry and Physiology Part C: Toxicology and Pharmacology*, *149*(2), 196-209.

Landrum, P. F., Lee, H., & Lydy, M. J. (1992). Toxicokinetics in Aquatic Systems - Model Comparisons and Use in Hazard Assessment. *Environmental Toxicology and Chemistry*, 11(12), 1709–1725.

Laurent, P. (1984). 2 Gill Internal Morphology. In *Fish Physiology* (Vol. 10, pp. 73-183). Academic Press.

Law, F. C. P., Abedini, S., & Kennedy, C. J. (1991). A biologically based toxicokinetic model for pyrene in rainbow trout. *Toxicology and Applied Pharmacology*, *110*(3), 390-402.

Le Fol, V., Brion, F., Hillenweck, A., Perdu, E., Bruel, S., Aït-Aïssa, S., ... & Zalko, D. (2017). Comparison of the *in vivo* biotransformation of two emerging estrogenic contaminants, BP2 and BPS, in zebrafish embryos and adults. *International Journal of Molecular Sciences*, *18*(4), 704.

Lee, J. W., Kim, Y. H., Yoon, S., & Lee, S. K. (2014a). Cytochrome P450 system expression and DNA adduct formation in the liver of *Zacco platypus* following waterborne benzo[*a*]pyrene exposure: implications for biomarker determination. *Environmental Toxicology*, *29*(9), 1032-1042.

Lee, Y. S., Lee, D. H., Delafoulhouze, M., Otton, S. V., Moore, M. M., Kennedy, C. J., & Gobas, F. A. (2014b). *In vitro* biotransformation rates in fish liver S9: Effect of dosing techniques. *Environmental Toxicology and Chemistry*, *33*(8), 1885-1893.

Lee, J. W., Yoon, H. G., & Lee, S. K. (2015). Benzo (a) pyrene-induced cytochrome p4501A expression of four freshwater fishes (*Oryzias latipes, Danio rerio, Cyprinus carpio, and Zacco platypus*). *Environmental Toxicology and Pharmacology*, *39*(3), 1041-1050.

Lerebours, A., Stentiford, G. D., Lyons, B. P., Bignell, J. P., Derocles, S. A., & Rotchell, J. M. (2014). Genetic alterations and cancer formation in a European flatfish at sites of different contaminant burdens. *Environmental Science and Technology*, 48(17), 10448-10455.

Leguen, I., Carlsson, C., Perdu-Durand, E., Prunet, P., Pärt, P., & Cravedi, J. P. (2000). Xenobiotic and steroid biotransformation activities in rainbow trout gill epithelial cells in culture. *Aquatic Toxicology*, *48*(2-3), 165-176.

Levine, W. G. (1978). Biliary excretion of drugs and other xenobiotics. *Annual Review of Pharmacology and Toxicology*, *18*(1), 81-96.

Levine, S. L., Oris, J. T., & Wissing, T. E. (1994). Comparison of P-4501A1 monooxygenase induction in gizzard shad (*Dorosoma cepedianum*) following intraperitoneal injection or continuous waterborne-exposure with benzo[*a*]pyrene: temporal and dose-dependent studies. *Aquatic Toxicology*, *30*(1), 61-75.

Levine, S. L., & Oris, J. T. (1997). Induction of CYP1A mRNA and catalytic activity in gizzard shad (*Dorosoma cepedianum*) after waterborne exposure to benzo[*a*]pyrene. *Comparative Biochemistry and Physiology Part C: Pharmacology, Toxicology and Endocrinology*, *118*(3), 397-404.

Levine, S. L., & Oris, J. T. (1999). CYP1A expression in liver and gill of rainbow trout following waterborne exposure: implications for biomarker determination. *Aquatic Toxicology*, *46*(3-4), 279-287.

Levy, R., & Herzberg, G. R. (1995). Effects of dietary fish oil and corn oil on bile flow and composition in rats. *Nutrition Research*, *15*(1), 85-98.

Li, Z., Kroll, K. J., Jensen, K. M., Villeneuve, D. L., Ankley, G. T., Brian, J. V., … Watanabe, K. H. (2011). A computational model of the hypothalamic - pituitary - gonadal axis in female fathead minnows (*Pimephales promelas*) exposed to 17α-ethynylestradiol and 17β-trenbolone. *BMC Systems Biology*, *5*(1), 63.

Lien, G. J., Nichols, J. W., McKim, J. M., & Gallinat, C. A. (1994). Modeling the accumulation of three waterborne chlorinated ethanes in fathead minnows (*Pimephales promelas*): A physiologically based approach. *Environmental Toxicology and Chemistry: An International Journal*, 13(7), 1195-1205.

Lindström-Seppä, P., Koivusaari, U., & Hänninen, O. (1981). Extrahepatic xenobiotic metabolism in North-European freshwater fish. *Comparative Biochemistry and Physiology Part C: Comparative Pharmacology*, *69*(2), 259-263.

Lipscomb, J. C., Teuschler, L. K., Swartout, J., Popken, D., Cox, T., & Kedderis, G. L. (2003). The impact of cytochrome P450 2E1-dependent metabolic variance on a risk-relevant pharmacokinetic outcome in humans. *Risk Analysis: An International Journal*, *23*(6), 1221-1238.

Liu, D., Pan, L., Yang, H., & Wang, J. (2014). A physiologically based toxicokinetic and toxicodynamic model links the tissue distribution of benzo [a] pyrene and toxic effects in the scallop *Chlamys farreri*. *Environmental Toxicology and Pharmacology*, *37*(2), 493-504.

Liu, Wiseman, Wan, Doering, Hecker, Lam, & Giesy. (2012). Multi-species comparison of the mechanism of biotransformation of MeO-BDEs to OH-BDEs in fish. *Aquatic Toxicology*, 114-115(C), 182-188.

Livingstone, D. R. (1998). The fate of organic xenobiotics in aquatic ecosystems: quantitative and qualitative differences in biotransformation by invertebrates and fish. *Comparative Biochemistry and Physiology Part A: Molecular & Integrative Physiology*, *120*(1), 43-49.

Lo, J. C., Allard, G. N., Otton, S. V., Campbell, D. A., & Gobas, F. A. (2015). Concentration dependence of biotransformation in fish liver S9: Optimizing substrate concentrations to estimate hepatic clearance for bioaccumulation assessment. *Environmental Toxicology and Chemistry*, *34*(12), 2782-2790.

Long, A., & Walker, J. D. (2003). Quantitative structure-activity relationships for predicting metabolism and modeling cytochrome P450 enzyme activities. *Environmental Toxicology and Chemistry: An International Journal*, *22*(8), 1894-1899.

Lu, Y., Ludsin, S. A., Fanslow, D. L., & Pothoven, S. A. (2008). Comparison of three microquantity techniques for measuring total lipids in fish. *Canadian Journal of Fisheries and Aquatic Sciences*, *65*(10), 2233-2241.

Lu, D., Harvey, R. G., Blair, I. A., & Penning, T. M. (2011). Quantitation of benzo [a] pyrene metabolic profiles in human bronchoalveolar (H358) cells by stable isotope dilution liquid chromatography–atmospheric pressure chemical ionization mass spectrometry. *Chemical Research in Toxicology*, *24*(11), 1905-1914.

MacDonald, D. (2009). Contaminants in white sturgeon (*Acipenser transmontanus*) from the upper Fraser River, British Columbia, Canada. *Environmental Toxicology and Chemistry,*16(3), 479-490.

Mackay, D., & Shiu, W. Y. (1977). Aqueous solubility of polynuclear aromatic hydrocarbons. *Journal of Chemical and Engineering Data*, *22*(4), 399-402.

Maren, T. H., Embry, R., & Broder, L. E. (1968). The excretion of drugs across the gill of the dogfish, *Squalus acanthias*. *Comparative Biochemistry and Physiology*, *26*(3), 853-864.

Marlowe, J. L., & Puga, A. (2005). Aryl hydrocarbon receptor, cell cycle regulation, toxicity, and tumorigenesis. *Journal of Cellular Biochemistry*, *96*(6), 1174-1184.

McAdam, S. O., Walters, C. J., & Nistor, C. (2005). Linkages between White Sturgeon Recruitment and Altered Bed Substrates in the Nechako River, Canada. *Transactions of the American Fisheries Society*, 134(6), 1448–1456.

McAdam, S. O., & Jonsson, B. (2011). Effects of substrate condition on habitat use and survival by white sturgeon (*Acipenser transmontanus*) larvae and potential implications for recruitment. *Canadian Journal of Fisheries and Aquatic Sciences*, 68(5), 812–822.

McElroy, A. E., Barron, M. G., Beckvar, N., Driscoll, S. B. K., Meador, J. P., Parkerton, T. F., ... & Steevens, J. A. (2011). A review of the tissue residue approach for organic and organometallic compounds in aquatic organisms. *Integrated Environmental Assessment and Management*, *7*(1), 50-74.

McKim, J., Schmieder, P., & Veith, G. (1985). Absorption dynamics of organic chemical transport across trout gills as related to octanol-water partition coefficient. *Toxicology and Applied Pharmacology*, *77*(1), 1-10.

McKim, J. M., & Erickson, R. J. (1991). Environmental impacts on the physiological mechanisms controlling xenobiotic transfer across fish gills. *Physiological Zoology*, *64*(1), 39-67.

McKim, J. M., Lien, G. J., Hoffman, A. D., & Jenson, C. T. (1999). Respiratory–cardiovascular physiology and xenobiotic gill flux in the lake trout (*Salvelinus namaycush*). *Comparative Biochemistry and Physiology Part A: Molecular & Integrative Physiology*, *123*(1), 69-81.

Mdegela, R., Myburgh, J., Correia, D., Braathen, M., Ejobi, F., Botha, C., ... & Skaare, J. U. (2006). Evaluation of the gill filament-based EROD assay in African sharptooth catfish (*Clarias gariepinus*) as a monitoring tool for waterborne PAH-type contaminants. *Ecotoxicology*, *15*(1), 51.

Meyer-Alert, H., Ladermann, K., Larsson, M., Schiwy, S., Hollert, H., & Keiter, S. H. (2018). A temporal high-resolution investigation of the Ah-receptor pathway during early development of zebrafish (*Danio rerio*). *Aquatic Toxicology*, *204*, 117-129.

Meyer-Alert, H., Larsson, M., Hollert, H., & Keiter, S. H. (2019). Benzo [a] pyrene and 2, 3-benzofuran induce divergent temporal patterns of AhR-regulated responses in zebrafish embryos (*Danio rerio*). *Ecotoxicology and Environmental Safety*, *183*, 109505.

Miller, M. M., Wasik, S. P., Huang, G. L., Shiu, W. Y., & Mackay, D. (1985). Relationships between octanol-water partition coefficient and aqueous solubility. *Environmental Science and Technology*, *19*(6), 522-529.

Miller, K. P., & Ramos, K. S. (2001). Impact of cellular metabolism on the biological effects of benzo[*a*]pyrene and related hydrocarbons. *Drug Metabolism Reviews*, 33(1), 1–35.

Mondou, M., Hickey, G. M., Rahman, H. T., Maguire, S., Pain, G., Crump, D., ... & Basu, N. (2020). Factors affecting the perception of New Approach Methodologies (NAMs) in the ecotoxicology community. *Integrated Environmental Assessment and Management*, *16*(2), 269-281.

Moserová, M., Kotrbová, V., Aimová, D., Šulc, M., Frei, E., & Stiborová, M. (2009). Analysis of benzo [a] pyrene metabolites formed by rat hepatic microsomes using high pressure liquid chromatography: optimization of the method. *Interdisciplinary Toxicology*, *2*(4), 239-244.

Murphy, P. G., & Murphy, J. V. (1971). Correlations between respiration and direct uptake of DDT in the mosquito fishGambusia affinis. *Bulletin of Environmental Contamination and Toxicology*, *6*(6), 581-588.

Nebert, D. W., Roe, A. L., Dieter, M. Z., Solis, W. A., Yang, Y. I., & Dalton, T. P. (2000). Role of the aromatic hydrocarbon receptor and [Ah] gene battery in the oxidative stress response, cell cycle control, and apoptosis. *Biochemical Pharmacology*, 59(1), 65-85.

Nacalai Tesque Inc. (2017) Cosmosil.Cosmocore Technical Notes. Retrieved from https://www.nacalai.co.jp/global/cosmosil/technicalnote/index.html. Date accessed July 14, 2020.

Nagel, R. (2002). DarT: the embryo test with the zebrafish *Danio rerio*—a general model in ecotoxicology and toxicology. *Altex*, *19*(Suppl 1), 38-48.

Nestorov, I. (2001). Modelling and simulation of variability and uncertainty in toxicokinetics and pharmacokinetics. *Toxicology Letters*, *120*(1-3), 411-420.

Newman, M. (1995). Quantitative methods in aquatic ecotoxicology (Advances in trace substances research). Boca Raton: Lewis.

Ng, C. A., & Hungerbühler, K. (2013). Bioconcentration of perfluorinated alkyl acids: how important is specific binding?. *Environmental Science and Technology*, *47*(13), 7214-7223.

Nichols, J. W., McKim, J. M., Andersen, M. E., Gargas, M. L., Clewell, H. J., & Erickson, R. J. (1990). A physiologically based toxicokinetic model for the uptake and disposition of waterborne organic chemicals in fish. *Toxicology and Applied Pharmacology*, 106(3), 433–447.

Nichols, J. W., McKim, J. M., Lien, G. J., Hoffman, A. D., & Bertelsen, S. L. (1991). Physiologically based toxicokinetic modeling of three waterborne chloroethanes in rainbow trout (*Oncorhynchus mykiss*). *Toxicology and Applied Pharmacology*, 110(3), 374–389.

Nichols, J. W., McKim, J. M., Lien, G. J., Hoffman, A. D., Bertelsen, S. L., & Gallinat, C. A. (1993). Physiologically-based toxicokinetic modeling of three waterborne chloroethanes in channel catfish, *Ictalurus punctatus. Aquatic Toxicology*, 27(1–2), 83–111.

Nichols, J., Rheingans, P., Lothenbach, D., McGeachie, R., Skow, L., & McKim, J. (1994). Three-dimensional visualization of physiologically based kinetic model outputs. *Environmental Health Perspectives*, 102(11), 952.

Nichols, J. W., McKim, J. M., Lien, G. J., Hoffman, A. D., Bertelsen, S. L., & Elonen, C. M. (1996). A physiologically based toxicokinetic model for dermal absorption of organic chemicals by fish. *Toxicological Sciences*, 31(2), 229-242.

Nichols, J. W., Jensen, K. M., Tietge, J. E., & Johnson, R. D. (1998). Physiologically based toxicokinetic model for maternal transfer of 2, 3, 7, 8-tetrachlorodibenzo-p-dioxin in brook trout (*Salvelinus fontinalis*). *Environmental Toxicology and Chemistry: An International Journal*, 17(12), 2422-2434.

Nichols, J. W., Fitzsimmons, P. N., Whiteman, F. W., Dawson, T. D., Babeu, L., & Juenemann, J. (2004). A physiologically based toxicokinetic model for dietary uptake of hydrophobic organic compounds by fish: I. Feeding studies with 2, 2′, 5, 5′- tetrachlorobiphenyl. *Toxicological Sciences*, 77(2), 206-218.

Nichols, J., Schultz, I., & Fitzsimmons, P. (2006). *In vitro-in vivo* extrapolation of quantitative hepatic biotransformation data for fish - I. A review of methods, and strategies for incorporating intrinsic clearance estimates into chemical kinetic models. *Aquatic Toxicology*,78(1), 74-90.

Nichols, J. W., Fitzsimmons, P. N., & Burkhard, L. P. (2007). *In vitro-in vivo* extrapolation of quantitative hepatic biotransformation data for fish. II. Modeled effects on chemical bioaccumulation. *Environmental Toxicology and Chemistry*, 26(6), 1304–1319.

Nichols, J. W., Hoffman, A. D., & Fitzsimmons, P. N. (2009). Optimization of an isolated perfused rainbow trout liver model: Clearance studies with 7-ethoxycoumarin. *Aquatic toxicology*, *95*(3), 182-194.

Nichols, J. W., Hoffman, A. D., ter Laak, T. L., & Fitzsimmons, P. N. (2013a). Hepatic clearance of 6 polycyclic aromatic hydrocarbons by isolated perfused trout livers: prediction from *in vitro* clearance by liver S9 fractions. *Toxicological Sciences*, *136*(2), 359-372.

Nichols, J., Huggett, D., Arnot, J., Fitzsimmons, P., & Cowan-Ellsberry, C. (2013b). Toward improved models for predicting bioconcentration of well-metabolized compounds by rainbow trout using measured rates of *in vitro* intrinsic clearance. *Environmental Toxicology and Chemistry*, 32(7), 1611-1622.

Nirmaier, H. P., Fischer, E., Meyer, A., & Henze, G. (1996). Determination of polycyclic aromatic hydrocarbons in water samples using high-performance liquid chromatography with amperometric detection. *Journal of Chromatography A*, *730*(1-2), 169-175.

Nogami, Y., Imaeda, R., Ito, T., & Kira, S. (2000). Benzo (a) pyrene adsorbed to suspended solids in fresh water. *Environmental Toxicology: An International Journal*, *15*(5), 500-503.

Nguyen, N. T., Hanieh, H., Nakahama, T., & Kishimoto, T. (2013). The roles of aryl hydrocarbon receptor in immune responses. *International Immunology*, 25(6), 335-343.

OECD (2012), Test No. 229: Fish Short Term Reproduction Assay, OECD Guidelines for the Testing of Chemicals, Section 2, OECD Publshing, Paris.

OECD (2013), Test No. 236: Fish Embryo Acute Toxicity (FET) Test, OECD Guidelines for the Testing of Chemicals, Section 2, OECD Publishing, Paris.

OECD (2018), Test No. 319B: Determination of *in vitro* intrinsic clearance using rainbow trout liver S9 sub-cellular fraction (RT-S9), OECD Guidelines for the Testing of Chemicals, Section 3, OECD Publishing, Paris.

Opperhulzen, A., Veide, E. W., Gobas, F. A., Liem, D. A., Steen, J., & Hutzinger, O. (1985). Relationship between bioconcentration in fish and steric factors of hydrophobic chemicals. *Chemosphere;(United States)*, *14*.

Oros, D. R., Ross, J. R., Spies, R. B., & Mumley, T. (2007). Polycyclic aromatic hydrocarbon (PAH) contamination in San Francisco Bay: a 10-year retrospective of monitoring in an urbanized estuary. *Environmental Research*, 105(1), 101-118.

Ortiz-Delgado, J. B., Segner, H., Arellano, J. M., & Sarasquete, C. (2007). Histopathological alterations, EROD activity, CYP1A protein and biliary metabolites in gilthead seabream Sparus aurata exposed to benzo[*a*]pyrene. *Histology and Histopathology (Cellular and Molecular Biology),* 22(4): 417-432.

Otte, J. C., Schmidt, A. D., Hollert, H., & Braunbeck, T. (2010). Spatio-temporal development of CYP1 activity in early life-stages of zebrafish (*Danio rerio*). *Aquatic Toxicology*, *100*(1), 38-50.

Ou, X., & Ramos, K. S. (1994). Benzo[*a*]pyrene inhibits protein kinase C activity in subcultured rat aortic smooth muscle cells. *Chemico-biological Interactions*, *93*(1), 29-40.

Pannetier, P., Morin, B., Clérandeau, C., Lacroix, C., Cabon, J., Cachot, J., & Danion, M. (2019). Comparative biomarker responses in Japanese medaka (*Oryzias latipes*) exposed to benzo [a] pyrene and challenged with betanodavirus at three different life stages. *Science of The Total Environment*, 652, 964-976.

Paragamian, V. L., McDonald, R., Nelson, G. J., & Barton, G. (2009). Kootenai River velocities, depth, and white sturgeon spawning site selection–a mystery unraveled?. *Journal of Applied Ichthyology*, *25*(6), 640-646.

Parhizgari, Z., & Li, J. (2014). A physiologically-based pharmacokinetic model for disposition of 2,3,7,8-TCDD in fathead minnow and medaka. *Environmental Toxicology and Chemistry*, 33(5), 1064–1071.

Parra, G., & Yúfera, M. (2001). Comparative energetics during early development of two marine fish species, *Solea senegalensis* (Kaup) and *Sparus aurata* (L.). *Journal of Experimental Biology*, *204*(12), 2175-2183.

Pastor, D., Boix, J., Fernandez, V., & Albaiges, J. (1996). Bioaccumulation of organochlorinated contaminants in three estuarine fish species (*Mullus barbatus, Mugil cephalus* and *Dicentrarcus labrax*). *Marine Pollution Bulletin*, *32*(3), 257-262.

Paustenbach, D. J. (2000). The practice of exposure assessment: A state-of-the-art review. *Journal of Toxicology and Environmental Health - Part B: Critical Reviews*, 3(3), 179–291.

Pelissero, C., & Sumpter, J. P. (1992). Steroids and "steroid-like" substances in fish diets. *Aquaculture*, *107*(4), 283-301.

Penning, T M, Ohnishi, S T, Ohnishi, T, & Harvey, R G. (1996). Generation of reactive oxygen species during the enzymatic oxidation of polycyclic aromatic hydrocarbon transdihydrodiols catalyzed by dihydrodiol dehydrogenase. *Chemical Research in Toxicology*, 9(1), 84-92.

Peters, L. D., O'hara, S. C. M., & Livingstone, D. R. (1996). Benzo [a] pyrene metabolism and xenobiotic-stimulated reactive oxygen species generation by subcellular fraction of larvae of turbot (*Scophthalmus maximus L.*). *Comparative Biochemistry and Physiology Part C: Pharmacology, Toxicology and Endocrinology*, *114*(3), 221-227.

Peters, L. D., Morse, H. R., Waters, R., & Livingstone, D. R. (1997). Responses of hepatic cytochrome P450 1A and formation of DNA-adducts in juveniles of turbot (*Scophthalmus maximus L.*) exposed to water-borne benzo[*a*]pyrene. *Aquatic toxicology*, *38*(1-3), 67-82.

Pettem, C. M., Briens, J. M., Janz, D. M., & Weber, L. P. (2018). Cardiometabolic response of juvenile rainbow trout exposed to dietary selenomethionine. *Aquatic Toxicology*, *198*, 175-189.

Pery, A. R., Devillers, J., Brochot, C., Mombelli, E., Palluel, O., Piccini, B., ... & Beaudouin, R. (2013). A physiologically based toxicokinetic model for the zebrafish *Danio rerio*. *Environmental Science and Technology*, 48(1), 781-790.

Phillips, D. H. (1983). Fifty years of benzo[a]pyrene. *Nature*, *303*(5917), 468.

Pikitch, E. K., Doukakis, P., Lauck, L., Chakrabarty, P., & Erickson, D. L. (2005). Status, trends and management of sturgeon and paddle fish fisheries. *Wildlife Conservation*, 233–265.

Pritchard, J. B., Karnaky Jr, K. J., Guarino, A. M., & Kinter, W. B. (1977). Renal handling of the polar DDT metabolite DDA (2, 2-bis [p-chlorophenyl] acetic acid) by marine fish. *American Journal of Physiology-Renal Physiology*, *233*(2), F126-F132.

Pritchard, J. B., & Bend, J. R. (1984). Mechanisms controlling the renal excretion of xenobiotics in fish: effects of chemical structure. *Drug Metabolism Reviews*, *15*(4), 655-671.

Pritchard, J., & Bend, J. R. (1991). Relative roles of metabolism and renal excretory mechanisms in xenobiotic elimination by fish. *Environmental Health Perspectives*, *90*, 85-92.

Puga, A., Xia, Y., & Elferink, C. (2002). Role of the aryl hydrocarbon receptor in cell cycle regulation. *Chemico-biological Interactions*, *141*(1-2), 117-130.

Puga, A., Ma, C., & Marlowe, J. L. (2009). The aryl hydrocarbon receptor cross-talks with multiple signal transduction pathways. *Biochemical Pharmacology*, *77*(4), 713-722.

Ramesh, M., Thilagavathi, T., Rathika, R., & Poopal, R. K. (2018). Antioxidant status, biochemical, and hematological responses in a cultivable fish *Cirrhinus mrigala* exposed to an aquaculture antibiotic Sulfamethazine. *Aquaculture*, *491*, 10-19.

Randall, D., Lin, H., & Wright, P. A. (1991). Gill water flow and the chemistry of the boundary layer. *Physiological Zoology*, *64*(1), 26-38.

Rey-Salgueiro, L., Costa, J., Ferreira, M., & Reis-Henriques, M. A. (2011). Evaluation of 3-hydroxy-benzo[a]pyrene levels in Nile tilapia (*Oreochromis niloticus*) after waterborne exposure to Benzo[a]pyrene. *Toxicological and Environmental Chemistry*, *93*(10), 2040-2054.

Reynaud, S., & Deschaux, P. (2006). The effects of polycyclic aromatic hydrocarbons on the immune system of fish: a review. *Aquatic Toxicology*, *77*(2), 229-238.

Richardson, S.J, Bai, A., A Kulkarni, A., & F Moghaddam, M. (2016). Efficiency in drug discovery: liver S9 fraction assay as a screen for metabolic stability. *Drug Metabolism Letters*, *10*(2), 83-90.

Rowland, M., & Tozer, Thomas N. (2011). Clinical pharmacokinetics and pharmacodynamics : Concepts and applications (4th ed.). Philadelphia: Wolters Kluwer Health/Lippincott William & Wilkins.

Roy, N. K., Courtenay, S., Maxwell, G., Yuan, Z., Chambers, R. C., & Wirgin, I. (2002). Cytochrome P4501A1 is induced by PCB 77 and benzo[*a*]pyrene treatment but not by exposure to the Hudson River environment in Atlantic tomcod (*Microgadus tomcod*) post-yolk sac larvae. *Biomarkers*, *7*(2), 162-173.

Saarikoski, J., Lindström, R., Tyynelä, M., & Viluksela, M. (1986). Factors affecting the absorption of phenolics and carboxylic acids in the guppy (*Poecilia reticulata*). *Ecotoxicology and Environmental Safety*, *11*(2), 158-173.

Salmina, E. S., Wondrousch, D., Kühne, R., Potemkin, V. A., & Schüürmann, G. (2016). Variation in predicted internal concentrations in relation to PBPK model complexity for rainbow trout. *Science of the Total Environment*, 550, 586-597.

Sandvik, M., Einar Horsberg, T., Utne Skaare, J., & Ingebrigtsen, K. (1997). Hepatic CYP1A induction in rainbow trout (*Oncorhynchus mykiss*) after exposure to benzo[*a*]pyrene in water. *Biomarkers*, *2*(3), 175-180.

Sandvik, M., Einar Horsberg, T., Utne Skaare, J., & Ingebrigtsen, K. (1998). Comparison of dietary and waterborne exposure to benzo a pyrene: bioavailability, tissue disposition and CYP1A induction in rainbow trout *Oncorhynchus mykiss*. *Biomarkers*, *3*(6), 399-410.

Santos, E., Souza, M. R., Junior, A. R. V., Soares, L. S., Frena, M., & Alexandre, M. R. (2018). Polycyclic aromatic hydrocarbons (PAH) in superficial water from a tropical estuarine system: Distribution, seasonal variations, sources and ecological risk assessment. *Marine Pollution Bulletin*, *127*, 352-358.

Schiwy, S., Bräunig, J., Alert, H., Hollert, H., & Keiter, S. H. (2015). A novel contact assay for testing aryl hydrocarbon receptor (AhR)-mediated toxicity of chemicals and whole sediments in zebrafish (*Danio rerio*) embryos. *Environmental Science and Pollution Research*, *22*(21), 16305-16318.

Schlenk, D., Celander, M., Gallagher, E. P., George, S., James, M., Kullman, S. W., ... & Willett, K. (2008). Biotransformation in fishes. *The Toxicology of Fishes*, 153-234.

Schmieder, P. K., & Henry, T. R. (1988). Plasma binding of 1-butanol, phenol, nitrobenzene and pentachlorophenol in the rainbow trout and rat: a comparative study. *Comparative Biochemistry and Physiology. C, Comparative Pharmacology and Toxicology*, *91*(2), 413-418.

Schultz, I.R., Barron, M.G., Newman, M.C., Vick, A.M. (1999). Blood flow distribution and tissue allometry in channel catfish. *Journal of Fish Biology*, 54, 1275–1286.

Schwerte, T., Voigt, S., & Pelster, B. (2005). Epigenetic variations in early cardiovascular performance and hematopoiesis can be explained by maternal and clutch effects in developing zebrafish (*Danio rerio*). *Comparative Biochemistry and Physiology Part A: Molecular & Integrative Physiology*, *141*(2), 200-209.

Seibert, H., Mörchel, S., & Gülden, M. (2002). Factors influencing nominal effective concentrations of chemical compounds *in vitro*: medium protein concentration. *Toxicology In Vitro*, *16*(3), 289-297.

Semakula, S., & Larkin, P. (1968). Age, Growth, Food, and Yield of the White Sturgeon (*Acipenser transmontanus*) of the Fraser River, British Columbia. *Journal of the Fisheries Research Board of Canada, 25*(12), 2589-2602.

Simmons, J. E., Boyes, W. K., Bushnell, P. J., Raymer, J. H., Limsakun, T., McDonald, A., ... & Evans, M. V. (2002). A physiologically based pharmacokinetic model for trichloroethylene in the male Long-Evans rat. *Toxicological Sciences*, *69*(1), 3-15.

Shen, J., Zhang, Q., Ding, S., Zhang, S., & Coats, J. R. (2005). Bioconcentration and elimination of avermectin B1 in sturgeon. *Environmental Toxicology and Chemistry*, *24*(2), 396-399.

Sloman, K. A., & McNeil, P. L. (2012). Using physiology and behaviour to understand the responses of fish early life stages to toxicants. *Journal of Fish Biology*, *81*(7), 2175-2198.

Sloman, K. A., Bouyoucos, I. A., Brooks, E. J., & Sneddon, L. U. (2019). Ethical considerations in fish research. *Journal of Fish Biology*, *94*(4), 556-577.

Smolowitz, R. M., Schultz, M. E., & Stegeman, J. J. (1992). Cytochrome P4501A induction in tissues, including olfactory epithelium, of topminnows (*Poeciliopsis spp.)* by waterborne benzo[*a*]pyrene. *Carcinogenesis*, *13*(12), 2395-2402.

Sobol, I.M., Tarantola, S., Gatelli, D., Kucherenko, S. S., & Mauntz, W. (2007). Estimating the approximation error when fixing unessential factors in global sensitivity analysis. *Reliability Engineering and System Safety*, *92*(7), 957-960.

Spacie, A., & Hamelink, J. L. (1982). Alternative models for describing the bioconcentration of organics in fish. *Environmental Toxicology and Chemistry: An International Journal*, *1*(4), 309-320.

Stadnicka, J., Schirmer, K., & Ashauer, R. (2012). Predicting concentrations of organic chemicals in fish by using toxicokinetic models. *Environmental Science and Technology*, 46(6), 3273–3280.

Stadnicka-Michalak, J., Tanneberger, K., Schirmer, K., & Ashauer, R. (2014). Measured and modeled toxicokinetics in cultured fish cells and application to *in vitro-in vivo* toxicity extrapolation. *PLoS One*, *9*(3), e92303.

Stegeman, J. J., & Lech, J. J. (1991). Cytochrome P-450 monooxygenase systems in aquatic species: carcinogen metabolism and biomarkers for carcinogen and pollutant exposure. *Environmental Health Perspectives*, *90*, 101-109.

Strobel, A., Burkhardt-Holm, P., Schmid, P., & Segner, H. (2015). Benzo[*a*]pyrene metabolism and EROD and GST biotransformation activity in the liver of red-and white-blooded Antarctic fish. *Environmental Science and Technology*, *49*(13), 8022-8032.

Talbot, C., & Higgins, P. J. (1982). Observations on the gall bladder of juvenile Atlantic salmon *Salmo salar L*., in relation to feeding. *Journal of Fish Biology*, *21*(6), 663-669.

Tan, Z., Chang, X., Puga, A., & Xia, Y. (2002). Activation of mitogen-activated protein kinases (MAPKs) by aromatic hydrocarbons: role in the regulation of aryl hydrocarbon receptor (AHR) function. *Biochemical Pharmacology*, *64*(5-6), 771-780.

Tang, C., Tan, J., Fan, R., Zhao, B., Tang, C., Ou, W., ... & Peng, X. (2016). Quasi-targeted analysis of hydroxylation-related metabolites of polycyclic aromatic hydrocarbons in human urine by liquid chromatography–mass spectrometry. *Journal of Chromatography A*, *1461*, 59-69.

TenBrook, P.L., Kendall, S.M., & Tjeerdema, R.S. (2006). Toxicokinetics and biotransformation of p-nitrophenol in white sturgeon (*Acipenser transmontanus*). *Ecotoxicology and Environmental. Safety, 64(3),* 362-368.

Tierney, K. B., Kennedy, C. J., Gobas, F., Gledhill, M., & Sekela, M. (2013). Organic contaminants and fish. In *Fish Physiology* (Vol. 33, pp. 1-52). Academic Press.

Timchalk, C., Nolan, R. J., Mendrala, A. L., Dittenber, D. A., Brzak, K. A., & Mattsson, J. L. (2002). A physiologically based pharmacokinetic and pharmacodynamic (PBPK/PD) model for the organophosphate insecticide chlorpyrifos in rats and humans. *Toxicological Sciences*, *66*(1), 34-53.

Tjeerdema, R. S., & Crosby, D. G. (1987). The biotransformation of molinate (Ordram) in the striped bass (*Morone saxatilis*). *Aquatic Toxicology*, *9*(6), 305-317.

Tjeerdema, R. S., & Crosby, D. G. (1988a). Comparative biotransformation of molinate (Ordram®) in the white sturgeon (*Acipenser transmontanus*) and common carp (*Cyprinus carpio*). *Xenobiotica*, *18*(7), 831-838.

Tjeerdema, R. S., & Crosby, D. G. (1988b). Disposition, biotransformation, and detoxication of molinate (Ordram) in whole blood of the common carp (*Cyprinus carpio*). *Pesticicide Biochemical Physiology*, *31*(1), 24-35.

Trushin, N., Alam, S., El-Bayoumy, K., Krzeminski, J., Amin, S. G., Gullett, J., ... & Prokopczyk, B. (2012). Comparative metabolism of benzo [a] pyrene by human keratinocytes infected with high-risk human papillomavirus types 16 and 18 as episomal or integrated genomes. *Journal of Carcinogenesis*, *11*.

Turney, G. L., & Goerlitz, D. F. (1990). Organic contamination of ground water at gas works park, Seattle, Washington. *Groundwater Monitoring & Remediation*, *10*(3), 187-198.

U.S. Environmental Protection Agency (EPA). (2006) Approaches for the Application of Physiologically Based Pharmacokinetic (PBPK) Models and Supporting Data in Risk Assessment. National Center for Environmental Assessment, Washington, DC; EPA/600/R-05/043F. Available from: National Technical Information Service, Springfield, VA, and online at http://epa.gov/ncea/.

U.S. Environmental Protection Agency (EPA). (1998). Guidelines for Ecological Risk Assessment. National Center for Environmental Assessment, Washington, DC; EPA/630/R-95/002F. Available from: National Technical Information Service, Springfield, VA, and online at http://epa.gov/ncea/.

U.S. Fish and Wildlife Service. 1999. Recovery plan for the white sturgeon (*Acipenser transmontanus*): Kootenai River population. U.S. Fish and Wildlife Service, Portland, Oregon. 96 pp. plus appendices.

Van den Heuvel, W. J. A., Halley, B. A., Ku, C. C., Jacob, T. A., Wislocki, P. G., & Forbis, A. D. (1996). Bioconcentration and depuration of avermectin B1a in the bluegill sunfish. *Environmental Toxicology and Chemistry*, *15*(12), 2263-2266.

van den Hurk, P., Gerzel, L. E., Calomiris, P., & Haney, D. C. (2017). Phylogenetic signals in detoxification pathways in Cyprinid and Centrarchid species in relation to sensitivity to environmental pollutants. *Aquatic Toxicology*, *188*, 20-25.

van Pul, W. A. J., De Leeuw, F. A. A. M., Van Jaarsveld, J. A., Van der Gaag, M. A., & Sliggers, C. J. (1998). The potential for long-range transboundary atmospheric transport. *Chemosphere*, *37*(1), 113-141.

Van Veld, P. A., Vogelbein, W. K., Cochran, M. K., Goksøyr, A., & Stegeman, J. J. (1997). Route-specific cellular expression of cytochrome P4501A (CYP1A) in fish (*Fundulus heteroclitus*) following exposure to aqueous and dietary benzo[*a*]pyrene. *Toxicology and Applied Pharmacology*, *142*(2), 348-359.

Vardy, D. W., Tompsett, A. R., Sigurdson, J. L., Doering, J. A., Zhang, X., Giesy, J. P., & Hecker, M. (2011). Effects of subchronic exposure of early life stages of white sturgeon (*Acipenser transmontanus*) to copper, cadmium, and zinc. *Environmental Toxicology and Chemistry*, 30(11), 2497-2505.

Vardy, D. W., Oellers, J., Doering, J. A., Hollert, H., Giesy, J. P., & Hecker, M. (2013). Sensitivity of early life stages of white sturgeon, rainbow trout, and fathead minnow to copper. *Ecotoxicology*, *22*(1), 139-147.

Vives i Batlle, J., Wilson, R. C., & McDonald, P. (2007). Allometric methodology for the calculation of biokinetic parameters for marine biota. *Science of the Total Environment*, *388*(1-3), 256-269.

Wan, Y., Zhang, K., Dong, Z., & Hu, J. (2013). Distribution is a major factor affecting bioaccumulation of decabrominated diphenyl ether: Chinese sturgeon (*Acipenser sinensis*) as an example. *Environmental Science and Technology*, 47(5), 2279-2286.

Wang, L., Camus, A. C., Dong, W., Thornton, C., & Willett, K. L. (2010). Expression of CYP1C1 and CYP1A in *Fundulus heteroclitus* during PAH-induced carcinogenesis. *Aquatic Toxicology*, *99*(4), 439-447.

Wessel, N., Santos, R., Menard, D., Le Menach, K., Buchet, V., Lebayon, N., ... & Akcha, F. (2010). Relationship between PAH biotransformation as measured by biliary metabolites and EROD activity, and genotoxicity in juveniles of sole (*Solea solea*). *Marine Environmental Research*, 69, S71-S73.

White, F.C., Kelly, R., Kemper, S., Schumacker, P.T., Gallagher, K.R., Laurs, R.M., 1988. Organ blood flow haemodynamics and metabolism of the albacore tuna *Thunnus alalunga* (*Bonnaterre*). *Journal of Experimental Biology*, 47, 161–169

Wold, P. A., Hoehne-Reitan, K., Cahu, C. L., Infante, J. Z., Rainuzzo, J., & Kjørsvik, E. (2009). Comparison of dietary phospholipids and neutral lipids: effects on gut, liver and pancreas histology in Atlantic cod (*Gadus morha L.*) larvae. *Aquaculture Nutrition*, *15*(1), 73-84.

Wright, P., Heming, T. O. M., & Randall, D. (1986). Downstream pH changes in water flowing over the gills of rainbow trout. *Journal of Experimental Biology*, *126*(1), 499-512.

Yang, F., Sun, N., Sun, Y. X., Shan, Q., Zhao, H. Y., Zeng, D. P., & Zeng, Z. L. (2013). A physiologically based pharmacokinetics model for florfenicol in crucian carp and oral-to intramuscular extrapolation. J*ournal of Veterinary Pharmacology and Therapeutics*, 36(2), 192-200.

Yu, R. M. K., Ng, P. K. S., Tan, T., Chu, D. L. H., Wu, R. S. S., & Kong, R. Y. C. (2008). Enhancement of hypoxia-induced gene expression in fish liver by the aryl hydrocarbon receptor (AhR) ligand, benzo[*a*]pyrene (BaP). *Aquatic Toxicology*, *90*(3), 235-242.

Yuan, L., Lv, B., Zha, J., & Wang, Z. (2017). Benzo[*a*]pyrene induced p53-mediated cell cycle arrest, DNA repair, and apoptosis pathways in Chinese rare minnow (*Gobiocypris rarus*). *Environmental Toxicology*, *32*(3), 979-988.

Yun, W. A. N. G., ZHENG, R., Zhenghong, Z. U. O., Yixin, C. H. E. N., & Chonggang, W. A. N. G. (2008). Relation of hepatic EROD activity and cytochrome P4501A level in *Sebastiscus marmoratus* exposed to benzo[*a*]pyrene. *Journal of Environmental Sciences*, *20*(1), 101-104.

Yunker, M. B., Macdonald, R. W., Vingarzan, R., Mitchell, R. H., Goyette, D., & Sylvestre, S. (2002). PAHs in the Fraser River basin: a critical appraisal of PAH ratios as indicators of PAH source and composition. *Organic Geochemistry*, *33*(4), 489-515.

Zaharko, Dedrick, & Oliverio. (1972). Prediction of the distribution of methotrexate in the sting rays *Dasyatidae sabina* and *sayi* by use of a model developed in mice. *Comparative Biochemistry and Physiology -- Part A: Physiology*,42(1), 183-194.

Zhang, L., Dong, L., Ren, L., Shi, S., Zhou, L., Zhang, T., & Huang, Y. (2012). Concentration and source identification of polycyclic aromatic hydrocarbons and phthalic acid esters in water of the Yangtze River Delta, China. *Journal of Environmental Sciences*, *24*(2), 335-342.

Zheng, B., Wang, L., Lei, K., & Nan, B. (2016). Distribution and ecological risk assessment of polycyclic aromatic hydrocarbons in water, suspended particulate matter and sediment from Daliao River estuary and the adjacent area, China. *Chemosphere*, *149*, 91-100.

Zhu, S., Li, L., Thornton, C., Carvalho, P., Avery, B. A., & Willett, K. L. (2008). Simultaneous determination of benzo [a] pyrene and eight of its metabolites in *Fundulus heroclitus* bile using ultra-performance liquid chromatography with mass spectrometry. *Journal of Chromatography B*, *863*(1), 141-149.

Zimmer, K. D., Hanson, M. A., & Butler, M. G. (2001). Effects of fathead minnow colonization and removal on a prairie wetland ecosystem. *Ecosystems*, *4*(4), 346-357.

APPENDICES

The appendices correspond to the supplementary materials associated with Chapters 2 and 3. There is an overlap of some appendices for each chapter, while some appendices are divided further by species, i.e., fathead minnow (Chapter 2) and white sturgeon (Chapter 3).

Appendix A. Test organism maintenance and housing

A.1 Fathead minnows housing

Adult fathead minnows used for adult exposures were housed in glass-fiber reinforced plastic tanks (700 L) containing aerated dechlorinated facility water at 22 °C ± 1 °C and a 12 h-light:12 h-dark photoperiod. Fish were fed a diet of frozen *Chironomidae* larvae twice daily (Hikari Sales Inc. Haywards, CA, USA). A second group of adult fathead minnows was used as breeding stock and housed in 20 L aquaria containing facility water within an environmental chamber at a ratio of 2 males: 3 females per tank, at 25 °C ± 1 °C and a 16 h-light:18 h-dark photoperiod. Fish were fed a diet of *Chironomidae* larvae (Hikari Sales Inc.) three times daily. Each breeding tank contained two halves of a PVC pipe to act as a breeding location. Embryos were collected twice daily and placed in glass Petri dishes for immediate use in embryo-larval life stage studies. Water quality parameters (temperature, dissolved oxygen, pH, ammonia) were measured weekly. Temperature (°C), pH, and dissolved oxygen (%) were measured with YSI Professional Plus probe (YSI Incorporated., Yellow Springs, OH, USA), while ammonia was measured using the colorimetric API ammonia test kit (Mars Fishcare, Chalfont, PA, USA).

Appendix B. Waterborne B[*a*]P exposures

B.1 Fathead minnow exposures

Waterborne chronic B[*a*]P exposures were conducted to evaluate uptake by and biotransformation of B[*a*]P in the embryo-larval and adult life stages of fathead minnows. Nominal concentrations for both exposures were 1.3, 4.0 or 12.0 µg B[*a*]P/L (benzo[*a*]pyrene, CAS 50-32-8, Sigma-Aldrich, Oakville, ON, CAN) by use of 0.02% DMSO (≥ 99.9% dimethyl sulfoxide, Fisher Scientific Co., Ottawa, ON, CAN) as the solvent carrier, or 0.02% DMSO only as the solvent control. The embryo-larval exposure also included facility water as a water control.

In the first experiment, fathead minnow embryos (<10 hours post-fertilization) were exposed for 32 days. For the first seven days of exposure, embryos were maintained in a daily 50% static renewal system in glass Petri dishes. Two sets of Petri dishes were maintained with 10 (lipid endpoint: *n*=2 per treatment per sampling point) or 20 (chemical analysis: *n*=2 per treatment per sampling point; biochemical endpoints: *n*=3 per treatment per sampling point) embryos each that

were sampled after three and seven days of exposure. One additional set of Petri dishes was maintained with 30 embryos each (n=5 per treatment) that were sampled after 14 and 32 days of exposure. At eight days of exposure, larvae from these Petri dishes were transferred to 7-L aquaria containing 5 L of water under flow-through conditions, and the tank volume was replaced four times per day. The temperature was maintained at 25°C ± 1°C. After the 32 days of exposure, three remaining larvae per tank (n=5 per treatment) underwent a depuration phase in clean, filtered facility water for an additional seven days. Fish were fed a diet of one or two-day-old *Artemia spp.* nauplii three times daily *ad libitum* starting prior to swim-up, i.e. five days of exposure.

In the second experiment, adult fathead minnow breeding groups consisting of two males and three females were exposed for 21 days (sampling day four and 21 of exposure: n=5 per treatment; sampling day seven, 14 and depuration: n=2 per treatment) following OECD 229: Fish Short Term Reproduction Assay (OECD, 2012) in 20-L flow-through tanks at approximately three full water replacements per day under a 16 h-light:8 h-dark photoperiod, and 25°C ± 1°C. Tanks were allocated to treatment groups by fecundity (the best 5 performing tanks were randomly assigned to the first replicate of each treatment group, then the next best 5 performing tanks to the second replicate of each treatment group, and so on) to ensure uniform fecundity between treatments at the start of exposure, and the number of eggs produced from each tank was recorded daily for the remainder of the exposure. Post-exposure, remaining tanks underwent a seven-day depuration phase during which they were switched to facility water. Fish were fed *ad libitum* a diet of frozen *Chironomidae* larvae three times daily during all phases of exposure.

Water quality parameters temperature (°C), dissolved oxygen (%), pH, conductivity (µS/cm), ammonia (mg/L), nitrates (mg/L), nitrites (mg/L), hardness (mg/L), and alkalinity (mg/L) were recorded daily from a manual selection of tanks to ensure each tank was tested once weekly. Temperature, dissolved oxygen, pH, and conductivity were measured using a hand-held digital instrument (YSI Professional Plus, YSI Inc.). Nitrates and nitrites were measured using colorimetric kits, and hardness and alkalinity were measured using titrations kits from LaMotte Co. (Chestertown, MD, USA). Ammonia was measured using the colorimetric API ammonia test kit (Mars Fishcare).

Table B.1. Time-resolved aqueous B[*a*]P concentrations for the embryo-larval and adult fathead minnow exposures

Embryo-larval exposure sampling times (day)	Low concentration (µg B[*a*]P/L)	Medium concentration (µg B[*a*]P/L)	High concentration (µg B[*a*]P/L)
1	0.03	0.30	2.00
15	0.12	0.62	3.54
30	0.32	1.64	8.11

Adult exposure sampling times (day)	Low concentration (µg B[*a*]P/L)	Medium concentration (µg B[*a*]P/L)	High concentration (µg B[*a*]P/L)
2	0.04	0.07	1.18
11	0.02	0.09	0.73
20	0.03	0.11	2.1

B.2 Embryo-larval white sturgeon exposure

A chronic waterborne B[*a*]P exposure was conducted for 49 days to evaluate the uptake and biotransformation of B[*a*]P during the egg, yolk, and free-feeding developmental stages of the white sturgeon. Embryos (<24 hours post-fertilization) were initially exposed in glass jars containing facility water from the supplier spiked with B[*a*]P (CAS 50-32-8, Sigma-Aldrich, Oakville, ON, CAN) to obtain nominal concentrations of 1.3, 4.0, and 12.0 µg B[*a*]P/L using 0.02% DMSO (≥ 99.9% dimethyl sulfoxide, Fisher Scientific Co., Ottawa, ON, CAN) as the solvent carrier, or 0.02% DMSO only as the solvent control, or facility water as the water control (*n*=4 per treatment). Five days post fertilization (dpf), the exposed embryos were transported to the Aquatic Toxicology Research Facility (ATRF) at the University of Saskatchewan, and the jars were placed into 7-L aquaria containing 50% RO water, 50% ATRF facility water as water bath, which maintained a temperature of 14°C ± 1°C. At hatch, the embryos within the jars were carefully emptied into the aquaria for the remainder of exposure. After 49 days of exposure, three remaining larvae (*n*=4 per treatment) underwent a seven-day depuration period in which all tanks were switched to clean water. A 50% daily static renewal system was maintained throughout all phases of exposure. The larvae were fed a diet of one or two-day-old *Artemia spp.* nauplii three times daily *ad libitum* starting prior to swim-up, i.e., ~10 days post-hatch.

Water quality parameters temperature (°C), dissolved oxygen (%), pH, conductivity (µS/cm), ammonia (mg/L), nitrates (mg/L), nitrites (mg/L), hardness (mg/L), and alkalinity (mg/L) were recorded from a random distribution of tanks weekly. Temperature, dissolved oxygen, pH, and conductivity were measured using a hand-held digital instrument (YSI Professional Plus, YSI Inc.). Nitrates and nitrites were measured using colorimetric kits, and hardness and alkalinity were measured using titrations kits from LaMotte Co. (Chestertown, MD, USA). Ammonia was measured using the colorimetric API ammonia test kit (Mars Fishcare).

Table B.2. Time-resolved aqueous B[*a*]P concentrations for the embryo-larval white sturgeon exposure

Embryo-larval exposure sampling times (day)	Low concentration (µg B[*a*]P/L)	Medium concentration (µg B[*a*]P/L)	High concentration (µg B[*a*]P/L)
1	0.00	0.93	4.08
14	3.67	7.32	9.67
22	1.30	N/A[a]	6.71
28	1.73	4.23	9.01
35	3.70	3.95	14.49
49	N/A[a]	N/A[a]	10.68

[a] N/A (not available), an error occurred during analysis and a concentration could not be calculated

Appendix C. Analytical analysis of B[*a*]P metabolites

The major metabolites 3-hydroxy-benzo[*a*]pyrene (OH-B[*a*]P) and 3-hydroxy-benzo[*a*]pyrene *O*-glucuronide (Gluc-B[*a*]P) were quantified using ultra-high-performance liquid chromatography high-resolution mass spectrometry (UPLC-HRMS) using a modified method described by Beach et al. (2000), Zhu et al. (2008), Lu et al., (2011), and Tang et al. (2016). The quantification method was developed due to the lack of standards available for gluc-B[*a*]P metabolites. Improvements to the standard method, in which total PAH equivalent concentrations were quantified by their quantitative enzymatic conversion into OH-PAHs (Kammann, 2007), were made by being able to obtain measurements that provide information on the relative concentrations of the major metabolite classes.

Metabolite analysis was conducted using a Vanquish UHPLC and Q-Exactive™ HF Quadrupole-Orbitrap™ mass spectrometer (Thermo-Fisher, Waltham, MA, USA). An Acclaim Vanquish 2.2-µm C18 LC column (150 x 2.1 mm) (Thermo-Fisher) using gradient elution with water and acetonitrile (ACN), both containing 0.1% formic acid at a flow rate of 0.25 mL/min and column temperature of 30°C was used for LC separation. The run time was 25 minutes in total using a gradient of 25% ACN from 0-3 min, increasing 25% to 100% ACN from 3-15 minutes, 100% ACN from 15-18 minutes, and re-equilibration for 7 minutes to 25% ACN. The retention time of OH-B[*a*]P was 12.74 and Gluc-B[*a*]P was 8.39

Samples were ionized by negative mode heated electrospray ionization (HESI) followed by a full MS/parallel reaction monitoring (PRM) method which monitored the [M-H]⁻ parent ion m/z 267.080 for OH-B[*a*]P and both parent and daughter ions for Gluc-B[*a*]P (m/z 443.113 → 267.080). HESI source parameters were as follows: sheath gas flow = 35; aux gas flow = 8; sweep gas flow = 1; aux gas heater = 325°C; spray voltage = 2.7 kV; S-lens RF = 55; capillary temperature = 300°C. The PRM scan settings were: 60,000/30,000 resolution, AGC target = $1x10^6/2x10^5$, max. injection time = 100ms/100ms, full MS scan range of 80-500 *m/z,* PRM isolation window of 2.0 m/z, and normalized collision energy = 30.

Stock solutions of OH-B[*a*]P (CAS 13345-21-6, Toronto Research Chemicals, ON, CAN) were made in HPLC grade methanol/ACN (Fisher Scientific, Waltham, MA, USA). A six-point OH-B[*a*]P calibration curve (0.3, 1, 3, 10, 30, 100 ng/ml, r^2 = 0.9959) was used for semi-quantification of the B[*a*]P metabolites. Concentrations of OH-B[*a*]P were quantified directly with the use of analytical standards and external calibration. To quantify Gluc-B[*a*]P concentrations, a semi-quantification method was used. A representative set of bile samples from B[*a*]P-exposed rainbow trout (*Oncorhynchus mykiss*) were analyzed untreated (25 µL bile, 100 µL purified water), or treated with glucuronidase (25 µL bile, 95 µL purified water, 5 µL 30/60 U/mL glucuronidase;

CAS 9001-45-0, Roche, Basel, Switzerland) to convert the glucuronide metabolites into OH-B[*a*]P. The samples were incubated in a shaking incubator (New Brunswick™, Innova 40®) at 200rpm and 37°C for two hours. Following incubation, the samples were diluted 1:10 in ACN and centrifuged at 1,700×g for 15 minutes. The supernatant was subsequently sampled for quantification of OH-B[*a*]P and Gluc-B[*a*]P following the methods outlined above. These samples provided an instrument relative response factor for semi-quantification. The response factors for glucuronide was calculated as (Eq. S1):

$$Response\ factor = \frac{Peak\ Area\ [OH-BaP]_{treated}}{Peak\ Area\ [Gluc-BaP]_{untreated}} \qquad (S1)$$

The average response factor for Gluc-B[*a*]P was 7.4. This suggests that for equimolar amounts of OH- and Gluc-B[*a*]P, the OH-B[*a*]P response was 7.4 times less sensitive. To obtain an external calibration curve for each metabolite, response factors were used to convert peak areas of OH-B[*a*]P from the standard curve to Gluc-B[*a*]P peak areas. Concentrations of each metabolite measured in the extracted whole-body embryo or adult bile samples could then be determined from the peak areas.
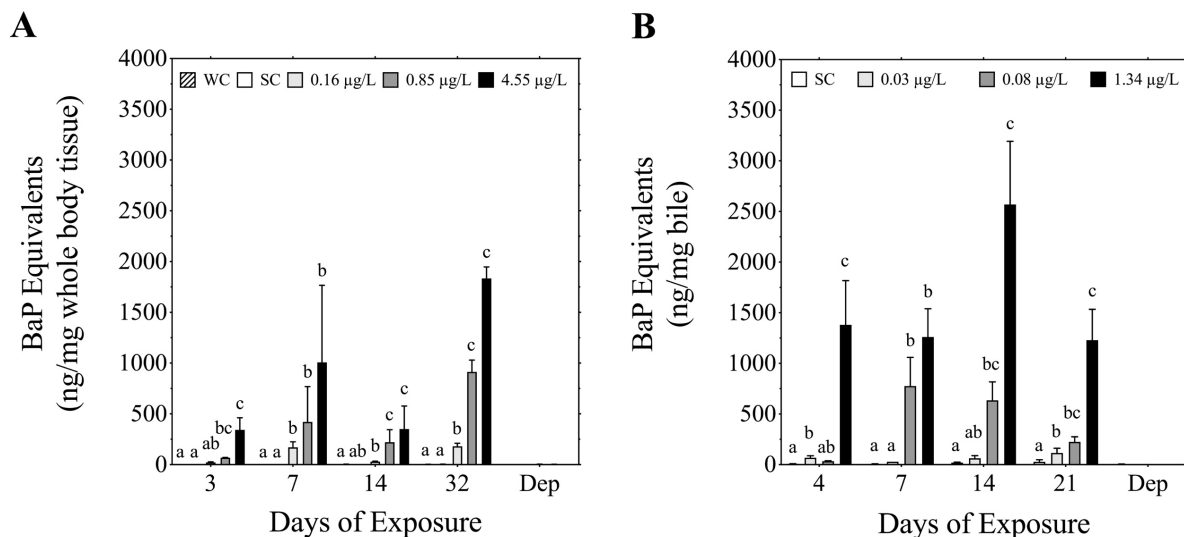
Figure C.1. Abundance of B[*a*]P equivalents (ng/mg whole body tissue or ng/mg bile) in whole-body embryo-larval (A) or the bile of adult (B) fathead minnows after three, seven, 14 and 32 or four, seven, 14 and 21 days of exposure to increasing concentrations of B[*a*]P as well as water control (WC) and solvent control (SC), respectively. B[*a*]P equivalents were calculated as mass concentrations that are independent of differences in molecular weight of the parent B[*a*]P and the metabolites from measured concentrations of 3-OH-B[*a*]P and associated glucuronide (metabolite specific data provided in the main document Figure 1). Data are expressed as mean ± S.E.M. Different letters denote a significant difference in B[*a*]P equivalents among treatment groups within each respective time point (2-way ANOVA with Tukey's HSD, $\alpha = 0.05$).
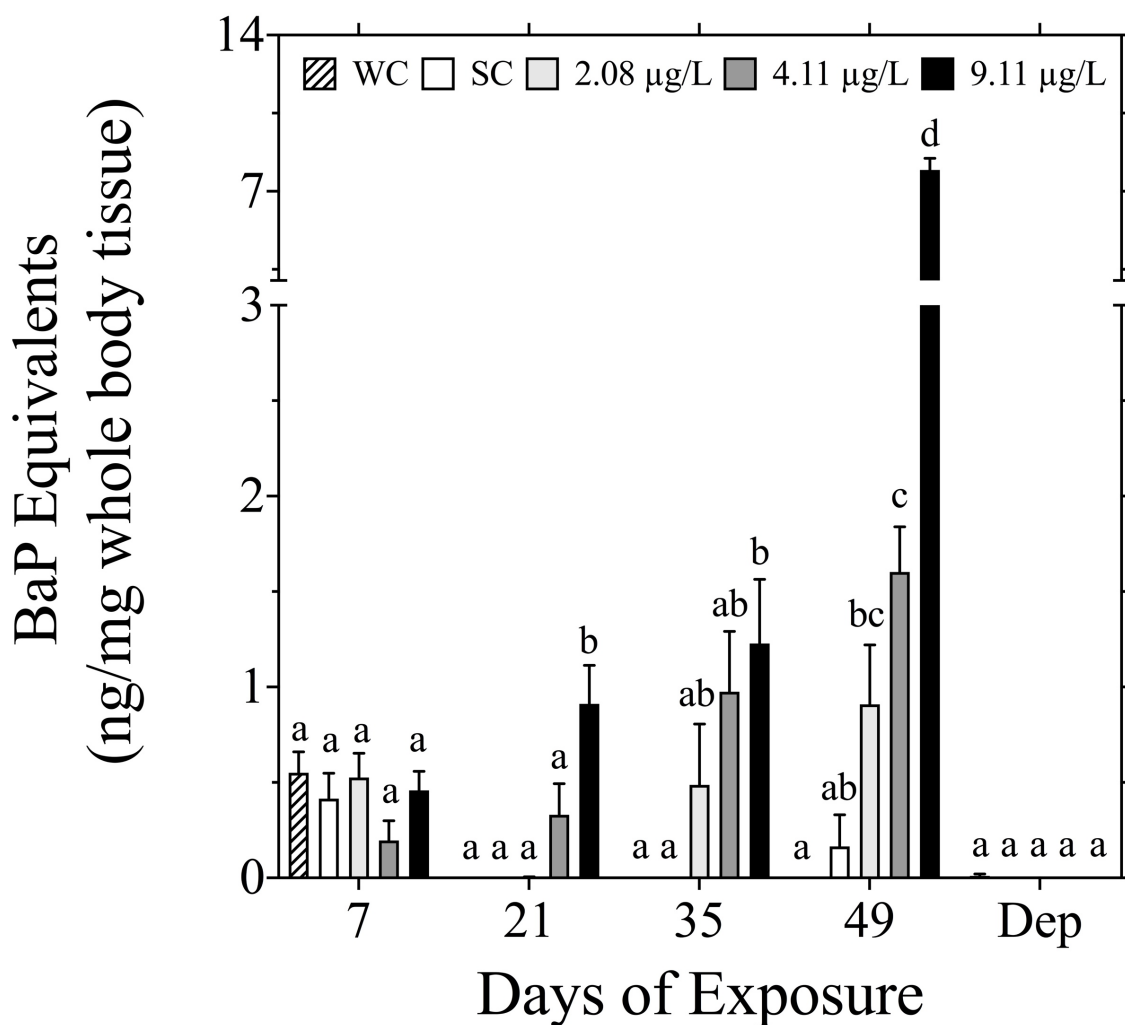
Figure C.2. Abundance of B[*a*]P equivalents (ng/mg whole body tissue) in whole-body embryo-larval white sturgeon after seven, 12, 21, 35, and 49 days of exposure to increasing concentrations of B[*a*]P as well as water control (WC) and solvent control (SC). B[*a*]P equivalents were calculated as mass concentrations that are independent of differences in molecular weight of the parent B[*a*]P and the metabolites from measured concentrations of 3-OH-B[*a*]P and associated glucuronide (metabolite specific data provided in the main document Figure 1). Data are expressed as mean ± SEM. Different letters denote a significant difference in B[*a*]P metabolites between treatment groups within each respective time point (One-way ANOVA with Tukey's HSD, α = 0.05).

Appendix D. Measurement of intrinsic clearance

Intrinsic clearance was measured in triplicates following the protocol described in OECD319b (OECD, 2018) with modifications. ATP (adenosine triphosphate, CAS 34369-07-8), NADPH (nicotinamide adenine dinucleotide phosphate reduced, CAS 100929-71-3), G6P (glucose-6-phosphate, CAS 54010-71-8), GSH (glutathione reduced, CAS 70-18-8), and UDPGA (uridine 5'-diphosphoglucuronic acid, CAS 63700-19-6) were purchased from Sigma-Aldrich. Two replicates of three pooled fathead minnow livers, and three replicates of three pooled white sturgeon livers, were used to obtain the S9 fraction. Liver tissue was homogenized in 5 µL homogenization buffer: 1 mg tissue for fathead minnow, and in 3 µL homogenization buffer: 1 mg tissue for white sturgeon, and centrifuged at 9,000 × g for 20 minutes. The supernatant (S9) was sampled for use in the *in vitro* clearance assay, and the protein concentration of the S9 was determined using the BCA (bicinchoninic acid) protein assay. A co-substrate mixture described by Richardson et al. (2016) was generated, with modifications, using ATP (11.1 mM), G6P (5.55 mM), GSH (2.77 mM), NADPH (0.55mM), and UDPGA (0.55mM) reconstituted in phosphate buffer (pH 7.4; 100 mM potassium phosphate, 5 mM magnesium chloride, 5 mM magnesium sulfate), to create a PAPS (3'-phosphoadenosine-5'-phosphosulfate) regenerating system. In a glass cell culture tube, S9 and the co-substrates were combined. The solution was spiked with 250µM B[*a*]P in ACN to obtain a concentration of 0.5 µM B[*a*]P and immediately incubated at 25°C in a shaking incubator (New Brunswick^{TM}, Innova 40®). Fathead minnow sub-samples of the solution were taken after 0, 20, 40, 60, 80, 100, and 120 minutes, and white sturgeon sub-samples were taken after 0, 30, 60, 90, 120, 180, and 240 minutes. The sub-samples were immediately quenched in ice-cold ACN. Samples were centrifuged at 1700×g for 15 minutes. The supernatant was subsequently analyzed for parent B[*a*]P concentrations using synchronous fluorescence spectrophotometry in a quartz cuvette (Lumina, Thermo Fisher Scientific, Ottawa, ON, CAN). Parent B[*a*]P signaled between 400-440 nm and the B[*a*]P metabolites between 420-480 nm, measured and validated using neat B[*a*]P and OH-B[*a*]P standards. The peak area of the B[*a*]P curve was interpolated from a 6-point standard curve (0.00, 0.03, 0.06, 0.13, 0.25, and 0.50 µM; $r^2 = 0.9989$) and concentrations were plotted against time. The depletion curve was *log*-transformed, and the first-order depletion rate constant (k) was determined by multiplying the slope of the line by -2.3. Intrinsic clearance (Cl$_{int, in vitro}$) was calculated as (Eq. S2):

$$Cl_{int,in\ vitro}(mL\ h^{-1}mg^{-1}) = \frac{k(h^{-1})\cdot volume\ of\ the\ reaction\ (mL)}{reaction\ protein\ concentration\ (mg\ L^{-1})} \qquad (S2)$$

Appendix E. EROD assay

EROD (7-ethoxyresorufin-O-deethylase) activity was measured in triplicates following the protocol previously described by Kennedy & Jones (1994), with modifications. BSA (bovine serum albumin, CAS 9048-46-8), EDTA (Ethylenediaminetetraacetic acid, CAS 6381-92-6), DTT (DL-dithiothreitol, CAS 3483-12-3), fluorescamine (CAS 38183-12-9), HEPES (CAS 7365-45-9), KCL (potassium chloride, CAS 7447-40-7), NADPH (nicotinamide adenine dinucleotide phosphate reduced, CAS 100929-71-3), resorufin (CAS 653-78-9), sucrose (CAS 57-50-1), and Tris-HCl (Trizma®Base, CAS 77-86-1) were purchased from Sigma-Aldrich (Oakville, ON, CAN). Ethoxyresorufin (CAS 5725-91-7) was purchased from Fisher Scientific Co. (Ottawa, ON, CAN). The post-mitochondrial supernatant fraction was generated from the whole-body larvae and adult liver samples following a modified protocol of what is described by OECD 319B (OECD, 2018). Tissue was homogenized in homogenization buffer (150 mM Tris-HCl, 150 mM KCl, 2 mM EDTA, 1 mM DTT, 250 mM sucrose) at a ratio of 20 µL buffer: 1 mg tissue then centrifuged at $10,000 \times g$. Six-point resorufin (0, 1.9, 3.8, 7.5, 15, 60 µM) and protein (0, 0.006, 0.012, 0.024, 0.036, 0.48 µM) standard curves were produced by adding HEPES buffer (0.05 M, pH 7.8), BSA (2 mg/mL in HEPES), and resorufin (1.9 µM in HEPES) to six sets of triplicate wells of a 96 well plate. Ethoxyresorufin (250 µM in HEPES; 30 µL) was added to all used wells and the plate was incubated at room temperature, in darkness, for 10 minutes. Following incubation, NADPH (0.3 mM in HEPES, 10 µL) was added to all wells, except the sample blanks, to initiate the reaction, and the plate was incubated at 25 °C in darkness for 30 minutes. The reaction was stopped by the addition of fluorescamine in ACN (600 µg/mL; 60 µL) to all used wells, and the plate was incubated at room temperature in darkness for 15 minutes. Fluorescence of resorufin was read at 570 nm excitation/ 630 nm emission and proteins at 365 nm excitation/ 480 nm emission using a multi-well plate reader (POLARstar Optima, BMG Labtech, Ortenberg, Germany).
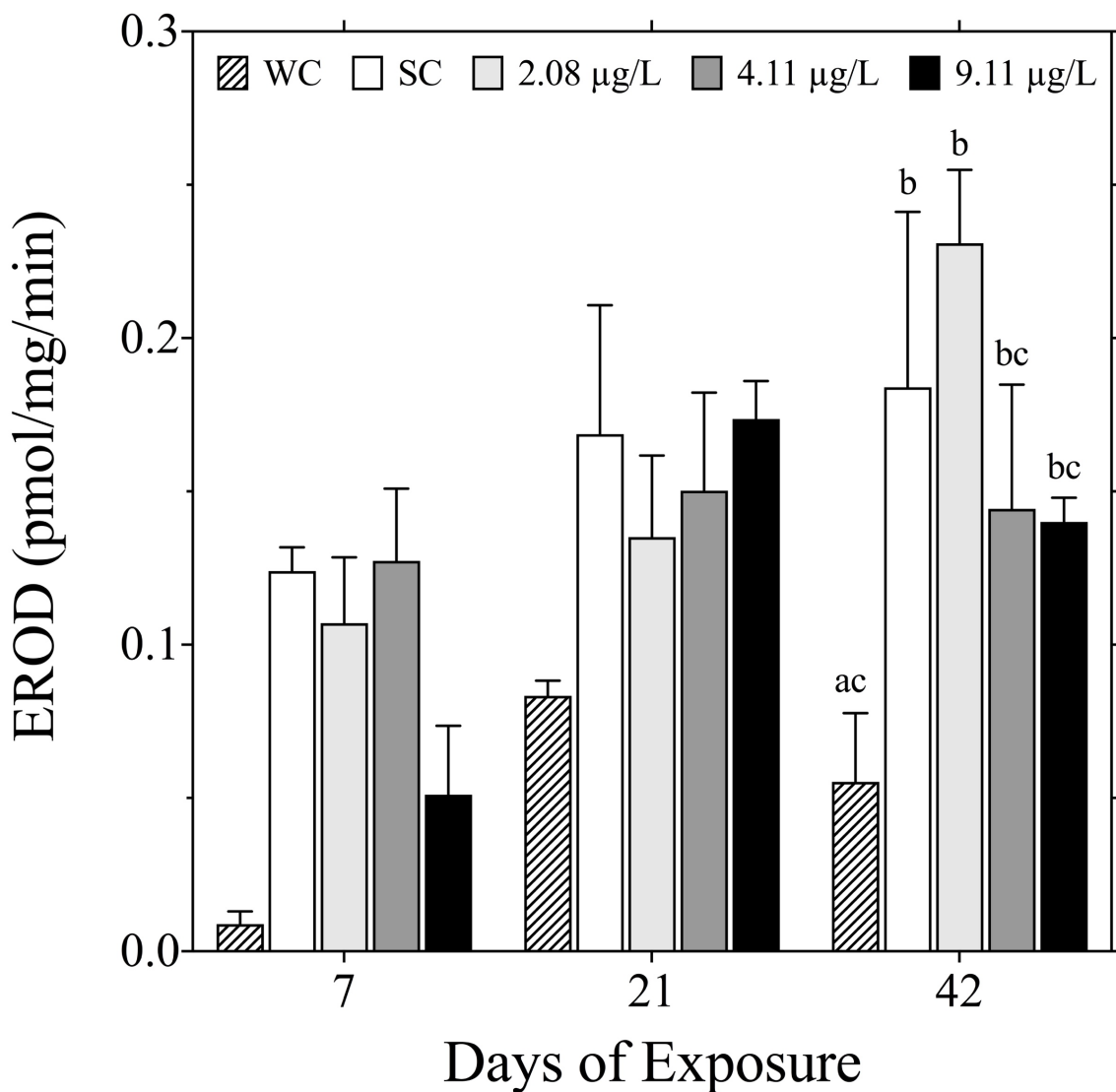
Figure E.1. EROD activity (pmol/mg/min) for whole-body embryo-larval white sturgeon after seven, 21, and 42 days of exposure to increasing concentrations of B[a]P as well as water control (WC) and solvent control (SC), respectively. Data are expressed as mean ± SEM. Different letters denote a significant difference in EROD activity among treatment groups within each respective time point (2-way ANOVA, $\alpha = 0.05$). No differences existed among treatment groups on day 12 or 21 of exposure.

Appendix F. GST assay

GST (glutathione-*S*-transferase) activity was measured in triplicates following the protocol described by Habig et al. (1974), adapted to microplates. The reagents CDNB (1-Chloro-2,4-dinitrobenzene, CAS 97-00-7), GSH (glutathione reduced, CAS 70-18-8), and potassium phosphate were purchased from Sigma-Aldrich. The post-mitochondrial supernatant fraction was produced as described for the EROD assay. Phosphate buffer (0.1 M, pH 6.5, 275 µL or 250 µL) was added to all wells for sample blanks and active wells respectively, followed by the post-mitochondrial supernatant fraction (20 µL) and CDNB (25 mM in ethanol; 10 µL). To initiate the reaction, GSH (11.4 mM in phosphate buffer; 25 µL) was added to active wells. A kinetic reading of absorbance was immediately started at 340 nm and 25°C for 10 minutes using a multi-well plate reader (POLARstar Optima, BMG Labtech). The concentration of CDNB was calculated using the Lambert-beer law. To calculate GST activity (nmol CDNB/mg protein/min), the molar extinction coefficient of 9.6 1/(mM cm) was used. The protein concentration of the post-mitochondrial supernatant fraction was measured using the BCA (bicinchoninic acid) protein assay kit (SKU BCA1; Sigma-Aldrich).
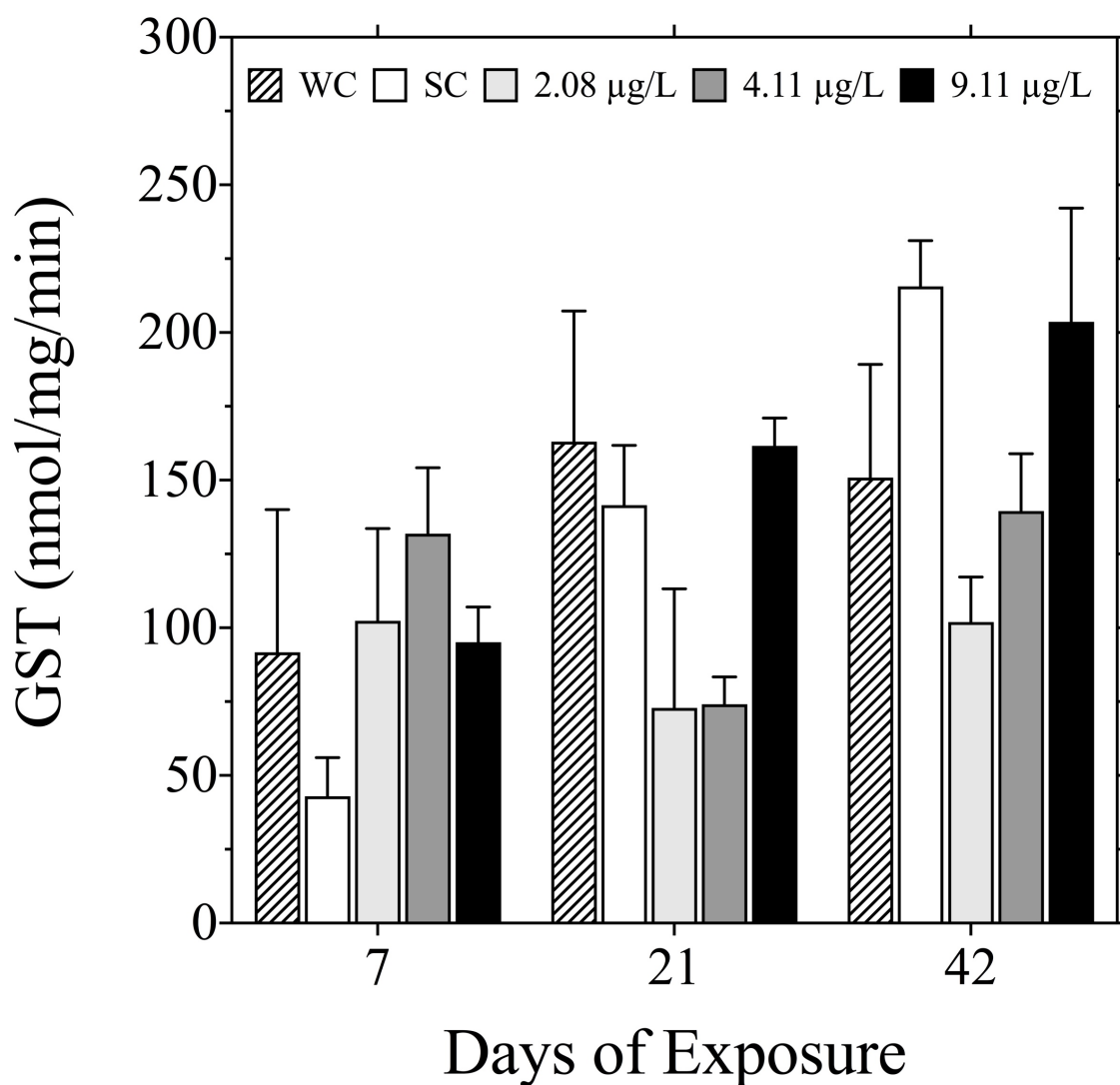
Figure F 1. GST activity (nmol/mg/min) of whole-body embryo-larval white sturgeon after seven, 21, and 42 days of exposure to increasing concentrations of B[*a*]P as well as water control (WC) and solvent control (SC), respectively. Data are expressed as mean ± SEM. No differences existed among treatment groups within each respective time point (2-way ANOVA, $\alpha = 0.05$).

Appendix G. Lipid analysis

Total whole-body lipid content in both life stages was quantified using a modification of the microcolorimetric sulfophosphovanillin (SPV) described by Lu et al. (2008). Sulphuric acid (CAS 7664-93-9) and phosphoric acid (CAS 7664-38-2) were purchased from Thermo Fisher Scientific, and vanillin (CAS 48-53-8) was purchased from Sigma-Aldrich. Lipids were extracted in triplicates using whole-body fish (embryo-larval fathead minnow, 10-50 mg wet weight; embryo-larval white sturgeon, 30-120 mg wet weight, adult fathead minnow, 10-50 mg homogenized sub-sample) or homogenized sub-samples of adult tissues (20-100mg sub-sample; liver, kidney, spleen, muscle, brain, gills, viscera, and carcass). The samples were homogenized in a 2:1 mixture (v/v) of chloroform and methanol followed by saline (200µl) for lipid purification. In instances in which sample weight exceeded 50 mg, extra chloroform:methanol (200 µL) was added to ensure complete homogenization of the sample and appropriate lipid concentrations. Lipid extracts (200 µL) were evaporated in 5-mL glass culture tubes using a dry bath heater, and lipids subsequentially quantified by the addition of sulphuric acid (62.5 µL) and SPV reagent (1.25 mL of a solution containing 0.75 g vanillin in 0.125 L deionized water and 0.5 L phosphoric acid). Absorbance was measured at 525nm from a 96-well plate using a multi-well plate reader (POLARstar Optima, BMG Labtech, Ortenberg, Germany). A 6-point standard curve (0.00, 0.16, 0.31, 0.63, 1.25, 5.00 mg/mL; $r^2 = 0.9971$) was developed from a serial dilution of cod liver oil (CAS 8001-69-2, Sigma Aldrich) in 2:1 (v/v) chloroform:methanol and used to determine total lipid content of the samples.

Appendix H. Gene Expression

H.1 Fathead minnow
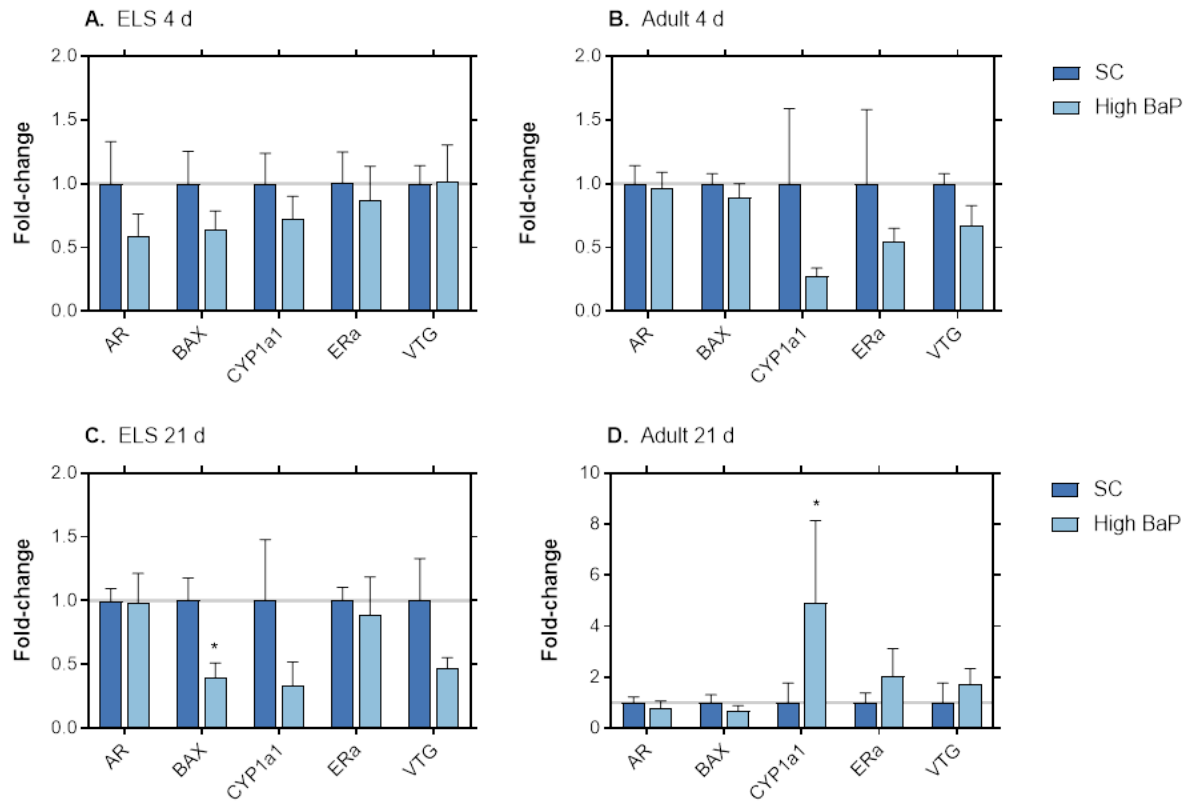
Figure H.1. Relative fold change of the genes androgen receptor (AR), BCL2 Associated (BAX), Cytochrome P450 family 1, subfamily A, polypeptide 1 (CYP1a1), estrogen receptor alpha (Era), and vitellogenin(VTG) in embryo-larval and adult female fathead minnows after a 4 and 21 day aqueous exposure to the solvent control (SC) and respective high B[*a*]P concentration from each exposure (embryo-larval, 4.55 µg B[*a*]P/L; adult, 1.34 µg B[*a*]P/L). Asterisks (*) represent a significant difference between treatment groups for the respective gene (p<0.05). This data was partially published by DeBofsky et al. (2020).

Appendix I. One-compartment embryo-larval life stage model

I.1 Embryo-larval fathead minnow model

The one-compartment bioaccumulation model described by Arnot and Gobas (2004) was adapted to predict the abundance of parent B[*a*]P and B[*a*]P metabolites in the ELS (embryo-larval stage) of fathead minnow exposed aqueously to B[*a*]P (Supplemental Table I.2). To adapt the model to account for biotransformation of B[*a*]P, a whole-body metabolism rate constant (k_{met}) was implemented into the model. The whole-body metabolism rate constant was calculated using an Excel spreadsheet provided by Nichols, Fitzsimmons, & Burkhard (2007), which used the parameters cardiac output, liver blood flow, and hepatic clearance (Table I.1). The model was implemented using Python 3.5® (Python Software Foundation, Wilmington, DE, USA) in Jupyter Notebook® (Project Jupyter, U.S. Patent & Trademark Office, Alexandria, VA, USA). A series of matrices were used for the parameters wet weight (w_w), whole-body lipid content (lipid), and the whole body chemical transformation rate constant (k_met) to describe the time function of parameters, i.e., the relationship between the parameter value and life stage (i.e., 0, 3, 7, 14, 32 or 39 days post fertilization (dpf)). A simulated exposure was run at the three measured average exposure concentrations, 0.16, 0.85, and 4.55 μg B[*a*]P/L for 32 days, 1000 iteration steps per day. Using the model, the accumulation of B[*a*]P and B[*a*]P metabolites were predicted in the whole-body fathead minnow larvae.

I.2 Embryo-larval white sturgeon model

The one-compartment bioaccumulation model described by Arnot and Gobas (2004) (Table I.2) was adapted to predict the abundance of parent B[*a*]P and B[*a*]P metabolites in the ELS (embryo-larval stage) of white sturgeon exposed aqueously to B[*a*]P. Biotransformation of B[*a*]P was integrated into the model through a whole-body biotransformation rate constant (k_{MET}). Because biotransformation could not be appropriately measured or scaled in the embryo-larval white sturgeon, k_{MET} was calibrated using a training data set consisting of 21 randomly selected data points out of the 42 measured values of B[*a*]P metabolite abundances. The k_{MET} values were obtained by adjusting *in vitro* clearance, in an allometric scaling equation (Table I.1) that uses estimates of cardiac output, until the highest achievable number of predictions were within one order of magnitude of the training set of measured values (Figure S4).

The model was implemented using Python 3.5® (Python Software Foundation, Wilmington, DE, USA) in Jupyter Notebook® (Project Jupyter, U.S. Patent & Trademark Office, Alexandria, VA, USA). A series of matrices were used for the parameters wet weight (w_w), whole-body lipid content (lipid), and the whole body biotransformation rate constant (k_met) to

describe the time function of parameters, i.e., the relationship between the parameter value and life stage (i.e., 0, 7, 12, 21, 35, 42, 49, or 56 days post fertilization (dpf)). A simulated exposure was run at the three measured average exposure concentrations, 2.08, 4.11, and 9.11 µg B[a]P/L for 49 days, 1000 iteration steps per day. The accumulation of B[a]P and B[a]P metabolites were predicted in the whole-body fathead minnow larvae using the model. Predictions of B[a]P metabolites were represented as B[a]P equivalents, i.e., mass concentrations that are independent of differences in molecular mass the parent B[a]P and the two measured metabolites. Therefore, for analysis of model performance, the measured abundances of B[a]P were also converted to B[a]P equivalents (Figure S3).
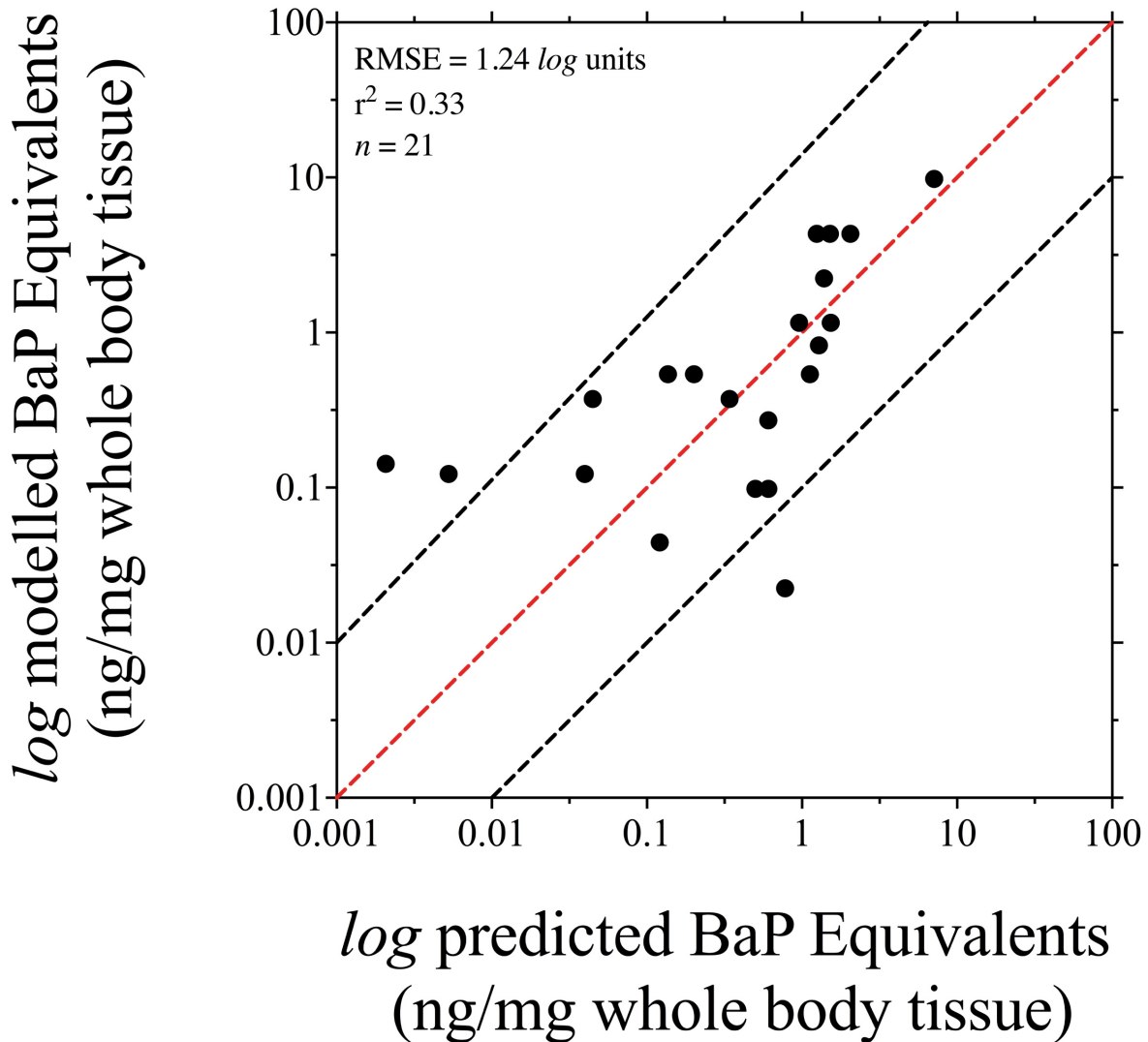
Figure I.1. Calibration of embryo-larval whole-body biotransformation in the white sturgeon. The figure shows the relationship between predicted and measured concentrations of B[*a*]P equivalents generated from the calibrated values of whole-body biotransformation. The dashed red line represents the equality line, and the dashed black lines represent the ± 10-fold deviation from equality. The parameter was determined using a training set of 21 data points and adjusted until the highest achievable number of predictions were within 1-order of magnitude from the measured values. Predicted B[*a*]P equivalents were obtained directly from model outputs, and measured B[*a*]P equivalents were calculated as mass concentrations that are independent of differences in molecular mass of the parent B[*a*]P and the two measured metabolites, OH-B[*a*]P and gluc-B[*a*]P. RMSE, root mean squared error.
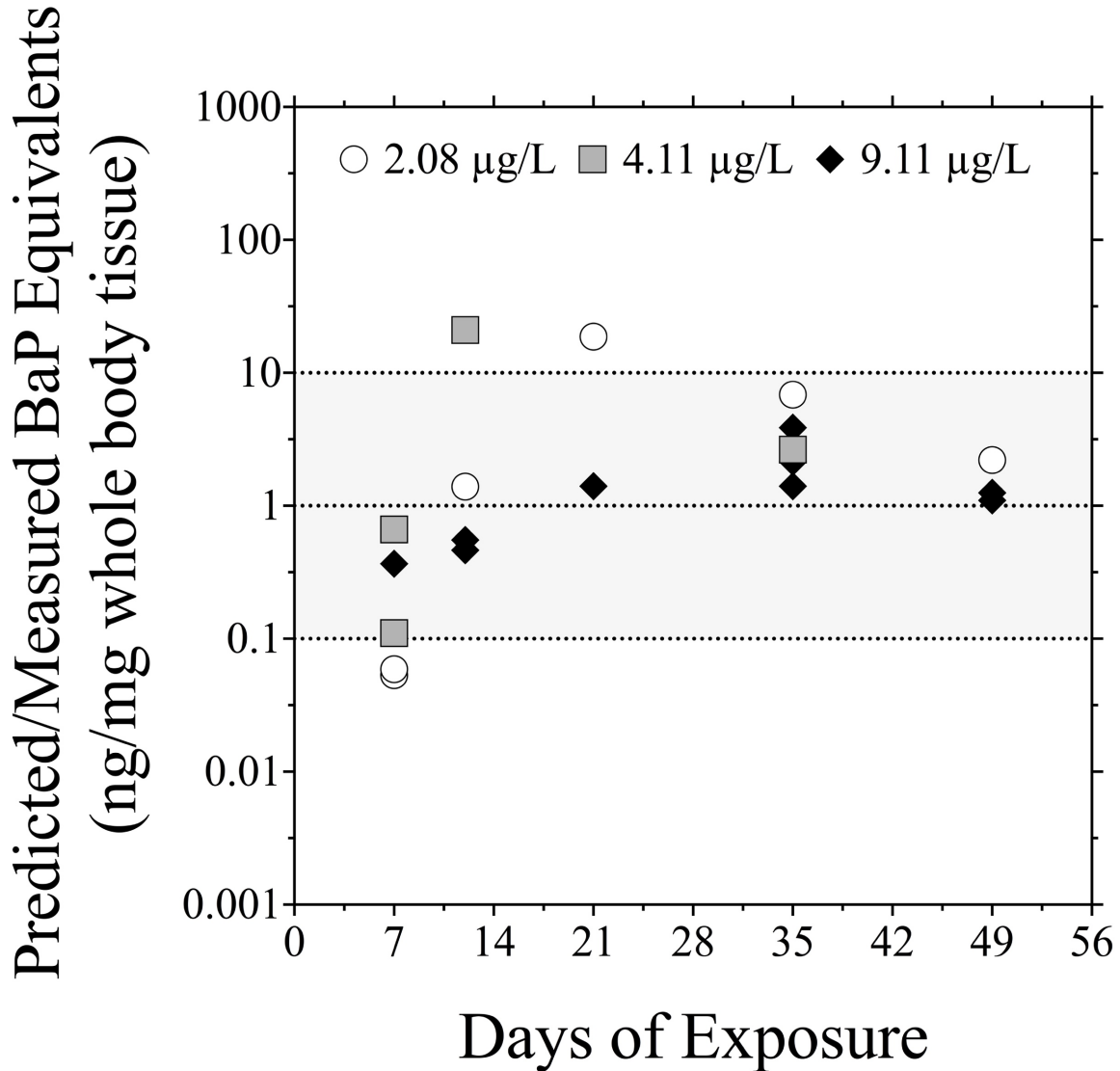
Figure I.2. Relationships between predicted and measured concentrations of B[*a*]P equivalents from the embryo-larval white sturgeon one compartment relative to the day of exposure with ± 10-fold error from equality (grey). Predicted B[*a*]P equivalents were obtained directly from model outputs. Measured B[*a*]P equivalents were calculated as mass concentrations that are independent of differences in molecular mass of the parent B[*a*]P and the two metabolites, OH-B[*a*]P and gluc-B[*a*]P, from measured metabolite concentrations in order to match model output units.

Table I.1. Spreadsheet inputs and parameters for the embryo-larval life stage of fathead minnow (*Pimephales promelas*) and white sturgeon (*Acipenser transmontanus*) to calculate whole-body metabolism rate. The table is based on Nichols, Fitzsimmons, & Burkhard (2007).

Symbol	Units	Description	Fathead minnow values			White Sturgeon values						
			Egg stage (0-3 dpf)	Yolk stage (3-7 dpf)	Free feeding stage (7-32 dpf)	Egg stage (0-12 dpf)	Yolk stage (12-21 dpf)		Free feeding stage (21-56 dpf)			
			3 dpf	14 dpf	32 dpf	7 dpf	12 dpf	21 dpf	35 dpf	42 dpf	49 dpf	56 dpf
Rate	h^{-1}	Depletion rate constant	– Adult value assumed (Table J.2)[a] –			0.00078[b]						
Bwg	g	Fish wet weight	0.00122	0.00079	0.00348	0.04911	0.03230	0.04009	0.04938	0.05950	0.08260	0.1242
log K_{ow}	-	Octanol-water partitioning coefficient	6.19									
C_{S9}	mg mL^{-1}	S9 protein concentration	– Adult value assumed (Table J.2) –									
L_{S9}	mg g liver^{-1}	Total liver S9 protein content	– Adult value assumed (Table J.2) –									
L_{FBW}	g liver g wet weight^{-1}	Fractional liver weight	– Adult value assumed (Table J.2) –									
V_{LWB}	-	Fractional whole-body lipid content	0.0182	0.017	0.029	0.0285	0.0362	0.0299	0.0254	0.0138	0.0047	0.0025
Q_C	L d^{-1} kg^{-1}	Cardiac output	34.980	110.868	39.528	34.980[c]	34.980[c]	110.868[c]	39.528[c]	39.528[c]	39.528[c]	39.528[c]
Q_{HFRAC}	-	Liver blood flow as a fraction of cardiac output	– Adult value assumed (Table J.2) –									
V_{WBL}	-	Fractional blood water content	– Adult value assumed (Table J.2) –									
f_u	-	Binding correction term	1.0 (assumed)									
$CL_{int,\ in\ vitro}$	mL h^{-1} mg S9 protein^{-1}	*In vitro* intrinsic clearance	– Equation S3 –									
$CL_{int,\ in\ vivo}$	L d^{-1} kg^{-1}	*In vivo* intrinsic clearance	– Equation S4 –									
Q_H	L d^{-1} kg^{-1}	Liver blood flow	– Equation S5–									
Cl_H	L d^{-1} kg^{-1}	Hepatic clearance	– Equation S6 –									

P_{bw}	-	Blood:water partitioning coefficient	– Equation S7 –
BCF_P	L kg^{-1}	Partitioning based BCF	– Equation S8 –
$V_{D,BL}$	L kg^{-1}	Volume of distribution to blood plasma	– Equation S9 –
k_{met}	d^{-1}	Whole-body metabolism rate	– Equation S10 –

[a]*derived from adult fathead minnow livers using methods described in OECD 319B: Determination of in vitro clearance using rainbow trout liver S9 sub-cellular fraction (RT-S9) (OECD, 2018)*

[a]*calibrated to produce k_{MET} values that resulted in the highest achievable number of predictions to be within 10-fold of the training set of measured values*

[b]*stage-matched and assumed to be equivalent to cardiac output measured in fathead minnow larvae (Grimard et al.[4])*

Spreadsheet equations for calculation of k$_{met}$ (Nichols et al., 2007)

In vitro intrinsic clearance

$$Cl_{int,in\ vitro} = \frac{rate}{C_{S9}} \text{ ; (mL h}^{-1} \text{ mg S9 protein}^{-1})$$

(Eq. S3)

In vivo intrinsic clearance

$$CL_{int,in\ vivo} = CL_{in\ vitro,int} \cdot L_{S9} \cdot L_{FBW} \cdot 24h \text{ ; (L d}^{-1} \text{ kg}^{-1})$$

(Eq. S4)

Liver blood flow

$$Q_H = Q_C \cdot Q_{HFRAC} \text{ ; (L d}^{-1} \text{ kg}^{-1})$$

(Eq. S5)

Hepatic clearance

$$CL_H = \frac{Q_H \cdot f_u \cdot CL_{in\ vivo,int}}{Q_H + f_u \cdot CL_{in\ vivo,int}} \text{ ; (L d}^{-1} \text{ kg}^{-1})$$

(Eq. S6)

Blood:water partition coefficient

$$P_{bw} = 10^{0.73 \cdot log\ K_{ow}} \cdot 0.16 + V_{WBL} \text{ ; (unitless)}$$

(Eq. S7)

Partitioning based bioaccumulation factor

$$BCF_P = V_{LWB} \cdot 10^{log\ k_{ow}} \text{ ; (L kg}^{-1})$$

(Eq. S8)

Volume of distribution to blood plasma

$$V_{D,BL} = \frac{BCF_P}{P_{BW}} \text{ ; (L kg}^{-1})$$

(Eq. S9)

Whole body metabolism rate

$$k_{met} = \frac{CL_H}{V_{D,BL}} \text{ ; (d}^{-1})$$

(Eq. S10)

Table I.2. Model inputs and parameters of the one-compartment model for the embryo-larval life stage of fathead minnow (*Pimephales promelas*) and white sturgeon (*Acipenser transmontanus*). The table is based on Arnot and Gobas (2004). The compartment is assumed to have a specific gravity of 1.0 (i.e., the units L and kg can be substituted for one another).

Symbol	Units	Description	Fathead minnow values			White Sturgeon values		
			Egg stage (0-3 dpf)	Yolk stage (3-7 dpf)	Free feeding stage (7-32 dpf)	Egg stage (0-12 dpf)	Yolk stage (12-21 dpf)	Free feeding stage (21-56 dpf)
w_w	kg (L)	Body wet weight (volume of the whole body)	– Model input –					
K_{ow}	-	Octanol-water partitioning coefficient	– Model input –					
S	%	Dissolved oxygen saturation	– Model input –					
T	°C	Water temperature	– Model input –					
C_w	µg L^{-1}	Chemical concentration in water	– Model input –					
f_lipid	%	Total lipid content (fraction of body weight)	– Model input –					
lipid	kg	Total lipid content	– Equation S11 –					
β	-	Sorption capacity constant	0.05[*]					
d_w	kg	Body dry weight	0.28 w_w					
f_NLOM	-	Fraction of non-lipid organic matter	– Equation S12 –					
f_water	-	Water content	– Equation S13 –					
K_{bw}	-	Fish – water partition coefficient	– Equation S14 –					
C_{ox}	mg O$_2$ L^{-1}	Dissolved oxygen concentration in water	– Equation S15 –					

151

G_v	L d^{-1}	Gill ventilation rate	– Equation S16 –
E_w	-	Gill chemical uptake efficiency	– Equation S17 –
k_{in}	L kg^{-1} d^{-1}	Aqueous uptake clearance rate constant	– Equation S18 –
k_{out}	kg kg^{-1} d^{-1}	Gill elimination rate constant	– Equation S19 –
k_G	d^{-1}	Growth dilution rate constant	– Equation S20 –
k_{met}	d^{-1}	Whole-body metabolism rate	– Equation S10 –
C_{int}	µg g^{-1}	Chemical internal concentration	– Equation S21 –
C_{met}	µg g^{-1}	Metabolite internal concentration	– Equation S22 –

[*] *Value is different than what is reported by Arnot & Gobas (2004). Value obtained from DeBruyn & Gobas (2007) as suggested by Stadnicka et al. (2012).*

Embryo-larval stage one-compartment model equations (from Arnot and Gobas, 2004)

Total lipid content

$$lipid = w\_w \cdot f\_lipid \; ; \text{(kg)} \hspace{4cm} \textbf{(Eq. S11)}$$

Fraction of non-lipid organic matter

$$f\_NLOM = \frac{d\_w - lipid}{w\_w} \; ; \text{(unitless)} \hspace{2.5cm} \textbf{(Eq. S12)}$$

Water fraction in fish

$$f\_water \; = \frac{w\_w - d\_w}{w\_w} \; ; \text{(unitless)} \hspace{2.5cm} \textbf{(Eq. S13)}$$

Fish – water partition coefficient

$$k_{bw} = f\_lipid \cdot K_{ow} + f\_NLOM \cdot \beta \cdot K_{OW} + f\_water \; ; \text{(unitless)} \hspace{0.5cm} \textbf{(Eq. S14)}$$

Dissolved oxygen concentration

$$C_{ox} = (-0.24 \cdot T + 14.04) \cdot \frac{S}{100} \; ; \text{(mg O}_2 \text{ L}^{-1}) \hspace{1.5cm} \textbf{(Eq. S15)}$$

Gill ventilation rate

$$G_v = 1400 \cdot \frac{w\_w^{0.65}}{C_{ox}} \; ; \text{(L d}^{-1}) \hspace{3cm} \textbf{(Eq. S16)}$$

Gill chemical uptake efficiency

$$E_w = \frac{1}{1.85 + \frac{155}{K_{ow}}} \; ; \text{(unitless)} \hspace{3cm} \textbf{(Eq. S17)}$$

Aqueous uptake clearance rate constant

$$k_{in} = \frac{E_w \cdot G_v}{w\_w} \; ; \text{(L kg}^{-1} \text{d}^{-1}) \hspace{3cm} \textbf{(Eq. S18)}$$

Gill elimination rate constant

$$k_{out} = \frac{k_{in}}{k_{bw}} \; ; \text{(kg kg}^{-1} \text{d}^{-1}) \hspace{3cm} \textbf{(Eq. S19)}$$

Growth dilution rate constant

$$k_G = 0.005 \cdot w\_w^{-0.2} \; ; \text{(d}^{-1} \text{ for temperatures around 10°C)}$$

$$\textbf{(Eq. S20)}$$

$$k_G = 0.00251 \cdot w\_w^{-0.2} \; ; \text{(d}^{-1} \text{ for temperatures around 25°C)}$$

Chemical internal concentration

$$\frac{dC_{int}(t)}{dt} = \frac{k_{in}}{1000} \cdot C_w(t) - (k_{out} + K_G) \cdot C_{int}(t) \; ; \; (\mu g \; g^{-1} \; d^{-1}) \qquad \textbf{(Eq. S21)}$$

Additional model equation (implementation of whole-body chemical biotransformation)

Metabolite internal concentration

$$\frac{dC_{met}(t)}{dt} = k_{met} \cdot C_{int}(t) \; ; \; (\mu g \; g^{-1} \; d^{-1}) \qquad \textbf{(Eq. S22)}$$

Appendix J. Adult multi-compartment physiologically based toxicokinetic (PBTK) model

J.1 Adult fathead minnow model

A multi-compartment PBTK (physiologically based toxicokinetic) model was adapted to predict the abundance of parent B[*a*]P in the tissues and B[*a*]P metabolites in the bile of adult life stage fathead minnow (Stadnicka, Schirmer, & Ashauer, 2012; Brinkmann et al., 2016). The model was adapted to integrate biotransformation of parent B[*a*]P by incorporating an *in vivo* intrinsic clearance parameter calculated using an Excel spreadsheet provided by Nichols, Fitzsimmons, & Burkhard (2007) (Table J.2). The *in vivo* intrinsic clearance parameter was used to calculate hepatic clearance, using the well-stirred model of hepatic clearance, which was further used to calculate hepatic biotransformation. A bile compartment was implemented into the existing model structure by combining hepatic biotransformation with bile volume and bile flow, which simulated the mass flux of B[*a*]P metabolites exiting the liver and entering the bile (Table J.3). The model was implemented using Python 3.5® (Python Software Foundation, Wilmington, DE, USA) in Jupyter Notebook® (Project Jupyter, U.S. Patent & Trademark Office, Alexandria, VA, USA). A simulation was run using input data from 157 adult fathead minnows. The physiological parameters wet weight and bile volume were described for each individual fish along with the exposure parameters, chemical concentration in the water, exposure time, simulation time, temperature, and dissolved oxygen. Simulated exposures were run for either 96, 168, 336, or 504 hours, with 5000 iteration steps per hour, at the measured concentrations of either 0.03, 0.08, or 1.34 µg B[*a*]P/L. The model predicted the accumulation of parent B[*a*]P in the whole body, as well as the liver, fat, richly perfused tissues, and poorly perfused tissues, and the accumulation of B[*a*]P metabolites in the bile of adult fathead minnows. Outputs of bile metabolites were multiplied by 0.6 (Equation 40) to represent specific fractions of hydroxy B[*a*]P and the associated glucuronide, which was determined to between 58-66% of total B[*a*]P metabolites produced in adult fish (Zhu et al., 2008). It should also be noted that the kidney was not included in the model as physiological values for the kidney parameters were not available for fathead minnow. However, the model equations for the kidney are included in the event that the values become available, or the model is used for another species.

J.2 Sub-adult white sturgeon model

A multi-compartment PBTK (physiologically based toxicokinetic) (Stadnicka et al., 2012; Brinkmann et al., 2016) (Table J.3) model was re-parametrized to predict the abundance of multiple organic chemicals in sub-adult white sturgeon. In addition, the model was adapted to

integrate biotransformation by incorporating an *in vivo* intrinsic clearance parameter calculated using an Excel spreadsheet provided by Nichols et al. (2007). The *in vivo* intrinsic clearance parameter was used to calculate hepatic clearance, using the well-stirred model of hepatic clearance, which was further used to calculate hepatic biotransformation. A bile compartment was implemented into the existing model structure by combining hepatic biotransformation with bile volume and bile flow. This component of the model can be used for chemicals that are actively biotransformed and in which values for *in vitro* intrinsic clearance exist. In the present study, *in vitro* intrinsic clearance of B[*a*]P was measured in white sturgeon; however, since no data set pertaining to the bioaccumulation of B[*a*]P exists for any sturgeon species, this parameter could not be tested. Biotransformation was omitted for the simulations using our test chemicals avermectin-B1 (Shen et al., 2005), molinate (Tjeerdema & Crosby, 1988), sulfamethazine (SM$_2$) (Hou et al., 2003), or *p*-nitrophenol (PNP) (Tenbrook et al., 2006) as, to our knowledge, no *in vitro* clearance value exists for these chemicals in a sturgeon species.

The model was implemented using Python 3.5® (Python Software Foundation, Wilmington, DE, USA) in Jupyter Notebook® (Project Jupyter, U.S. Patent & Trademark Office, Alexandria, VA, USA). Monte Carlo-like simulations (200 simulations per data point) were run in which a random combination of parameter values from each parameter distribution was chosen, assuming that the parameters are independent. Predictions of the internal concentrations of organic contaminants were generated in the whole body, as well as the liver, fat, richly perfused tissues, and poorly perfused tissues. No predictions for the kidney were generated as, presently, the kidney compartment cannot be accurately parameterized. The model outputs were compared to published data sets of internal concentrations (C$_{int}$) or muscle concentrations (C$_m$) for sturgeon that were exposed to the organic contaminants avermectin-B1 (Shen et al., 2005), molinate (Tjeerdema & Crosby, 1988), sulfamethazine (SM$_2$) (Hou et al., 2003), or *p*-nitrophenol (PNP) (Tenbrook et al., 2006). Experimental data sets used for model test and validation purposes are shown in Table J.1.

Table J.1. Experimental data used for modelling internal and muscle chemical concentrations in white sturgeon (*Acipenser transmontanus*) using the PBTK model.

	Chemical	Log K_{ow}[a]	Wet weight	Temp	Exposure Time	Exposure Concentration	Measured C_m	Measured C_{int}
		(-)	(g ± S.D)	(°C)	(h)	(μg L^{-1})	(mg kg^{-1})	(mg kg^{-1})
1	Avermectin B1[b]	4.40	35.8 ± 4.6	20	72	0.2	0.0044	-
2	Avermectin B1[b]	4.40	35.8 ± 4.6	20	120	0.2	0.0066	-
3	Avermectin B1[b]	4.40	35.8 ± 4.6	20	192	0.2	0.0066	-
4	Avermectin B1[b]	4.40	35.8 ± 4.6	20	264	0.2	0.0072	-
5	Avermectin B1[b]	4.40	35.8 ± 4.6	20	336	0.2	0.0074	-
6	Avermectin B1[b]	4.40	35.8 ± 4.6	20	432	0.2	0.0077	-
7	Avermectin B1[b]	4.40	35.8 ± 4.6	20	528	0.2	0.0080	-
8	Avermectin B1[b]	4.40	35.8 ± 4.6	20	24	1	0.0054	-
9	Avermectin B1[b]	4.40	35.8 ± 4.6	20	72	1	0.0198	-
10	Avermectin B1[b]	4.40	35.8 ± 4.6	20	120	1	0.0272	-
11	Avermectin B1[b]	4.40	35.8 ± 4.6	20	192	1	0.0340	-
12	Avermectin B1[b]	4.40	35.8 ± 4.6	20	264	1	0.0364	-
13	Avermectin B1[b]	4.40	35.8 ± 4.6	20	336	1	0.0364	-
14	Avermectin B1[b]	4.40	35.8 ± 4.6	20	432	1	0.0383	-
15	Avermectin B1[b]	4.40	35.8 ± 4.6	20	528	1	0.0383	-
16	Molinate[c]	3.21	15.6 ± 1.9	18	50 + 24 depuration	100	-	2.748
17	Sulfamethazine[d]	0.53	28.2 ± 5.1	20	6	100	0.10	-
18	Sulfamethazine[d]	0.53	28.2 ± 5.1	20	12	100	0.097	-
19	Sulfamethazine[d]	0.53	28.2 ± 5.1	20	24	100	0.099	-
20	Sulfamethazine[d]	0.53	28.2 ± 5.1	20	48	100	0.102	-
21	Sulfamethazine[d]	0.53	28.2 ± 5.1	20	72	100	0.100	-
22	Sulfamethazine[d]	0.53	28.2 ± 5.1	20	96	100	0.097	-
23	Sulfamethazine[d]	0.53	28.2 ± 5.1	20	120	100	0.098	-
24	Sulfamethazine[d]	0.53	28.2 ± 5.1	20	144	100	0.097	-
25	Sulfamethazine[d]	0.53	28.2 ± 5.1	20	192	1000	0.097	-
26	Sulfamethazine[d]	0.53	28.2 ± 5.1	20	6	1000	0.094	-
27	Sulfamethazine[d]	0.53	28.2 ± 5.1	20	12	1000	0.479	-

28	Sulfamethazine[d]	0.53	28.2 ± 5.1	20	24	1000	0.574	-
29	Sulfamethazine[d]	0.53	28.2 ± 5.1	20	48	1000	0.747	-
30	Sulfamethazine[d]	0.53	28.2 ± 5.1	20	72	1000	0.795	-
31	Sulfamethazine[d]	0.53	28.2 ± 5.1	20	96	1000	0.779	-
32	Sulfamethazine[d]	0.53	28.2 ± 5.1	20	120	1000	0.811	-
33	Sulfamethazine[d]	0.53	28.2 ± 5.1	20	144	1000	0.795	-
34	Sulfamethazine[d]	0.53	28.2 ± 5.1	20	192	1000	0.820	-
35	p-nitrophenol[e]	1.91	9.9 ± 0.3	17	3	1000	-	8.350
36	p-nitrophenol[e]	1.91	9.9 ± 0.3	17	7	1000	-	12.700
37	p-nitrophenol[e]	1.91	9.9 ± 0.3	17	24	1000	-	15.020
38	p-nitrophenol[e]	1.91	9.9 ± 0.3	17	24	1000	-	15.816
39	p-nitrophenol[e]	1.91	9.9 ± 0.3	17	24 + 24 depuration	1000	-	1.680

[a] value obtained from PubChem® (U.S. National Library of Medicine)

[b] Shen et al. 2005

[c] Tjeerdema & Crosby, 1988

[d] Hou et al. 2003

[e] Tenbrook et al. 2006

Table J.2. Spreadsheet inputs and parameters for adult fathead minnow (*Pimephales promelas*) and white sturgeon (*Acipenser transmontaus*) to calculate hepatic clearance. The table is based on Nichols et al. (2007).

Symbol	Units	Description	Fathead minnow value	White sturgeon value
Rate	h^{-1}	Depletion rate constant[a]	0.786	0.219
C_{S9}	$mg\ mL^{-1}$	S9 protein concentration	1	1
L_{S9}	$mg\ g\ liver^{-1}$	Total liver S9 protein content	71	24
L_{FBW}	$g\ liver\ g\ wet\ weight^{-1}$	Fractional liver weight	0.018[b]	0.029[b]
Q_C	$L\ d^{-1}\ kg^{-1}$	Cardiac output	924.582[b]	81.88[b,c]
Q_{HFRAC}	-	Liver blood flow as a fraction of cardiac output	0.286[b]	0.071[b]
f_u	-	Binding correction term	1.0 (assumed)	
$CL_{int,\ in\ vitro}$	$mL\ h^{-1}\ mg\ S9\ protein^{-1}$	*In vitro* intrinsic clearance	– Equation S3 –	
$CL_{int,\ in\ vivo}$	$L\ d^{-1}\ kg^{-1}$	*In vivo* intrinsic clearance	– Equation S4 –	
Q_H	$L\ d^{-1}\ kg^{-1}$	Liver blood flow	– Equation S5 –	
Cl_H	$L\ d^{-1}\ kg^{-1}$	Hepatic clearance	– Equation S6 –	

[a]*Derived from methods described in OECD 319B: Determination of in vitro clearance using rainbow trout liver S9 sub-cellular fraction (RT-S9) (OECD, 2018)*
[b]*Data taken from adult fathead minnow and white sturgeon multi-compartment PBTK model (Appendix Table J.3*
[c]*Values were determined 3-year-old fish with a wet mass of 510 ± 105 g*

Table J.3. Model inputs and parameters of the multi-compartment PBTK model for adult fathead minnow (*Pimephales promelas*) and sub-adult white sturgeon (*Acipenser transmontanus*). The table is based on Stadnicka et al. (2012). Compartment volumes were expressed relative to the total body volume, while all compartments were assumed to have a specific gravity of 1.0 (i.e., the units L and kg can be substituted for one another).

Symbol	Units	Description	Fathead minnow value	White sturgeon value
w_w	kg (L)	Body wet weight (volume of the whole body)	– Model input –	
log K_{ow}	-	Octanol-water partitioning coefficient	– Model input –	
C_w	µg L^{-1}	Chemical concentration in inspired water	– Model input –	
T	°C	Water temperature	– Model input –	
C_{ox}	mg L^{-1}	Dissolved oxygen concentration in inspired water	– Model input –	
lipid	-	Total lipid content (fraction of body weight)	– Model input –	
K	-	Constant in equation S23, for T>10°C	3.05 10^{-4} [a]	
n	-	Constant in equation S23, for T>10°C	1.855[a]	
m	-	Constant in equation S23, for T>10°C	-0.138[a]	
α_b	-	Lipid content of blood tissue (fraction of wet weight)	0.019[a]	0.008
α_f	-	Lipid content of fat tissue (fraction of wet weight)	1.010[a]	– calculated –
α_k	-	Lipid content of kidney tissue (fraction of wet weight)	–	0.008
α_l	-	Lipid content of liver tissue (fraction of wet weight)	0.074[a]	0.306
α_m	-	Lipid content of muscle tissue (fraction of wet weight)	0.025[a]	0.0262
γ_b	-	Water content of blood tissue (fraction of wet weight)	0.876[a]	0.866
γ_f	-	Water content of fat tissue (fraction of wet weight)	0.016[a]	0.342
γ_k	-	Water content of kidney tissue (fraction of wet weight)	–	0.875
γ_l	-	Water content of liver tissue (fraction of wet weight)	0.766[a]	0.510

γ_m	-	Water content of muscle tissue (fraction of wet weight)	0.806[a]	0.763
$lipid_l$	-	Lipid content of lean tissue (fraction of wet weight)	– Equation S23 –	
V_f	L	Volume of the fat compartment	– Equation S24 –	
V_k	L	Volume of the kidney compartment	–	–
V_l	L	Volume of the liver compartment	0.018 w_w	0.029 w_w
V_m	L	Volume of the poorly perfused compartment	– Equation S25 –	
V_r	L	Volume of the richly perfused compartment	0.072 w_w	0.058 w_w
V_{bile}	L	Volume of bile compartment	– Model input –	
Q_c	L h^{-1}	Cardiac output	– Equation S26 –	
Q_f	L h^{-1}	Blood flow to the fat compartment	0.010 Q_c (assumued)	
Q_k	L h^{-1}	Blood flow to the kidney compartment	–	–
Q_l	L h^{-1}	Blood flow to the liver compartment	0.024 Q_c	0.071 Q_c
Q_m	L h^{-1}	Blood flow to the poorly perfused compartment	0.440 Q_c	0.717 Q_c
Q_r	L h^{-1}	Blood flow to the richly perfused compartment	0.526 Q_c	0.202 Q_c
Q_{bile}	L h^{-1}	Bile flow	0.5 V_{bile}	
VO_2	mg h^{-1}	Oxygen consumption rate normalized to 1 kg body weight	– Equation S27 –	
Q_w	L h^{-1}	Effective respiratory volume	– Equation S28 –	
P_{bw}	-	Blood:water partitioning coefficient	– Equation S29 –	
P_l, P_f, P_m	-	Liver/fat/muscle:blood partitioning coefficient	– Equation S30 –	
P_k	-	Kidney:blood partitioning coefficient	–	–
P_r	-	Richly perfused tissue:blood partitioning coefficient	– P_l –	

A_i	μg	Chemical amount in fat, poorly and richly perfused tissues	– Equation S32 –	
A_l	μg	Chemical amount in the liver compartment	– Equation S33 –	
$A_{l\_transform}$	μg	Hepatic biotransformation	– Equation S38 –	
A_k	μg	Chemical amount in the kidney compartment	–	–
A_{bile}	μg	Chemical amount in bile compartment	– Equation S39 –	
$CL_{int,\ in\ vivo}$	L d^{-1} kg^{-1}	*In vivo* intrinsic clearance	– Equation S4 –	
Cl_H	L d^{-1} kg^{-1}	Hepatic clearance	– Equation S6 –	
C_{int}	μg g^{-1}	Internal concentration in the whole fish	– Equation S35 –	
C_{art}	μg L^{-1}	Chemical concentration in arterial blood	– Equation S36 –	
C_{ven}	μg L^{-1}	Chemical concentration in venous blood	– Equation S37 –	
C_{bile}	μg L^{-1}	Metabolite concentration in bile	– Equation S40 –	

[a]Data taken from from Stadnicka et al. (2012)

Multi-compartment PBTK model equations (from Stadnicka et al. 2012)

Volume of the lean tissue compartment - cyprinids

$$lipid_l = \frac{V_l \cdot \alpha_l + V_r \cdot \alpha_r + V_m \cdot \alpha_m}{V_l + V_r + V_m} \; ; \text{(unitless)}$$
(Eq. S23)

Volume of the fat compartment

$$V_f = w\_w \cdot \frac{lipid - lipid_l}{\alpha_f - lipid_l} \; ; \text{(L)}$$
(Eq. S24)

Volume of the poorly perfused compartment - cyprinids

$$V_m = w\_w - (V_l + V_r + V_f) \; ; \text{(L)}$$
(Eq. S25)

Cardiac output

$$Q_c = (0.23 \cdot T - 0.78) \cdot \left(\frac{1000 \cdot w\_w}{500}\right)^{-0.1} \cdot w\_w^{0.75} \; ; \text{(L h}^{-1}\text{)}$$
(Eq. S26)

Oxygen consumption rate

$$VO_2 = K \cdot (32 + T \cdot \frac{9}{5})^n \cdot \left(\frac{w\_w}{0.4536}\right)^m \cdot \frac{10000}{24} \; ; \text{(mg h}^{-1}\text{)}$$
(Eq. S27)

Effective respiratory volume

$$Q_w = \frac{VO_2}{0.8 \cdot C_{ox}} \cdot w\_w^{0.75} \; ; \text{(L h}^{-1}\text{)}$$
(Eq. S28)

Blood:water partitioning coefficient

$$P_{bw} = 10^{0.72 \cdot \log Kow + 1.04 \cdot log(\alpha_b) + 0.86} + \gamma_b \; ; \text{(unitless)}$$
(Eq. S29)

Liver/fat/muscle:blood partitioning coefficient

$$P_{l,f,m} = \frac{10^{0.72 \cdot \log Kow + 1.04 \cdot log(\alpha_{l,f,m}) + 0.86 + \gamma_{l,f,m}}}{P_{bw}} \; ; \text{(unitless)}$$
(Eq. S30)

Kidney:blood partitioning coefficient

$$P_k = \frac{10^{0.72 \cdot \log Kow + 1.04 \cdot log(\alpha_k) + 0.86 + \gamma_k}}{P_{bw}} \; ; \text{(unitless)}$$
(Eq. S31)

Chemical amount in fat, poorly and richly perfused tissues

$$\frac{dA_i(t)}{dt} = Q_i \cdot \left(C_{art}(t) - \frac{A_i(t)}{V_i \cdot P_i} \right) ; (\mu g \; h^{-1}) \qquad \textbf{(Eq. S32)}$$

Chemical amount in the liver compartment

$$\frac{dA_l(t)}{dt} = Q_r \cdot \frac{A_r(t)}{V_r \cdot P_r} + Q_l \cdot C_{art}(t) - (Q_r + Q_l) \cdot \frac{A_l(t)}{V_l \cdot P_l} - A_{l\_transform}(t) ; (\mu g \; h^{-1}) \; \textbf{(Eq. S33)}$$

Chemical amount in the kidney compartment

$$\frac{dA_k(t)}{dt} = 0.6 \cdot Q_m \cdot \frac{A_m(t)}{V_m \cdot P_m} + Q_k \cdot C_{art}(t) - (0.6 \cdot Q_m + Q_k) \cdot \frac{A_k(t)}{V_k \cdot P_k} ; (\mu g \; h^{-1}) \; \textbf{(Eq. S34)}$$

Internal chemical concentration in the whole fish - cyprinids

$$C_{int}(t) = \frac{A_f(t) + A_m(t) + A_r(t) + A_l(t)}{1000 \cdot w\_w} ; (\mu g \; g^{-1}) \qquad \textbf{(Eq. S35)}$$

Chemical concentration in arterial blood

$$C_{art}(t) = \min (Q_w, Q_c \cdot P_{bw}) \cdot C_w - \frac{C_{ven}(t)}{P_{bw}} \cdot \frac{1}{Q_c} + C_{ven}(t) ; (\mu g \; L^{-1}) \qquad \textbf{(Eq. S36)}$$

Chemical concentration in venous blood - cyprinids

$$C_{ven}(t) = \left(Q_f \cdot \frac{A_f(t)}{V_f \cdot P_f} + Q_m \cdot \frac{A_m(t)}{V_m \cdot P_m} + (Q_r + Q_l) \cdot \frac{A_l(t)}{V_l \cdot P_l} \right) \cdot \frac{1}{Q_c} ; (\mu g \; L^{-1}) \qquad \textbf{(Eq. S37)}$$

Additional model equations (implementation of chemical biotransformation and bile compartment)

Hepatic biotransformation

$$\frac{dA_{l\_transform}(t)}{dt} = Cl_H \cdot \frac{A_l}{V_l \cdot P_l} ; (\mu g \; h^{-1}) \qquad \textbf{(Eq. 38)}$$

Chemical amount in the bile

$$A_{bile} = A_{bile} - A_{bile} \cdot \frac{Q_{bile}}{V_{bile}} ; (\mu g \; h^{-1}) \qquad \textbf{(Eq.39)}$$

Metabolite concentration in bile

$$C_{bile}(t) = \frac{A_{bile}}{V_{bile}} \cdot 0.60 ; (\mu g \; L^{-1}) \qquad \textbf{(Eq.40)}$$

Appendix K. Sensitivity analyses

K.1 Fathead minnow

Sensitivity analyses were run with the fathead minnow models to assess the influence of changes in several model parameters on model outputs. For the one-compartment ELS model, the parameters wet weight, lipid content, and k_{MET}, were increased and decreased two-fold, respectively. The parameters *in vivo* intrinsic clearance, bile volume, and bile flow were analyzed for the adult multi-compartment PBTK model. *In vivo* intrinsic clearance was changed three-fold, and bile volume was changed two-fold in each direction. Bile flow was decreased two-fold and increased by half a factor. Only one parameter was changed at a time by two steps in each direction, while the other parameters remained at their default value.

The sensitivity analysis for the one-compartment ELS model displayed that k_{MET} had the largest influence on model predictions (Supplemental Figure S2C). Model predictions were sensitive to wet weight at low values and became less sensitive as values increased. The model was insensitive to changes in lipid content. All three parameters analyzed for the adult multi-compartment PBTK model exhibited sensitivity at low values and became progressively insensitive to changes as values increased (Supplemental Figure S2D,E,F).
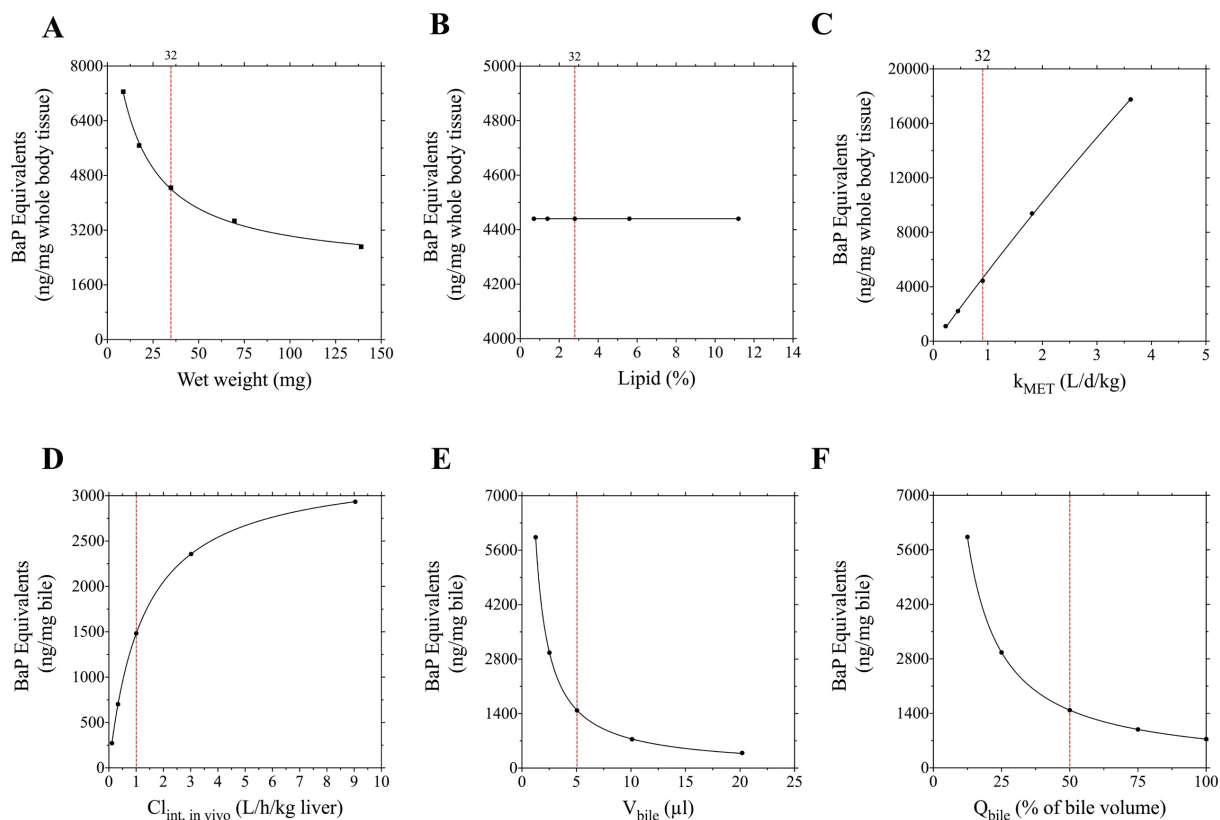
Figure K.1. Sensitivity analyses conducted for the fathead minnow using the ELS one-compartment model (run using the 4.55 μg B[*a*]P/L treatment) and the adult multi-compartment PBTK model (run using the 1.34 μg B[*a*]P/L treatment). The parameters wet weight (A), total lipid content (B), and biotransformation rate (k_{MET}; C) were analyzed for the ELS one-compartment model while the parameters *in vivo* intrinsic clearance ($Cl_{int,\ in\ vivo}$; D), bile volume (V_{bile}; E), and bile flow (Q_{bile}; F) were analyzed for the adult multi-compartment model. Model default values are denoted by a red dotted line. For the ELS one-compartment model, the default value is shown for 32 dpf; however, a value for zero, three, seven, and 14 dpf was also implemented for each parameter.